Reprinted from Journal of the Virtual Explorer, volume 27
http://virtualexplorer.com.au/
doi:10.3809/doi:10.3809/jvirtex.2007.00167

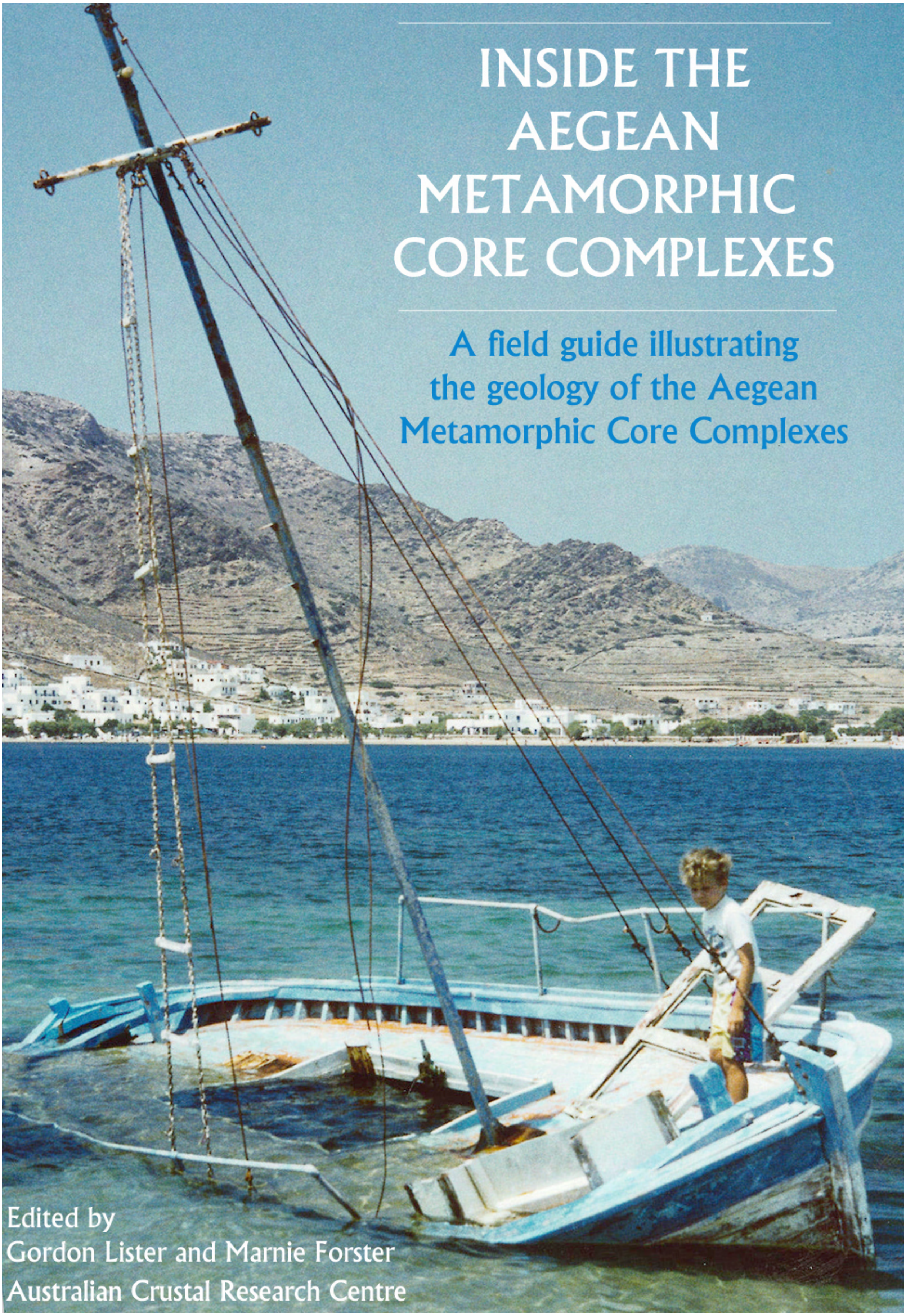

# Inside the Aegean Metamorphic Core Complexes:
## *A Field Trip Guide Illustrating the Geology of the Aegean Metamorphic Core Complexes Thera, Ios, Naxos and Paros*

**EDITED BY GORDON S. LISTER & MARNIE A. FORSTER**

*Australian Crustal Research Centre, Department of Earth Sciences, Monash University*

*Australian Crustal Research Centre, Technical Publication **45**, 110 pp., 1997*



The original field trip to the Aegean metamorphic core complexes took place in October 1996.
The excursion leaders were Marnie Forster (top), Sue Keay (bottom left), Gordon Lister(bottom right)

# TABLE OF CONTENTS

# Foreword

## A historical perspective

*Sue Keay, University of Queensland*

Travelling from Crete to Naxos we are following the famous voyage of Theseus, the hero of Athens, on his flight from the Minoans after slaying the evil minotaur.

Theseus was the son of King Aegeas of Athinna. At the time (~2000 BC), Athens was under the domination of King Minos of Crete. King Minos had invoked the wrath of Poseidon, God of the sea, who cursed Minos in retribution, causing a raging Bull to emerge from the sea and wreak destruction on Crete.

Another clause in the curse caused King Minos's wife Pasiphae to fall in love with Poseidon's creation. Hercules conquered the bull, but not before Pasiphae conceived a child by it. The baby was born half-man half-bull (a minotaur), and declared a monster. King Minos had his chief architect design a special labyrinth beneath the palace of Knossos near Heraklion, to contain the creature where it grew up alone and unloved in the dark.

King Minos already had two children, a boy and girl, Androgenes and Ariadne. Androgenes was murdered whilst visiting Athens and in a rage, King Minos blamed King Aegeas for not protecting his son and ordered as compensation the delivery of an annual tribute of seven maidens and seven young men to Crete. The fourteen sent away each year never returned to Athens, so the tribute ship always sailed with black sails, mourning the loss of Athens'youth. When they arrived in Crete the youths were sent into the labyrinth, where they were eventually found and eaten by the minotaur.

When rumours of the terrible fate befalling the human tribute reached Athens, Theseus determined to stop the slaughter. Much against his father's wishes Theseus volunteered to be sent as part of the next tribute to Crete. To ease his father's mind, Theseus agreed that if his voyage was successful, he would return to Athens with white sails flying.

The tribute ship arrived in Crete and Ariadne, daughter of King Minos, saw Theseus and instantly fell in love with him. She promised to help him escape from the labyrinth if he would take her back to Athens with him. Theseus agreed and she supplied him with a ball of string that he could unravel and use to find his way back out of the maze. Theseus entered the labyrinth and was able to slay the minotaur and escape with Ariadne.

Things did not progress smoothly between Theseus and Ariadne. Some say that Ariadne was a priestess for a particularly bloodthirsty religious cult which Theseus found abhorrent. At any rate, Theseus decided to abandon Ariadne before they reached Athens, and took his opportunity when his ship stopped at Naxos, leaving her sleeping on the beach while he and his crew sailed away.

There are several variations of the legend from here on, one version suggests that in her grief Ariadne cast herself off the nearest cliff. The other version (most popular with Naxians) is that the local God of the island, Dionysius (the God of Wine and a particularly popular God in the Cyclades) came across Ariadne while she slept, instantly fell in love with her and that the pair lived happily ever after on Naxos. Dionysius was apparently so enamoured of his bride that after their wedding he removed Ariadne's bridal crown and cast it into the sky where it can now be seen as the Corona Borealis.

Theseus more than paid for his callous abandonment of Ariadne. His thoughtlessness meant that when he returned to Athens he forgot to change his sails from black to white. On seeing the tribute ship returning to Athens with black sails King Aegeas, assuming that his son had been killed, threw himself into the sea from the cliffs of Sounion in his grief. Legend says that this is how the Aegean Sea gained its name.

### The Cyclades

The name Cyclades comes from the Greek word for circle (kikladhes) and denotes the shape the islands form around the sacred island of Delos, the birthplace of Apollo and Artemis, and the religious and commercial centre of Classical Greece.

### Culture

The Cyclades have evolved under the influence of a complicated series of invading armies and so it is impossible to qualify their origins. Greece is, and was, a melting pot for many different cultures. The islands have seen the rise and fall of important empires and peoples, including the Thracians, Carians, Minoans, Ionians, Arcadians, the odd Phoenician, Dorians, Persians, Athenians, Macedonians, Egyptians, Romans, Goths, Slavs, Venetians, Franks, Turks, Russians and finally the Tourists.

Most of the people (98%) belong to the Greek Orthodox church (with the rest of the religions being Roman Catholic, Jewish and Muslim). Founded in the 4th century, Orthodox churches make up one third of the world's Christian churches. The Greek Orthodox church acted as an important cultural anchor during the occupation of Greece by the Turks, and strove to protect Greek customs and traditions.

## Geography

Reports that islands such as Paros and Naxos were heavily forested date back from 1000AD. Recent reports indicate that much vegetation has been destroyed only within the last 100 years of settlement. With the advent of tourism, water has become an exceedingly precious commodity, and the heavy drain made on this resource has caused the water table to begin to fall at an alarming rate on many of the most popular islands. This in turn has resulted in significant damage to agriculture, and also acted to the detriment of local springs, and natural vegetation. The European Union has invested resources in the construction of dams on some islands (e.g., Ios and Naxos).

## Flora

One memory of the islands you are sure to take back home with you is the tangy scent of the assorted herbs which grow wild on deserted hillsides. Rosemary and thyme predominate, but lavender, oregano, camomile, fennel and sage can also be found.

The islands were once covered by forests but now, deforestation and the introduction of the goat has spelt the demise of most large trees and any edible flora. The most familiar vegetation are the thorny bushes: broom, knapweed and heather. In cultivated areas olive trees are ubiquitous, while along streams the oleander predominates. In villages geranium and bougainvillea are grown for their profusions of colour, while the village square will often house a towering plane tree. Mulberry trees are relicts from the old silk-worm trade. Citrus trees are cultivated and the lemons are used on Naxos for making the liqueur specialty "kitron".

## Fauna

Deforestation and the expansion of agriculture combined with the popularity of hunting in Greece has meant that very few wild animals are left in the country. While there are over 400-odd species of bird, wild animals are uncommon on the islands, comprising rabbits, lizards, turtles, snakes and rare wild goats. Dolphins may commonly be seen in the Aegean, while Greece is the only European home for the almost extinct monk seal, and the last loggerhead turtle colony.

There are significant numbers of snakes on the islands including beautiful carpet snakes (pythons). Some species have a deadly reputation and it has been suggested that considerable care be exerted in this respect. Two poisonous varieties abound: the asp of legendary fame (instrumental in Cleopatra's death) and the adder.

## Economy

The main staple products grown in the islands are wine, olive oil, potatoes, and cereals. The islanders often grow enough of their own fruit and vegetables to be self-sustaining. Goats, sheep, pigs and sometimes cattle are also raised.

## Minerals

The islands have a long history of resource exploitation. Naxos in particular has a strong tradition in mining, still visible today in the mountain communities of Moni, Apiranthos, and Koronida. Marble and emery have been mined on Naxos while, Thera exports pumice.

## Climate

As one might expect the Cyclades have a Mediterranean climate, with dry, hot summers and wet, mild winters. In October you can expect temperatures to range from 15-22°C (59-72°F) with up to 6 days of rain. The sea temperature (average 20°C) can sometimes exceed air temperature and this time of Autumn is often called the Summer of Saint Dimitri (to indicate its salubrious nature).

Conditions by mid-October are variable and could range from “shorts” to “long johns” weather depending on the prevailing wind. While storms sometimes afflict the islands in October, we should not experience the dreaded Meltemi, the strong northern winds which blow for weeks in July and August disrupting ferry schedules and making field work less than pleasant.

## History

Most of the islands retain some record of early inhabitation at approximately 5000 BC (see Fig. 1). At this time the area was inhabited by stone age people who left behind carved figures on rock surfaces. During the Early Bronze Age (3200-2000 BC) a highly developed culture evolved in the Cyclades. Numerous marble figurines and unique pottery from this era have been unearthed. The wealth of material found on the islands has led this era to be known as the Cycladic Period.

As the Minoan civilisation on Crete developed it expanded with Minoan influences on the Cycladic culture becoming noticeable by 2000 BC. Thera contains the best preserved settlement of these times at Akrotiri. When the Cretan-Minoan civilisation declined after the eruption of Thera (1400 BC), Mycenaean influences predominated until all of the islands were conquered by the Ionians around 1100 BC. This signified the start of the Geometric Epoch or Dark Ages with the Ionians doing their best to slaughter the original inhabitants of the islands.

On Paros this invasion was followed a mere 100 years later by an invasion of Arcadians (themselves fleeing the invasion of the Dorians further north). Under their leader, Paros, they intermarried with the Ionians and renamed the island. The Parians developed trade links with the Phoenicians and became a maritime power controlling most of the traffic through the Aegean by 800 BC. This developed into a form of piracy and Paros became the centre of the slave trade in the region, selling off people captured during various raids on other settlements.

During the Archaic Period (700-490 BC) Paros and Naxos waged war, the two islands had conflicting styles of government, democratic (Paros) versus oligarchic (Naxos) and the war continued off and on for centuries. This era also saw the peak of marble sculpture work with many of the marble offerings for Delos being constructed, such as the Lions of Delos from Naxos marble, and the many “kouros” statues (see Fig. 2).

By 500 BC the power of Paros had waned and Naxos became the dominant island, ruled by aristocrats. These noblemen were defeated by rebellious commoners led by the Ionian Lygdamis who installed a tyranny in 540 BC (see Fig. 3). The aristocrats appealed to the expanding empire of Persia for assistance. Lygdamis was overthrown in 524 BC but it was not until 490 BC that the Persians gained control of Naxos and the surrounding islands, signalling the beginning of the so-called "Classical Period" (490-336 BC).

Paros sided with the Persians who used Paros as a base for launching attacks on mainland Greece. The Naxians remained loyal to Athens. After the defeat of the Persians in the battle of Marathon and later in the battle at Salamis, Naxos came under the protection of the Delian-Attic sea alliance. An Athenian fleet was sent to Paros to take over the island (and to kill many of its inhabitants).

Athenian rule lasted until Sparta's victory in the Peloponnesian War. The islands briefly came under the influence of the Ptolemies of Egypt until Macedonia gained power, forging a huge Empire that lasted until the death of Alexander the Great. Rhodes briefly took control of much of the Aegean until the Romans took over from 146 BC to 330 AD (the Roman Epoch). Weakening of the Roman empire led to the islands becoming the haunt of pirates from 69 BC on, with the sacred island of Delos plundered by pirates and deserted. Paros was sacked by Goths in 267 AD.

330-1207 AD marked the Byzantine Period in Greece with Christianity widely practised. Attacks and looting by Vandals, Slavs and Saracens became a common occurrence, and the island inhabitants were forced to take refuge in inland towns, or hidden villages such as the chora

## HISTORICAL TIMES

| | |
|---|---|
| Neolithic Period | 5000 BC - 3200 BC |
| Cycladic Period | 3200 BC - 1100 BC |
| Geometric Epoch (Dark Ages) | 1100 BC - 700 BC |
| Archaic Period | 700 BC - 490 BC |
| Classical Period | 490 BC - 336 BC |
| Hellenistic Period | 336 BC - 146 BC |
| Roman Epoch | 146 BC - 330 AD |
| Byzantine Period | 330 AD - 1207 AD |
| Venetian Epoch | 1207 AD - 1566 AD |
| Turkish (Ottoman) Epoch | 1566 AD - 1821 AD |
| Independent Greece | 1821 AD - present |

**Figure 1** A chronology of historical events for the Aegean region.

**Figure 2** The Kouros at Apollon.

of Ios. In 675AD the Slavs attacked and killed most of the inhabitants of Paros and by 1000AD the island was almost deserted.

In 1207 a Venetian nobleman, Marco Sanudos conquered Naxos with a band of mercenaries and took over the surrounding Aegean islands (including Ios, Paros and Thera). The Franks took over Paros in 1389 building a number of castles to fortify the island. Incursions by Turks into the Cyclades around this time saw many of the islands plagued by pirate raids. In 1537 the Turks made a concerted attack on the Aegean with their dreaded admiral Barbarossa conquering the islands. The Turks installed representatives on each island but allowed the islanders to remain relatively independent, as long as they paid their taxes.

The Venetians and Turks continued to have long running battles over territory in the area waging war from 1644-1669 and 1684-1699. There was a sea battle in the straits between Naxos and Paros in 1651. During this time the Cyclades was pillaged by both armies and with no naval protection of their own, the islands became easy targets for pirates. Major pirate bases were established on the islands of Paros and Mykonos. Despite the fact that the Turks were able to establish sovereignty of the region in the 1700s, pirate attacks continued to plague the islands (see Byron's poem "The Corsair"). Turkish rule was briefly broken from 1770-1777 when the Russians captured the area during their war against the Ottoman Empire. When the War of Independence began in 1821 many of the islands sent volunteers. Amongst them was the heroine Manto Mavroyenous, from Paros (or perhaps from Mykonos), who took part in the siege of Tripolitsa and is claimed to have been responsible for setting explosives to blow up Turkish boats.

## Disclaimer

This information is an amalgamation of things I have read in tourist brochures and more serious books and from stories I have been told while on the islands. From these imperfect sources there may be errors or inconsistencies and certainly different interpretations are possible. This section is meant only for the enjoyment of the field trip participants.

## Selected Reading

Barber 1987, Boatswain & Nicolson 1989, Burn & Burn 1980, Dermopoulos 1990, Ellingham et al. 1992, Forbes-Boyd 1970, Marangou 1990, O'Sullivan 1993, Ucke 1988, Willett et al., 1996.

# Chapter One

## Geological overview of the Aegean area

*Vaios Avdis, I.G.M.E., Athens, Greece*

### INTRODUCTION

The Aegean area (Fig. 1.1) is a rapidly deforming area and presents similarities with island arcs in the western Pacific, both in terms of morphology and geophysical data. Several authors have described the morphology of the Aegean area (e.g., Jongsma et al. 1978, Agarwal et al. 1976, McKenzie 1978). Figure 1.2 shows the main features that these authors have described. Most of these features can be directly or indirectly linked to active tectonic processes, including subduction.

The Mediterranean ridge is characterised by extensive folding of the Messinian and Pliocene-Quaternary cover (Le Pichon et al. 1982). This zone is bordered by a series of deep basins extending from Kefallinia to Rhodes, and is referred to as the Hellenic trench. Maximum depth recorded in these basins is 5100 m. These basins are elongated and filled with unconsolidated sediments (to >500 m depth). Narrow linear structures west, and southeast of Crete are void of sediments however, suggesting active tectonism (Le Pichon & Angelier 1979).

North of the Hellenic trench is the Aegean volcanic arc, defined by a series of active volcanoes (Methana, Aegina, Poros, Milos, Santorini, Yali, and Nisyros, see Fig. 1.2). In

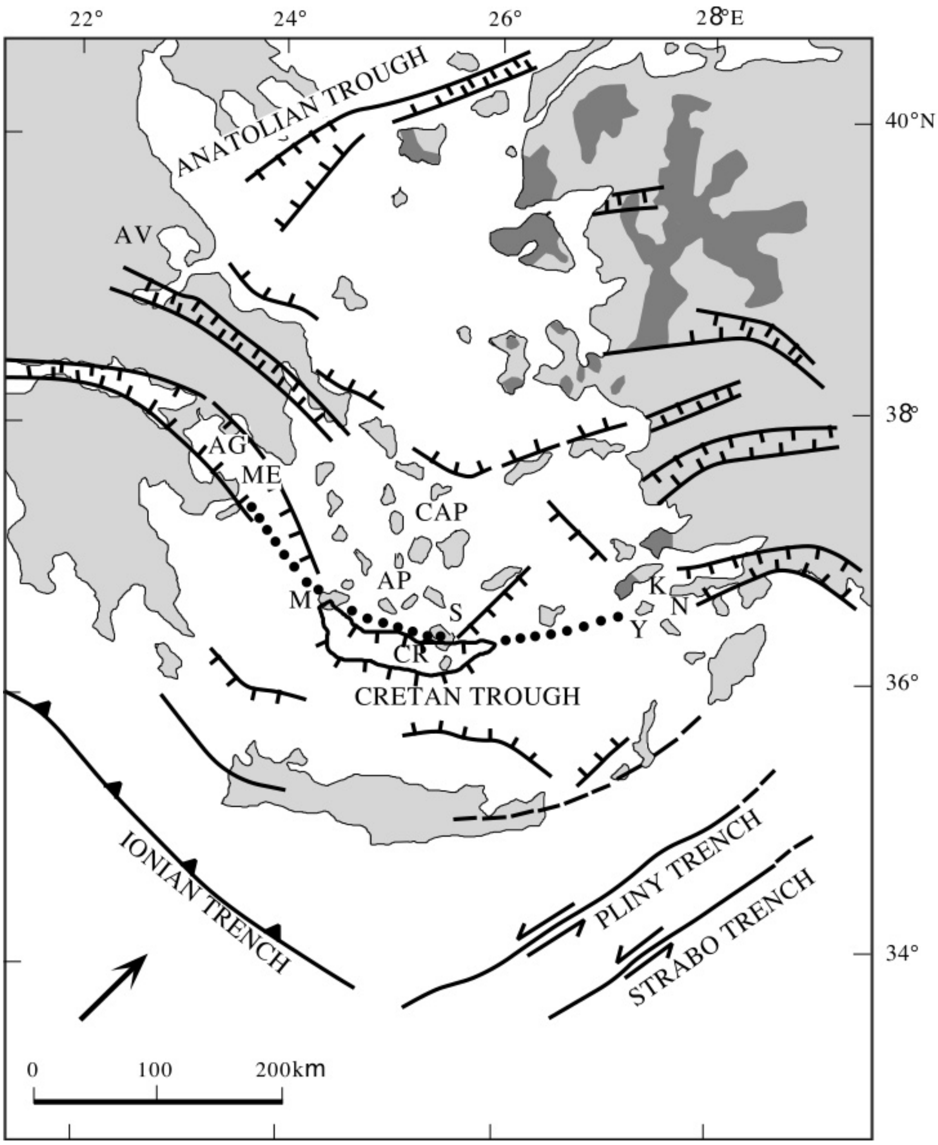


**Figure 1.1** A map of the Aegean area displaying the main tectonic features and the volcanoes of the area. The arrows point to the direction of current subduction. CAP: central aseismic plateau; N: Nisyros; K: Kos; Y: Yali; S: Santorini; Cr: Chris-tiana Islands; M: Milos; Ap: Antiparos; Me: Me-thana; P: Poros; Ag: Aegina [Modified from Jongsma et al. 1978, Agarwal et al. 1976, McKenzie 1978].

the northern Aegean a SW-NE trending trough forms the extension of the Anatolian fault (McKenzie 1978) or is relict of an older arc (Papazachos & Comninakis 1978).

## Geophysical Data

Bath (1983) estimated that the seismic energy released in Greece is ~2% of the total for Earth. Systematic and accurate recording of the earthquakes occurring in the area started in 1961 (Makris 1978). Most shallow shocks are restricted in a band between the Hellenic trench and the arc. The deepest shocks occur at 100-150 km in the northern Aegean. The central part of the Aegean is relatively aseismic. The distribution of epicenters is comparable to those in Pacific subduction zones (Benioff 1962, Sykes 1966). P-wave travel time residuals recorded at Greek stations suggest a high-velocity sinking slab and a low-velocity upper mantle in the Aegean. (Agarwal et al. 1976, Jacoby et al. 1978).

Deep N-S seismic sections (Makris & Vees 1977) show that the crust on both sides of the Hellenic trench has a con tinental character. The crust below the Pelopónnissos is 46 km thick and decreases gradually to 32 km thick towards the northeast. P-wave velocity gradually increases from 6.4 - 6.8 km s-1. P-wave velocity for the upper mantle is 7.5 - 7.7 km s-1. Strong PmP reflections indicate a sharp discontinuity at the Moho throughout the area.

A Bouguer gravity map of the Aegean was published by Makris (1977; 1978). The Aegean Sea, the Cyclades and Crete show (+) anomalies with maximum values in the sea of Crete (+175 mgal). The gravity difference between the Aegean and the Ionian sea (with a crustal thickness of 21 km) could not be explained by adjusted crustal velocities. This discrepancy led Makris to postulate a zone of low density (i.e., low velocity) below the crust of the Aegean Sea. This low density is commensurate with the effects of the rise of anomalously hot asthenosphere.

Magnetic surveys of the Aegean (Vogt & Higgs 1969, Woodside & Bowin 1970, Allan & Morelli 1971) show the Aegean Sea covered by numerous local anomalies. These appear to be related to geological structures (Makris 1978).

Heat flow measurements for the Aegean area were published by Jongsma (1973; 1974) (estimated heat flow is 8.71 x 10-2 watt/m2). Heat flow though the crust of the Aegean Sea is higher than the heat flow in the Eastern Mediterranean, which according to Erickson (1970) and Ryan et al. (1982) is 3.68 x 10-2 watt/m2.

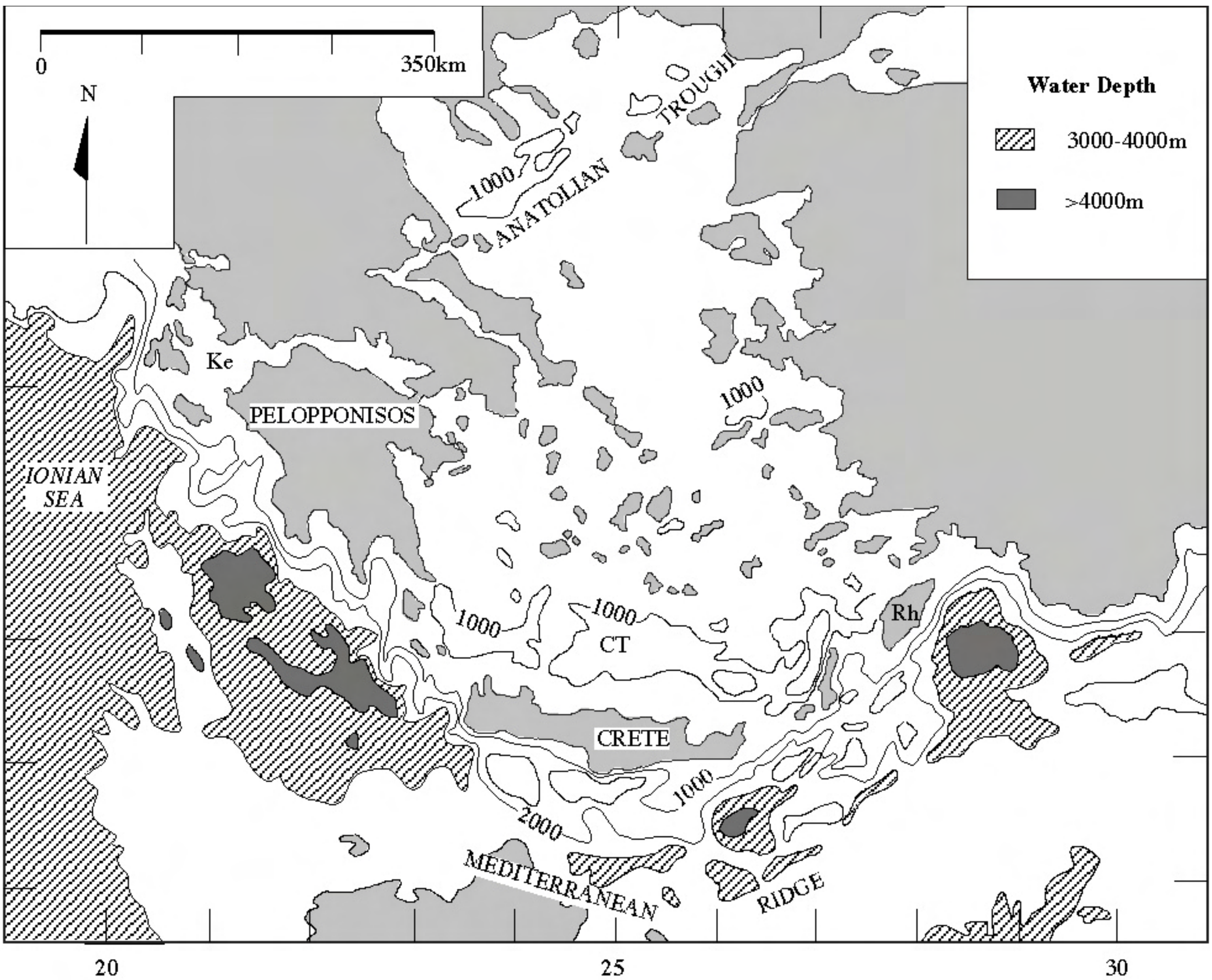


**Figure 1.2** Morphology of the Aegean area after McKenzie (1978). Isobaths at 1 km intervals. (CT= Cretan Trough; Ke = Kefallinia; Rh = Rhodes).

Data based on fault plane solutions for earthquakes in the Aegean area have been used by several authors to constrain geodynamic models for the area (McKenzie 1972, 1978, Ritsema 1974, Papazachos & Comninakis 1978, Le Pichon & Angelier 1979). The results of a study by McKenzie (1978) are briefly outlined below.

## A tectonic model for the Aegean

McKenzie (1972) has interpreted the geology and tectonics of the Aegean area in the light of plate tectonic concepts (see Fig. 1.4 after McKenzie 1972). The Aegean microplate overrides the African plate in a SW direction. Le Pichon & Angelier (1979) suggest that this process started at about 13 Ma. A Benioff zone with the shape of an amphitheatre dips at an angle of ~30° NE (Papazachos & Comninakis 1978) to a depth of ~220 km. Recent tomography indicates that the lithospheric slab penetrates to an even greater depth (Spakman et al. 1988), and that a horizontal tear in the slab runs from the NW towards western Crete. Recent calc-alkaline volcanism occurs (see Fig. 1.3) where the Benioff zone reaches a depth of 130 to 150 km below the Aegean Sea (Ninkovitch & Hays 1972).

Some doubt has been cast as to the validity of the model of a subducting slab beneath the Aegean Sea (Makris 1978). These criticisms are based on the lack of oceanic crust south of the Hellenic trench and the occurrence of intermediate-depth earthquakes on the convex side of the trench south of Crete. McKenzie (1978) suggested intermediate depth earthquakes might reflect inaccuracy in the location of earthquake hypocentres.

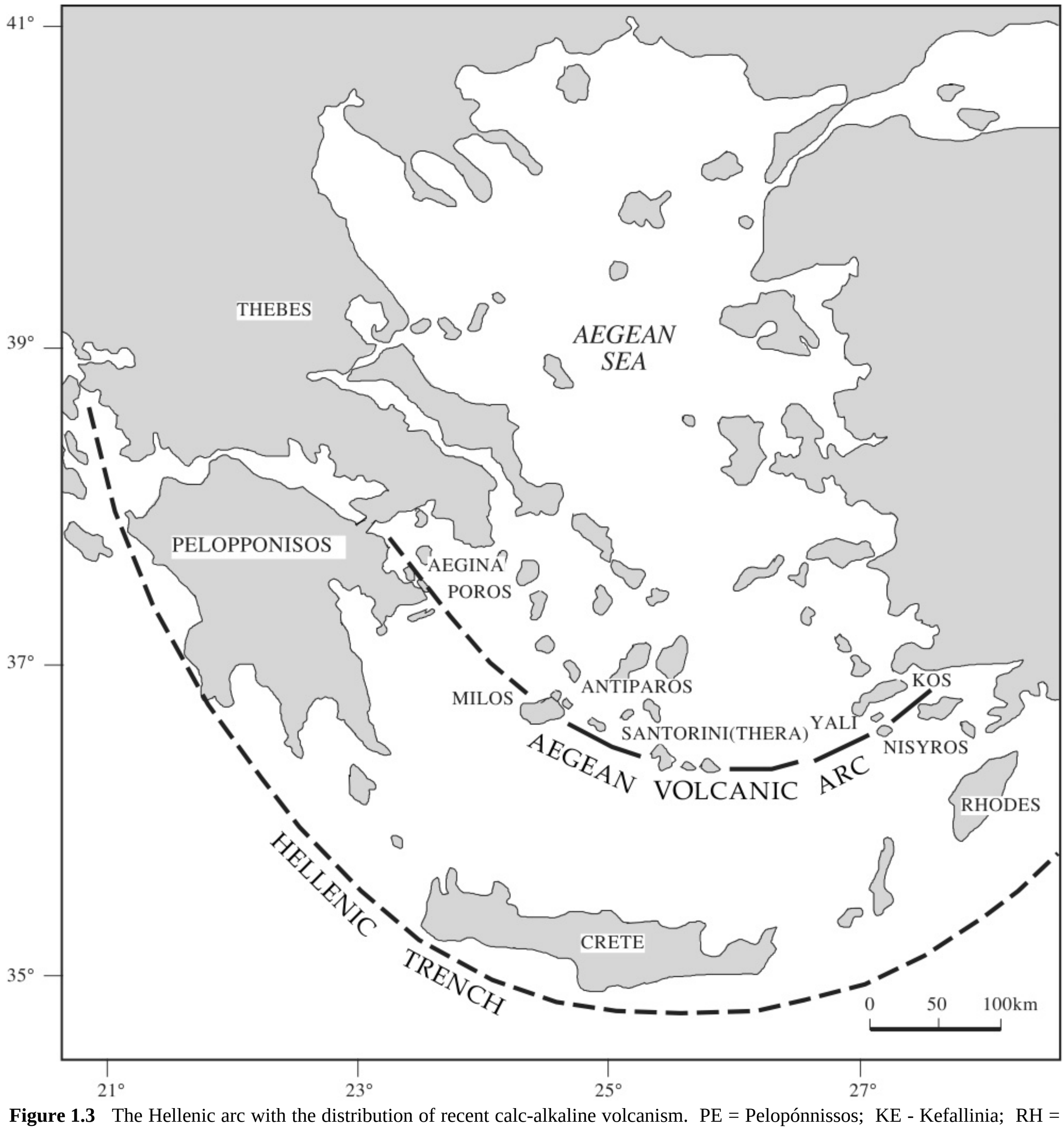


**Figure 1.3** The Hellenic arc with the distribution of recent calc-alkaline volcanism. PE = Pelopónnissos; KE - Kefallinia; RH = Rhodes. (Fytikas et al. 1976)

Boccaletti et al. (1974) and Papazachos & Comninakis (1978) explain them as due a gradual shift of the Benioff zone structure from north to south, or as the result of the breakup of the arc into several pieces along N-S trending faults, due to its sharp curvature (Richter & Strobach 1978).

Leydecker et al. (1978) proved the existence of Benioff zones in part of the area by projecting high precision hypocenter determinations onto several profiles across the Hellenic trench and arc, using seismic data collected between 1971 and 1974. The situation around Crete remains ambiguous, however. The geodynamic context strongly resembles the western Pacific. There is relatively high heat flow in the Aegean area. There is a low velocity of P-waves in the upper Aegean mantle, and a lower than normal density. Observed travel-time residuals are consistent with the model of a dipping Benioff zone. This fits the model of a subducting slab in a marginal sea back arc system, similar to the western Pacific model.

Several authors (e.g., Gass 1972, Schuiling & Kreulen 1973, Makris 1978) suggest that the Aegean is underlain by upwelling hot asthenosphere. The Aegean core complexes (see §2) may thus result from "hot spots" in the continental crust that formed as the result of mantle igneous activity (Lister 1990). Retreat of the flexure of the subducting African lithosphere can explain the anomalous mantle, because "roll back" will encourage asthenospheric flow into the back-arc region. The tectonic position of the Aegean core complexes is therefore compatible with the modern day geodynamic environment.

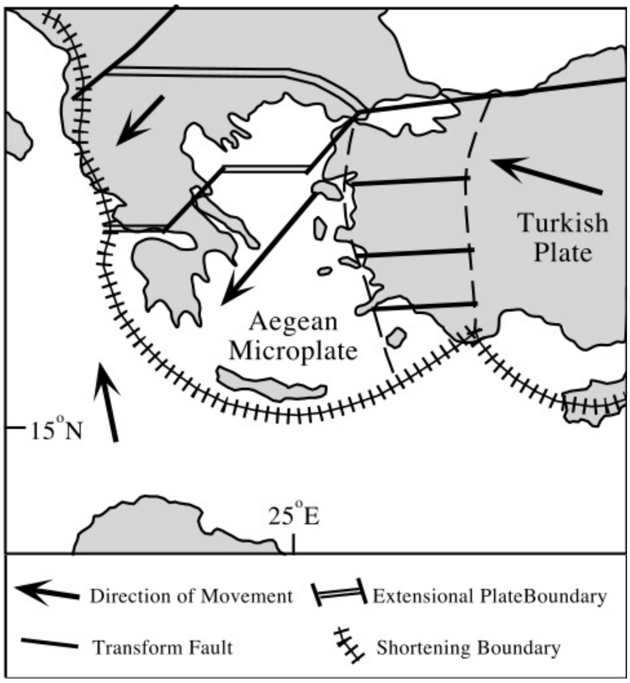


**Figure 1.4** Plate tectonic model in the Aegean area after McKenzie (1972). The arrows indicate the direction of motion relative to Eurasia and the magnitude of the velocity.

# Chapter Two

## The nature and the origin of the Aegean core complexes

*Gordon Lister and Marnie Forster*

### INTRODUCTION

The Aegean metamorphic core complexes were discovered as the result of a thesis study conducted by Greetje Banga (1983), studying at the Institute of Earth Sciences at the University of Utrecht. She sought permission and was granted leave to conduct a minor project in structural geology, in conjunction with her main study in petrology and geochemistry, which involved field work on the island of Ios. She conducted one of the first studies of the fabrics and microstructures of the Cycladic islands, and her work lead to the recognition of the major ductile shear zone that forms the mylonitic carapace of the Ios dome (see Lister et al. 1984).

Banga's thesis provided the basic data that led to the hypothesis that ductile stretching of the Aegean continental crust had taken place during Oligo-Miocene extensional tectonism. Lister et al. (1984) suggested the existence of metamorphic core complexes in the Cyclades that had formed during this period of extension, and compared the Aegean gneiss domes and the core complexes of the Colorado River extensional corridor in the U.S. Cordillera (e.g., see Davis & Lister 1988, Reynolds & Lister 1987).

The occasion of this field trip provides an appropriate moment to review some of the concepts that were developed in this early work, and to provide some context for the contributions that have been made by the different authors for the field guide. New work during the subsequent decade will also be introduced.

Figure 2.1 shows a sketch map of the Cyclades (modified after Altherr et al. 1982) showing the main islands of the Aegean and the structural domains of the west and central Cyclades.

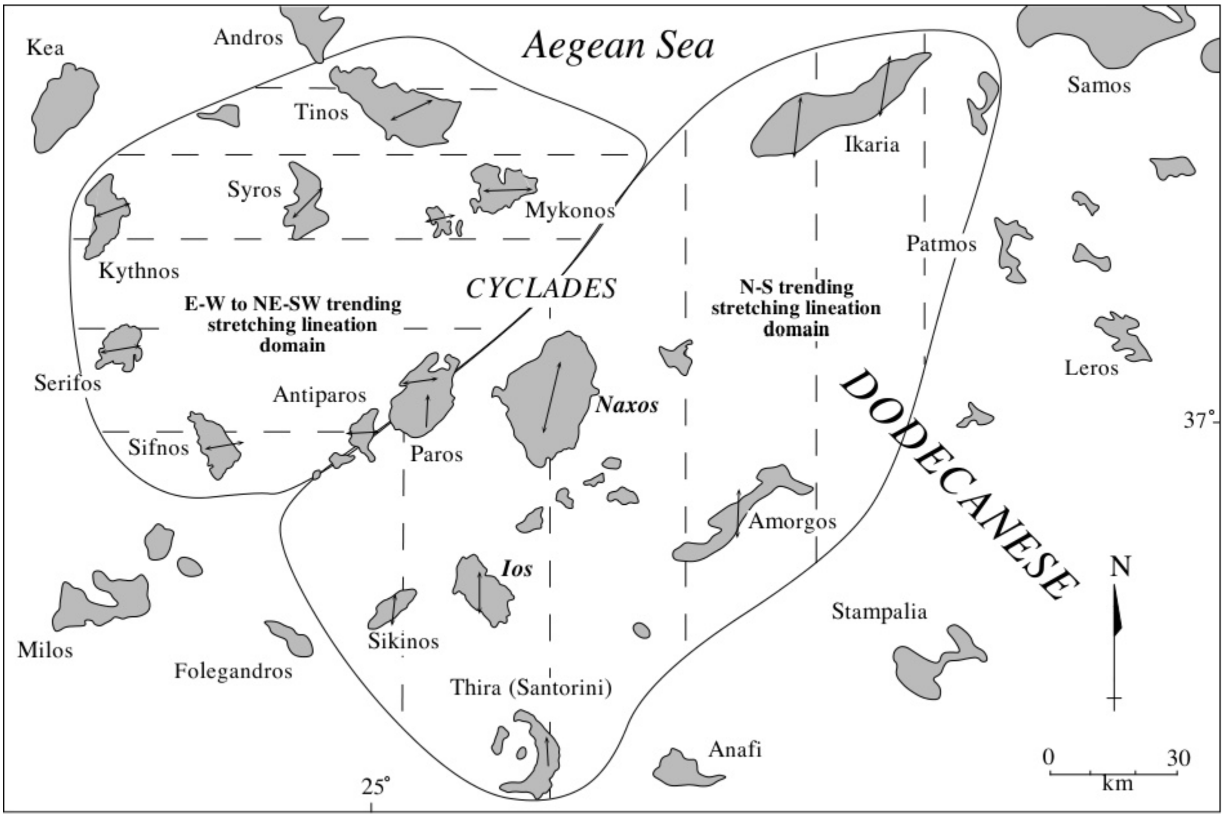


**Figure 2.1** Schematic geological map of the Cyclades, showing the two structural domains, and the islands mentioned in the text (modified from Altherr et al. 1982)

## DETACHMENT FAULTS IN THE AEGEAN CORE COMPLEXES

Structural work (e.g., Lister et al. 1984, Buick 1991a; b, Urai et al. 1990, Gautier et al. 1993, Gautier & Brun 1994, Avigad 1993) has led to the recognition that there are a number of (Miocene ?) low-angle normal faults developed throughout the Aegean region. These may be detachment faults similar to those recorded from the core complexes of the North American Cordillera (e.g., Davis & Lister 1988).

It should be noted, that although there are many points of similarity with the detachment faults of the Colorado River extensional corridor, there are also many points of dissimilarity. To illustrate the point, during this geological excursion we will demonstrate the presence of at least three generations of detachment faults. On Ios each fault system involves a network of anastomosing faults. The fact that there are several generations of detachment faults has not been recognized by previous research.

It is not possible to link up individual exposures of low-angle fault systems without considering the different generations of low-angle normal faults (LANFs). Current practice (e.g., Gautier et al 1993, see Fig. 2.2) is to link up individual exposures of low-angle faults, or suggested low-angle faults, over large distances. The reconstruction shown in Fig. 2.2 links low-angle normal faults on the east coast of Naxos with faults of quite different character in western Naxos, and thence to Paros. There is no data for in excess of 98% of the proposed fault trace, and it is more than likely that more than one fault is involved.

We suggest that in the Aegean, differently oriented detachment systems have operated at different times throughout the extensional history. Unlike the U.S. core complexes, the Aegean core complexes formed in a changing kinematic environment, and there is ample evidence of regionally significant changes in the orientation of stretching axes throughout the geological history (Forster 1996).

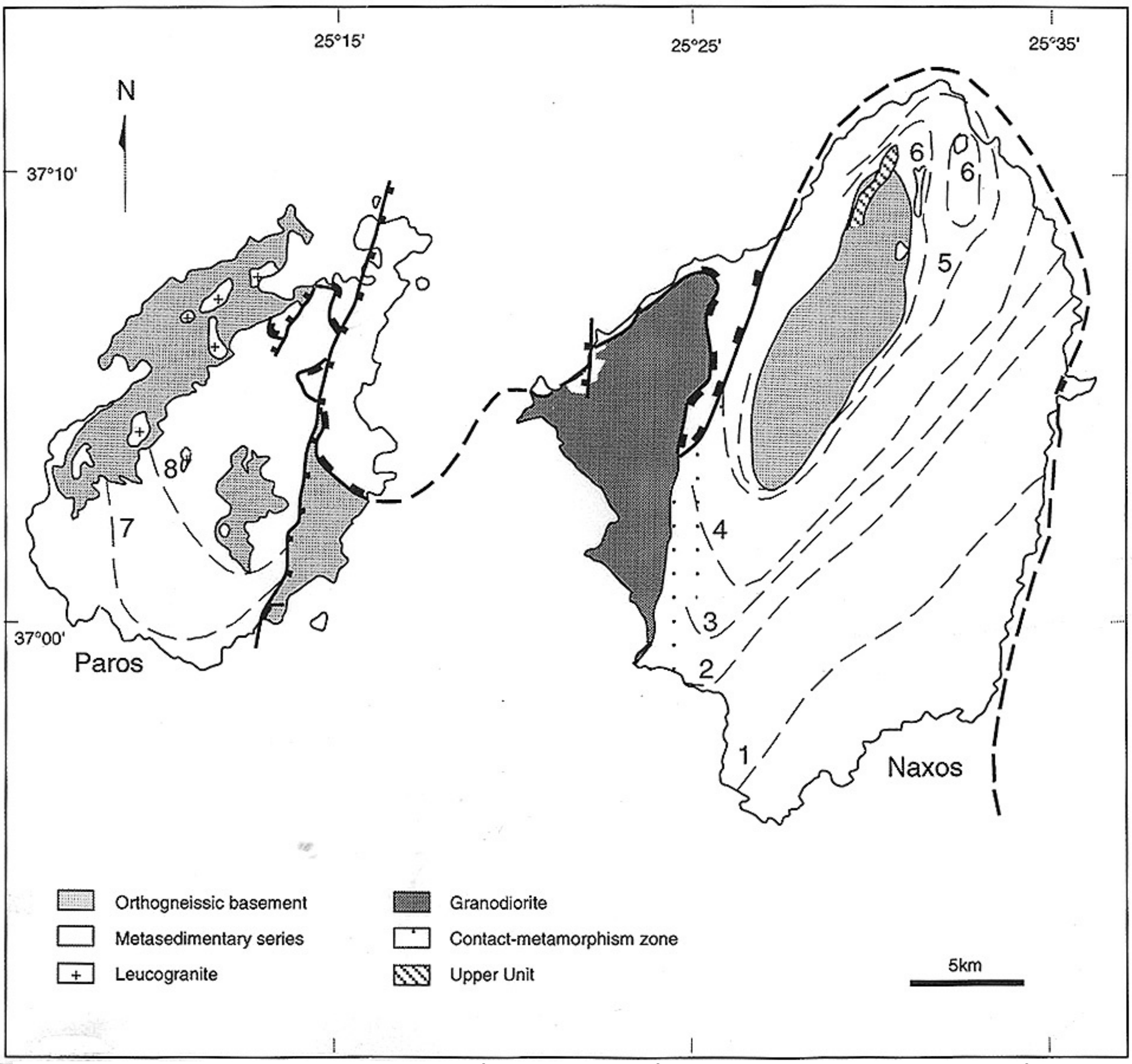


**Figure 2.2** It is not possible to link all exposures of low-angle normal faults into one single detachment system, for example as has been done in this diagram (modified after Gautier et al 1993). Asingle detachment fault surface has been extrapolated over a distance exceeding 100 km, based on a few hundred metres of outcrop.

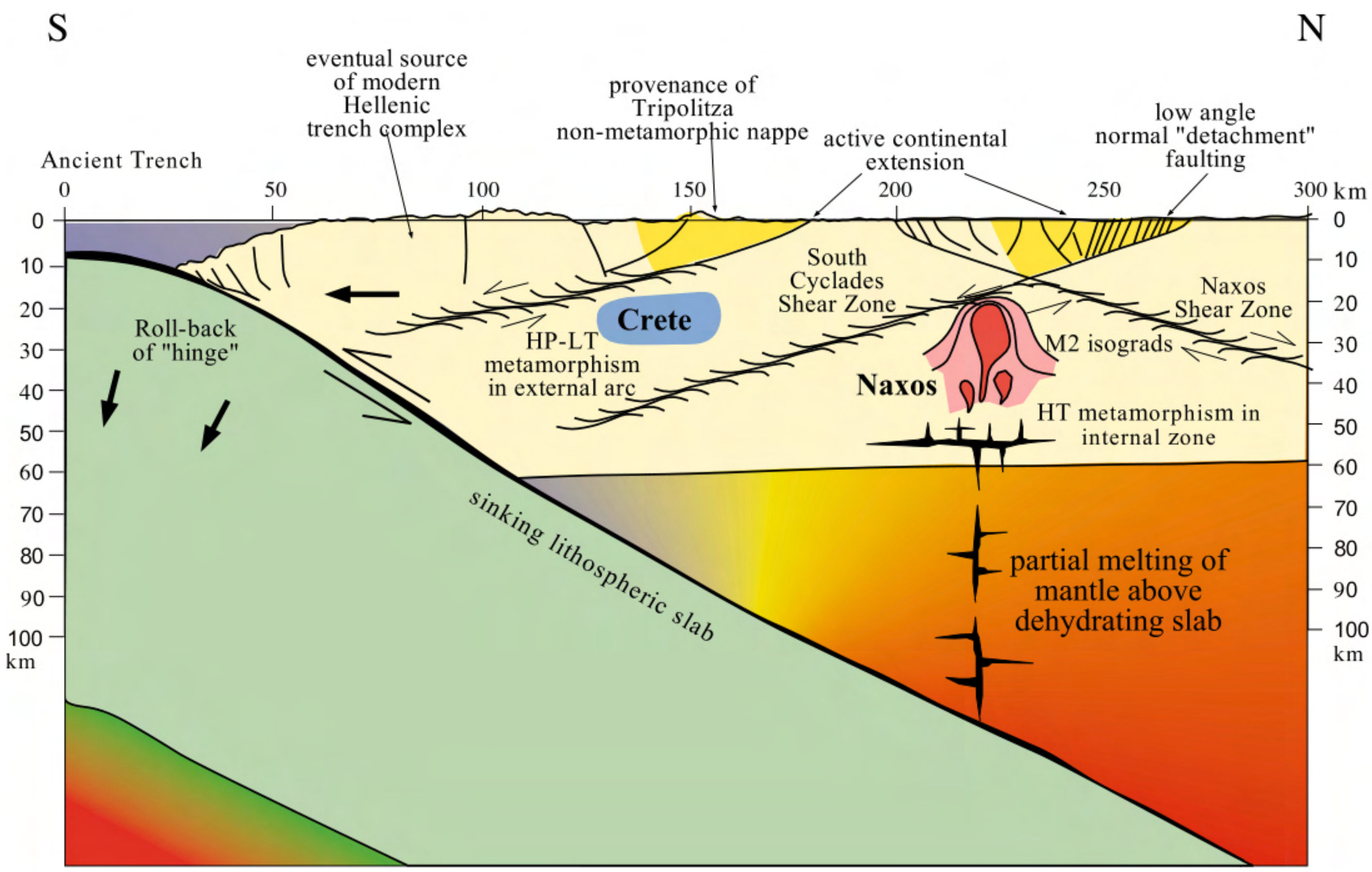


**Figure 2.3** An Oligo-Miocene cross-section through the Hellenic Trench, Sea of Crete and the Cyclades, prior to the tectonic denudation of the Aegean metamorphic core complexes. Note the overthickened continental crust above Crete, subject to Oligocene high pressure metamorphism (Seidel et al. 1982), and above the Cycladic terrane, subject to medium to high pressure high temperature metamorphism (Altherr et al. 1982). This is a classic "paired metamorphic belt" (in the sense of Miyashiro 1973). The proto- North Cycladic and South Cycladic Shear zones are indicated. These will contribute significantly to the exhumation of the Aegean core complexes.

## DUCTILE DEFORMATION DURING MIOCENE EXTENSION OF THE AEGEAN CONTINENTAL CRUST

A number of authors have suggested the existence of Miocene fabrics throughout the Aegean domain (e.g., Lister et al. 1984, Buick 1991a, b, Urai et al. 1990, Gautier et al. 1993, Avigad 1993). It has been suggested that ductile deformation during Oligo-Miocene extensional tectonism produced fabrics (e.g., foliations and lineations) that dominate the geology of the Cycladic islands.

This may be true, but it is easy to label fabrics and/or lineations indiscriminately, either by directly relating them to Eocene "collision", Miocene "extension" or to some (unspecified) "exhumation" process. It is dangerous to assume that the last formed fabric is related to Miocene extension.

For example, Avigad et al. (1988) referred to the last generation (D4) of ductile fabrics on Sifnos as related to Miocene extension. However, there is little evidence that would support a Miocene age for these fabrics. Raouzaios et al. (1996) show that cooling took place during the Oligocene, based on 40Ar/39Ar apparent age spectra and that D4 on Sifnos appears to be associated with large-scale recumbent folding. This suggests that D4 deformation that took place during crustal shortening.

40Ar/39Ar geochronological studies in progress do not necessarily support the assumption that Oligo-Miocene ductile deformation pervasively dominated rock fabrics throughout the Cyclades. There are older fabrics that survive in locations not affected by the late shearing (e.g., in areas of S2 not caught up in D4 shear zones).

Many of the fabrics observed in the Aegean are characterized by depressurization during the period of their formation (and thus these fabrics are sensu stricto produced during exhumation). The same is true for most deformation and metamorphic events throughout the whole of the Alpine chain. Thrusting during compressional orogeny can equally produce such fabrics, as can extensional tectonism during compressional orogeny, as well as the effects of extensional tectonism alone. Each of these scenarios can produce intensely lineated metamorphic tectonites with shallow dipping foliations, and develop during a period of depressurization. The term "exhumation-related" fabric has thus relatively little connotation.

## OPERATION OF MAJOR DUCTILE SHEAR ZONES DURING MIOCENE STRETCHING OF THE AEGEAN CONTINENTAL CRUST

Lister et al. (1984) suggested that a single (south-directed) crustal-scale shear zone operated in the central Cyclades during Oligo-Miocene extension of the Aegean continental crust. This shear zone (named the South Cyclades Shear Zone) was suggested to accomplish exhumation of Barrovian amphibolite to greenschist facies metamorphic rocks, in the lower plates of a sequence of metamorphic core complexes developed in the central Cyclades. We will have first hand opportunity to examine this shear zone during the excursion, and some of its equivalents to the north.

The concept of a single crustal-scale shear zone accomplishing denudation of the Aegean metamorphic core complexes was too simple. In hindsight, the observations made on Ios (Lister et al. 1984) should not have been extrapolated over such a wide area. Research carried out by the Lamont-Doherty excursion to Naxos in 1986, Urai et al. (1986), Buick (1991a, 1991b) and lately Gautier et al (1993) have demonstrated that major north-directed ductile shear zones affected the rocks of Paros, and Naxos, and were associated with the formation of the core complexes recognized on those islands.

The concept of a single crustal scale shear zone that accomplished tectonic denudation of the Aegean core complexes (Lister et al. 1984) has thus been shown to be incorrect. However, the existence of the (south-directed) South Cyclades Shear Zone is not in question. The north-directed shear zones of Naxos and Paros may be complementary ductile shear zones, with the opposite sense-of-shear to the South Cyclades Shear Zone. The relevant question is whether the different shear zones operated simultaneously, or whether they operated in sequence, as the geometry of this complex extensional terrain evolved.

Figure 2.3 & 2.4 illustrate the evolution of a crustal cross-section north-south through the Cyclades, to Crete. It is implied that extension was driven by “roll-back” of the flexure of the subducting African lithosphere, during formation of the Hellenic Arc which palaeomagnetic data (Kissel & Laj 1988) showed was taking place at that time.

## EARLIER PERIODS OF EXTENSIONAL TECTONISM

The blueschist facies rocks that abound throughout the Cyclades were in the upper-plate of the extensional systems at the time of Miocene extension. It is clear as the result of a number of different studies (e.g., Wijbrans & McDougall 1986; 1988, Avigad & Garfunkel 1991) that considerable exhumation of eclogite and/or blueschist facies rocks had already taken place in the Aegean, prior to this period of Miocene extension. This exhumation may also have involved extensional tectonism, but at an earlier stage of the Alpine orogenic history.

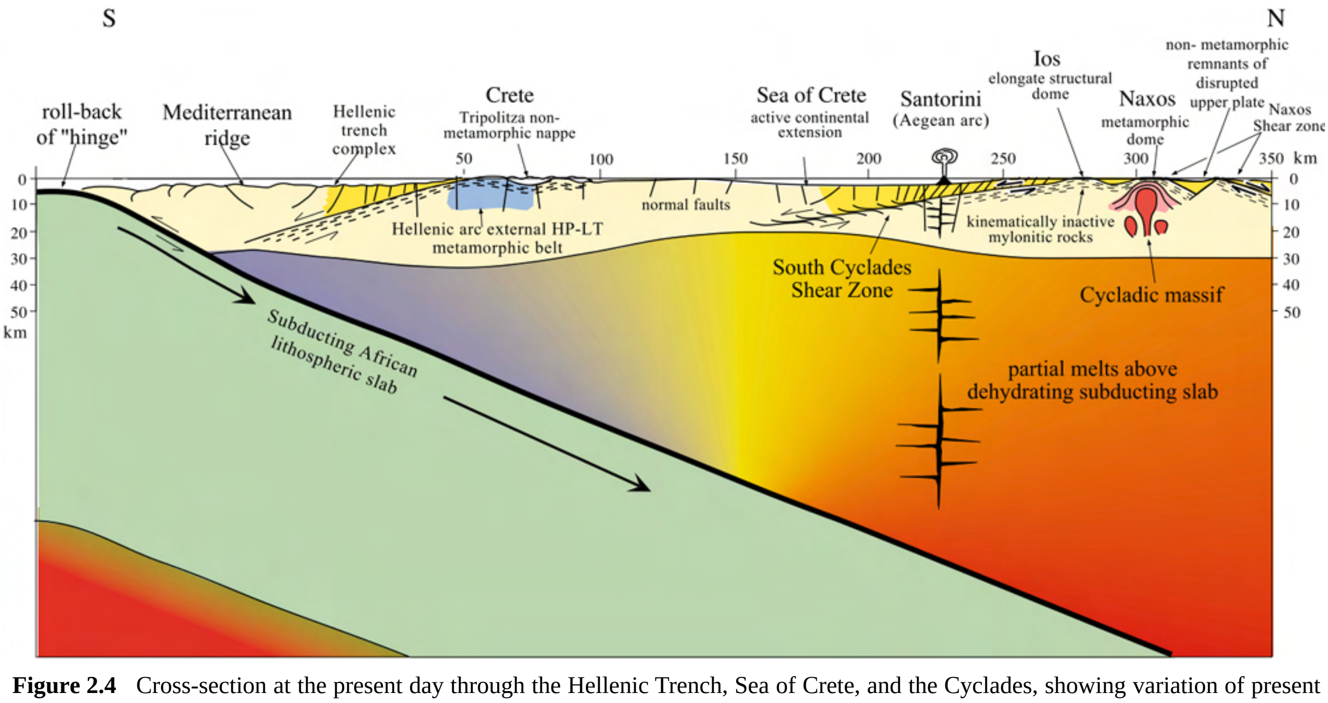


**Figure 2.4** Cross-section at the present day through the Hellenic Trench, Sea of Crete, and the Cyclades, showing variation of present day crustal thickness, and the geometry of the North and South Cyclades Shear Zones and associated detachment faults. This interpretation of the large scale geodynamics assumes that “roll back” of the flexure of the subducting African slab has driven extensional tectonism. The Mediterranean Ridge is the result of the tectonic denudation of medium pressure metamorphic rocks exposed in western Crete. The Aegean metamorphic core complexes result because tectonic denudation has resulted from the combination of the operation of crustal scale extensional shear zones and detachment faults.

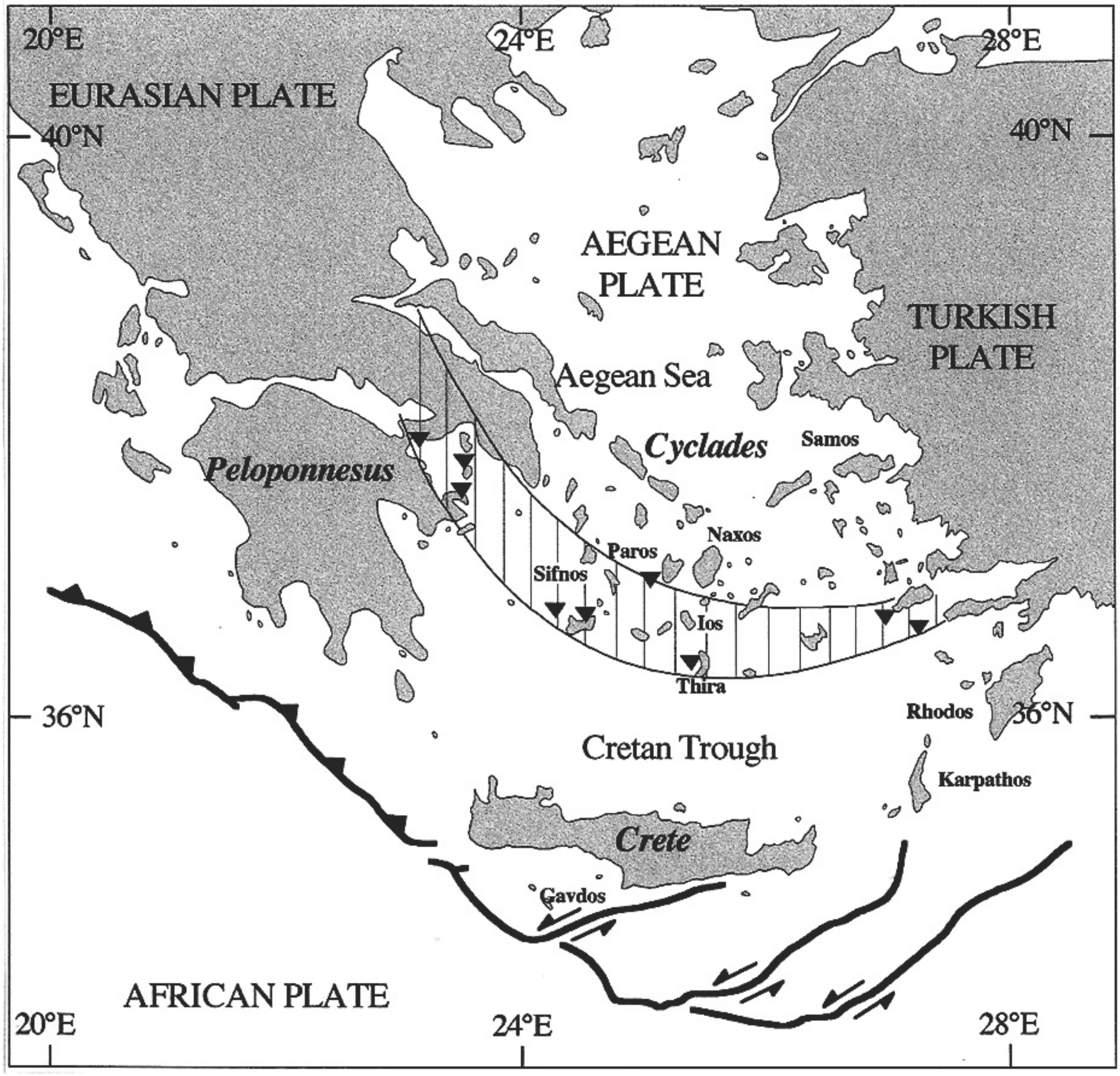


**Figure 2.5** The Aegean Plate, showing some of the major geological features of the Aegean Plate.

## MAGMATISM AND THE AEGEAN CORE COMPLEXES

Lister et al. (1984) also made specific predictions in relation to the timing of the regional Barrovian overprint of the high pressure (blueschist facies) metamorphic assemblages. It was suggested that this metamorphic event heralded the onset of extensional tectonism in the Aegean, after a long period of collisional orogeny.

Again this was too simple a concept. It is now clear that there are several different episodes of metamorphic mineral growth, both during the period of high pressure metamorphism (M1) and during the period of Barrovian facies metamorphism (M2). Because the distinction between these many different growth episodes has not been made, various authors have attributed Oligo-Miocene greenschist facies metamorphism, recognized throughout the Aegean, to a single event, rather than to a multitude of events with markedly different timing.

It is important to make the distinction. Greenschist facies events include: (a) a transitional blueschist-greenschist facies paragenesis on Sifnos (somewhere in the period ~30-40 Ma) (Lister & Razouzaios 1996); (b) high temperature medium pressure greenschist facies to amphibolite facies metamorphism on Naxos and Ios (somewhere between ~ 15-20 Ma); and (c) younger thermal pulses perhaps associated with granitoid intrusion (at ~12-14 Ma), which also cause greenschist to amphibolite (?) facies metamorphism. These latter results come from Sue Keay (pers. comm.), with her work dating zircons in the Aegean core complexes, Raouzaios & Lister (1993) for Sifnos, and Suzanne Baldwin, with her work on 40Ar/39Ar geochronology of the Aegean core complexes (Baldwin & Lister, in preparation).

Baldwin & Lister (in prep.) propose that the relatively cool lower plate of the Ios core complex records a history of Hercynian magmatism and metamorphism followed by intense deformation during the Alpine high pressure event.

The protolith of the central granite gneiss terrane on Ios consisted of a complex of igneous and metamorphic rocks that occupied a shallow crustal setting, with low ambient temperatures. They were subjected to the alpine orogeny, but temperatures remained low. During the Miocene the temperature briefly rose, and the entire complex was stretched in a (D4) Miocene ductile shear zone.

To explain markedly different argon release spectra have been obtained from adjacent samples it is necessary to postulate that the Miocene thermal pulses were short-lived, and that a period of very rapid deformation ensued thereafter. Plastic strain taking place during such thermal pulses may involve times frames possibly as short as 10,000 - 100,000 Yr. Yet large strains accumulated in these major ductile shear zones during the Miocene D4 event. Therefore strain rates must have been very rapid (in the order of 10-9 - 10-11 s-1 while strains involving as much as 70-80% shortening took place). Rapid cooling continued after the Miocene thermal pulse because the core complexes were unroofed due to ongoing extension.

The Baldwin & Lister (in prep.) study leads to a radically different vision of how crustal scale ductile shear zones interact with rising batholiths in extensional terranes. Rather than the slow and steady operation of a ductile shear zone over the 2-3 MYr that it takes to form a metamorphic core complex, we infer intermittent and very rapid shear events during and after batholith intrusion.

## THE NATURE AND ORIGIN OF DETACHMENT FAULTS IN THE AEGEAN CORE COMPLEXES

The planar almost polished top surface of the microbreccia ledge is a remarkable feature of core complexes in the Colorado River extensional corridor. Similar planar features are observed in the Aegean “detachment faults”, but these are not associated with microbreccia, or ultracataclasite. This is just one of the major distinctions to be made between the detachment faults of the Aegean core complexes and those in the core complexes of the Colorado River extensional corridor.

In the zone beneath the microbreccia ledge, in the U.S. core complexes there is a well developed zone of brecciation associated with chloritic alteration. These rocks are altered variants of the gneisses that underlie the zone of “chlorite breccia”. The Aegean core complexes are quite distinct in how the zone of rock beneath the “detachments” is affected by fault movement. The situation is highly variable. Some Aegean low-angle faults develop similar zones of chloritic alteration, but this is not a characteristic feature of their formation (Forster 1996).

The mylonites and mylonitic gneisses that lie at the lowest structural levels of the core complexes in the Colorado River extensional corridor are a deformed Precambrian gneiss protolith intruded by meta-igneous rocks of different ages. In the Nevadan core complexes Palaeozoic metasediments are involved, and Miocene magmatic complexes.

The Aegean core complexes differ substantially in that there is not a well defined upper- and a lower-plate. Instead several generations of detachment faults appear to have sliced through a sequence of thrust nappes, and extension has resulted in a number of different tectonic slices, each recording a variant of the metamorphic history to which the Aegean has been subjected (Forster 1996, Forster & Lister 1996a & b).

The rocks have been dragged to the surface from their position deep within the roots of an ancient mountain belt, travelling distances perhaps exceeding 50-80 km. It is our belief that by carefully unravelling the geology, we will learn considerably more about the processes that lead to the collapse and the destruction of orogenic welts.

## TRAVERSES THROUGH THE AEGEAN CORE COMPLEXES

To illustrate the various features of the Aegean core complexes, this field guide will describe a sequence of different traverses through different parts of different islands. This will enable points of similarity and points of dissimilarity to be adequately discerned.

The excursion will begin on the island of Thera, which to all extents and purposes appears to have been a “core complex” before it became a “volcano”. We will examine the “basement” rocks to the modern volcanic eruptions, and the participants will note that the rocks are similar in all aspects to those that they will visit on the immediately adjacent Aegean metamorphic core complex of Ios.

The Ios core complex has been intensively examined, but there is still much that has to be learned. The excursion will begin in the “basement” complex in the lower plate, and examine the rocks caught up in the South Cyclades Shear Zone. The chosen traverses will include visits to different localities where the different generations of “detachment faults” can be observed on Ios. Finally we will examine the high pressure metamorphism in the upper plate, so that we can compare and contrast the behaviour of the upper and lower plate of the Ios core complex.

The excursion will then move to the island of Naxos, where we can examine the opposite sense shear zones, and isolated outcrops of a few of the LANFs that have been discovered on this island. We will examine one of the “detachment” faults that juxtapose non-metamorphic rocks in the upper plate against highly deformed metamorphic rocks in the lower plate, and observe the enigmatic planar faults that slice through the basement rocks without heed or hindrance, unaffected by the orientation of the phyllitic schistosity though which they travel.

We will also examine the Barrovian facies high grade migmatitic core of the Naxos gneiss dome, and elucidate some of its complex structural and metamorphic history.

The excursion will finally end on the island of Paros, where we will examine a traverse through a major shear zone, which terminates at a major detachment fault. The detachment faults separates the strongly deformed Mesozoic marble sequence from the extremely mylonitized granitic rocks of the Hercynian "basement".

## RECOMMENDED FIELD GEAR

It is likely that you will be separated from your baggage during the excursion, except in the evenings. Ensure that you bring a day pack for your camera, water bottle, and jacket. You will probably also need a windproof jacket and warm clothes, as it can get cold and windy.

Be sure to bring strong walking boots, and a good hat. Sunglasses help on those days when the glare from the sea is strong. Sunscreen is essential, even late in the season.

There are snakes on these islands and spiders. These normally do not pose a problem, but field trip participants should exert due care.

In terms of other safety aspects, the only other point to make is that cliffs can crumble, and on hot days an adequate supply of water is essential.

View of the Naxos detachment at sunset, looking NorthWest. The island of Paros can be seen in the background, where another (older) detachment fault juxtaposes marble against marble against underlying Hercynian and Miocene granite schists.

Ios town is built around the southern side of a granite knoll. Sikinos can be seen in the background. The knoll is a boudin of Hercynian granite in the South Cyclades Shear Zone.

# Chapter Three

## Thera - the core complex that became a Volcano

*Leah Moore, Gordon Lister and Sue Keay*

### INTRODUCTION

In the Late Bronze Age, a paroxysmal eruption took place on Santorini volcano, referred to as the Minoan eruption (after the Minoan civilisation which inhabited the island at that time). The eruption produced a great volume of pumice and ash and almost certainly had a catastrophic effect on the people living in the southern Aegean at that time. The Minoan eruption resulted in the formation of the present day caldera, which measures 11.5x8 km2. There is still controversy concerning the exact date of the eruption, which is largely based on archaeological finds at the buried town of Akrotiri on Santorini.

Santorini is a group of islands lying 120 km north of Crete at the southern end of the Cycladic Group. It is the only volcano in the eastern Mediterranean to have been copiously active in historic times. The islands of Palaeo Kameni and Nea Kameni in the middle of the caldera have been constructed by post Minoan eruptions in 197 BC, AD (19?), 46, 726, 1570, 1707-1711, 1866-70, 1925-6, 1928, 1939-41 and 1950 (Georgalas 1962). These have largely been small, gas-poor eruptions characterised by weak volcanic explosions and the effusion of blocky lava flows. The eruption of 726 AD, however, produced considerable pumice.

The volcano is built up on a basement of Triassic limestones, forming the hills of Monte Elias and Platinamos, and Mesozoic schists near the port of Athinion (Pichler & Kussmaul 1972). Previous workers recognise several phases of activity at different centres in the construction of the volcano, beginning with the old and substantially altered Akrotiri group in the south.

Before the Minoan eruption there was probably only one island, known as Strongyli (Pichler & Kussmaul 1972). This had a steep sided central cone which, judging from the present profile of the volcano, rose to between 500 and 800 m above sea level. Repeated eruptions of blocky lavas similar to the historic lavas of Nea Kameni have infilled an old caldera in the NE of the island, a cross section of which is preserved in the caldera walls between Thera and Oia. To the south lay a low sloping plain formed by the pyroclastic accumulations from many prehistoric eruptions.

The Minoan eruption produced a thick, continuous layer of white pumice and ash that now covers the remnants of the volcano like icing on a cake. The products of the eruption were a Plinian pumice fall deposit succeeded by fine ash fall and base surge deposits, ignimbrite, mud-flows and mud-flow deposits.

### THE HISTORY OF THERA

Thera (Santorini) (population ~8000) has been known by many different names: Strongyli (round), Kalliste (most beautiful) and finally Thera (after a Greek hero). To tourists the island will always be known as Santorini, a name established by foreign sailors in the area, derived from the church of the island Agia Irini (St Irene).

Before the Minoan eruption, the original volcanic island was 600-1000m high. The island was inhabited from Neolithic times. After the eruption, the central portion of the island collapsed, forming one of the largest calderas in the world. This was subsequently flooded. Like Krakatoa, only the rims of the caldera remain. These were once the sides of the immense volcano. Now they form the islands of Thera, Therasia and Aspronisi.

After the eruption and the subsequent destruction of the Minoan civilisation, the island was eventually re-inhabited by Phoenicians (1200 BC) and then Dorians (1000 BC). The downfall of the Minoan civilisation was, for many years, the subject of intense speculation by archaeologists. Evidence from Crete suggested that the downfall had been very rapid but there was no evidence to indicate that an invading army had conquered the powerful Minoans, or that the people had been extinguished by plague or pestilence.

Excavations on Crete have revealed that many of the Minoan buildings have disrupted foundations, originally thought to have been caused by a major earthquake. The first person attributed with relating the destruction of the Minoan civilisation with the catastrophic eruption of Thera was Professor Spyros Marinatos in the 1930s. Evidence supporting this theory came to light with his discovery of the buried city of Akrotiri on Thera, a city preserved, Pompeii-like, in the ashes of the eruption.

Akrotiri was a Minoan settlement rich in decorative frescoes and decorated pottery. It is thought to have been abandoned before the eruption as no bodies have been found and it appears that all valuables were removed. Excavations begun in 1967 by Marinatos revealed the best-preserved settlement of the Bronze Age with intact walls and ceilings. Due to the friable nature of the supporting ash however, the structures are not well supported and Marinatos was killed by a collapsing wall during excavations.

It has been speculated that the eruption of Strongyli was at least twice as powerful as that of Krakatoa and generated a tsunami initially over 200 metres high. There is a wide extent of ejecta that can be related to this eruption.

Many believe that the Minoan civilisation based on Crete was literally washed away. This idea has also led to the resurgence of the myth of Atlantis, with several archaeologists suggesting that two of Atlantis's fabled major cities, Metropolis and Vasiliki Politeia (King's city) were based on Strongyli and Crete respectively and destroyed by the volcanic eruption when most of Strongyli did in fact sink beneath the sea.

## EVOLUTION OF THE SANTORINI VOLCANIC CENTRE

The Santorini Volcanic Centre is part of the Aegean island arc which is an arcuate chain of a dozen inactive or dormant volcanoes, 500 km long and 20-40 km wide, extending from the middle of the eastern coast of mainland Greece, through the central Aegean, to the western coast of Turkey (Fytikas et al. 1976, Ninkovich & Hays 1972). The Aegean Arc is the site of extensive Quaternary volcanism (Keller et al. 1990). The age of Aegean volcanism has been reviewed by Ferrara et al. (1980), Innocenti et al. (1981), Fytikas et al. (1984), and Keller (1982). Additional data have been contributed by Fytikas et al. (1986), Rehren (1988), and Keller et al. (1989).

The correspondence of the active volcanic arc with a Benioff zone depth of about 130 km is evidence of a role for subduction in the genesis of the arc (Gill 1981, Spiegelman & McKenzie 1987). The volcanism is voluminous, with individual centres having volumes above sea-level of the order of 10-30 km 3.

The geochemical character of the volcanic rocks of the South Aegean arc is typical of subduction-zone volcanoes, with a range of products varying from basaltic andesite through dacite to rhyolite (Mitropoulos et al. 1987). The greater abundance of basalt and andesite at Santorini, with asthenospheric isotopic characteristics (Gulen 1989), has been related by Mitropoulos & Tarney (1992) to a greater amount of lithospheric extension in the central part of the arc, leading to upwelling of fertile asthenosphere.

Volcanic activity of the Hellenic Arc started about 3-4 Ma. The main centres of explosive eruptions are located on Milos, Santorini, Kos, Nisyros and Yali. Explosive volcanism was particularly intense in the Upper Quaternary on Santorini, Kos and Nisyros. The Minoan eruption of Santorini is the most recent and one of the most powerful manifestation of this activity.

## VOLCANISM ON THERA

Thera has been the subject of intense geological study for over 100 years. Vent locations and caldera shapes are strongly controlled by regional structure, along a graben in an extensional environment, normal to the volcanic arc. The volcanic field contains multiple, overlapping calderas, consisting of flooded craters. There have been as many as four caldera-forming eruptions.

Volcanism at Santorini was focussed on a deep NE-SW basement fracture which has acted as a pathway for magma ascent. At least four major explosive eruptions began at a vent complex on this fracture. Composite volcanoes constructed north of the fracture were dissected by at least three caldera-collapse events associated with the pyroclastic eruptions. Southern Santorini consists of pyroclastic ejecta draped over a pre-volcanic island and a ridge of early to mid-Pleistocene volcanics. The southern half of the present day caldera basin is a long-lived essentially non-volcanic depression defined by topographic highs to the south and east, but deepened by subsidence associated with the main northern caldera complex, and is thus probably not a separate caldera.

The volcanic history of Santorini shows twelve major explosive cycles during the last 200,000 years. A similar frequency of explosive volcanism over approximately the same time span characterises the volcanic history of the eastern sector of the Hellenic arc, where Kos, Nisyros and Yali are prominent centres of important eruptions.

Kalogeropoulos & Paritsis (1990) indicate that Santorini is a group of five islands: Thera, Therasia, Aspronisi, Palaea Kameni and Nea Kameni, with an areal extent of 75 km2. The first three islands are arranged in a semicircle and define a caldera 8x5 km2 across. The flooded caldera reaches a depth of 370 m with Palaea Kameni and Nea Kameni islands rising at its centre. In the past ~3 Ma intermittent volcanic activity took place on Santorini, with several volcanoes active, operating successively or concurrently. At present volcanic activity is restricted to the Kameni islands with all the older volcanoes now extinct.

The older larger volume pyroclastic deposits at Thera range in age from 1.0 - 0.1 Ma. Post-caldera eruptive activity occurred along fissures located along overlapping caldera basins. Heiken & McCoy (1984) demonstrated that the Santorini caldera depression is a multiple structure formed by several collapse events. Druitt et al. (1989) have documented 12 major pyroclastic deposits of the caldera wall, each representing an eruption with volumes in excess of 1 km3, several of which should have produced a caldera collapse.

At least two earlier calderas are evident from unconformities and lava fill sequences in the caldera wall (Heiken & McCoy 1984, Druitt et al. 1989). Heiken & McCoy (1984) proposed that the Minoan collapse was confined to the northern depression and involved about 19 km3 of collapse.

Friedrich et al. (1988) and Eriksen et al. (1990) have recently documented compelling evidence for a pre-Minoan caldera in the north. They describe stromatolite clasts in Phase 3 Minoan deposits in northern Thera and Therasia with ages of ~0.17 Ma. The observations demonstrate that a substantial caldera depression already existed prior to the Minoan eruption, perhaps related to the 0.185 Ma Cape Riva event (Druitt 1985). For more information please read Keller et al. (1990), Druit et al. (1989), Bond & Sparks (1976), Heiken & McCoy (1990), Kalogeropoulos & Paritsis (1990).

Recent estimates for the timing of the Minoan eruption are C14 ages of 1615±17 BC based on carbonised wood (Hammer et al. 1987), and correlations with western USA tree ring dates which show a frost effect in 1626±2 Yr BC. These have been correlated with global climatic effects caused by the eruption. Narrow tree rings occur in Irish Oak trees from 1626-1628 BC (Baillie & Munro 1988), which may be related to global climatic change caused by the eruption.

The oldest radiometric ages obtained from Santorini are 1.59-0.63 Ma, in the Akrotiri volcanoes from which K/Ar dates have been obtained (Ferrara et al. 1980). Most of the volume of exposed volcanics has been erupted during the last 200,000 years, however.

## CALDERA FORMATION AND PHYSIOGRAPHY OF THE THERA IN THE LATE BRONZE AGE.

The Minoan eruption of Santorini discharged about 30 km3 of rhyodacitic magma, distributed ash over a large area of the eastern Mediterranean and Turkey and caused caldera collapse (Bond & Sparks 1976, Heiken & McCoy 1984, Watkins et al. 1978, Sullivan 1988, Sparks & Wilson 1990, Pyle 1990). The ejecta buried a major Bronze Age settlement at Akrotiri (Doumas 1983); the effects of tsunamis and ash fallout were probably felt on Crete, 120 km to the south.

Druitt & Francaviglia (1990) indicate that the present caldera is a composite structure, formed over the last 100 ka. Geomorphological mapping shows that the present day caldera wall is a complex assemblage of cliff surfaces of different ages, and that cliff collapse has repeatedly exhumed earlier caldera cliffs and unconformities. Cliffs bounding the southern, southeastern and northwestern rims of the caldera are morphologically fresh and probably formed during or soon after the Minoan eruption in the late Bronze Age. The well-scalloped shape of these cliffs is attributed to large-scale rotational landslip around the margins of the Minoan caldera. The deposit from one landslip is preserved subaerially.

Minoan landslips in southeast Santorini detached along the basement unconformity, exposing a cliff present in the prevolcanic island. The caldera wall in the north, northeast and east preserves evidence for three generations of cliff: those of Minoan age and two earlier generations of caldera wall. The two earlier calderas can be dated relative to a well established stratigraphy of lavas and tuffs. The presence of in situ Minoan tephra plastered onto the present day caldera wall provides evidence that these ancient caldera cliffs had already been exhumed prior to the Minoan eruption.

Field relationships permit reconstruction of the physiography of Bronze Age Santorini immediately before the Minoan eruption. Bronze Age Santorini had a large flooded caldera, formed 21 ka ago. This caldera acted as an excellent harbour for the inhabitants of the island. The 3.6 ka Minoan eruption deepened and widened the extant caldera. The volume of Minoan collapse (~25 km3) is in good agreement with published estimates for the volume of discharged magma of between 5 and 8 km3 of Minoan ignimbrite ponded as intracaldera tuff.

## NATURE OF THE DEPOSITS

The Minoan eruption of Santorini produced the following sequence of deposits: a Plinian pumice fall deposit, interbedded Surtseyan-type ash fall and base surge deposits, mud flow deposits and ignimbrite interbedded with very coarse, well-sorted flood deposits. The variation of thickness and grain size in the Plinian deposit indicates a vent 1 km west of Thera town. The base surges and Surteseyan-type activity is interpreted as the result of seawater entering the magma chamber.

The poorly sorted mudflow deposits and ignimbrite are distinguished on their grain size, and morphology. There must have been substantial rheological differences in the mass flows which produced them. Grain size analyses show wide ranges in the lithic contents of the different types of deposit: ignimbrite (35-60%), mud-flows (20-30%) and the pyroclastic fall and surge deposits (4-15%). The ignimbrite is enriched in crystals, in contrast to the in fine airfall ash beds that interstratify with the ignimbrite. The gas velocity of Plinian phase is estimated as 550 m/s, the eruption column height was greater than 20 km. Only particles of <2 mm could have reached Minoan Crete.

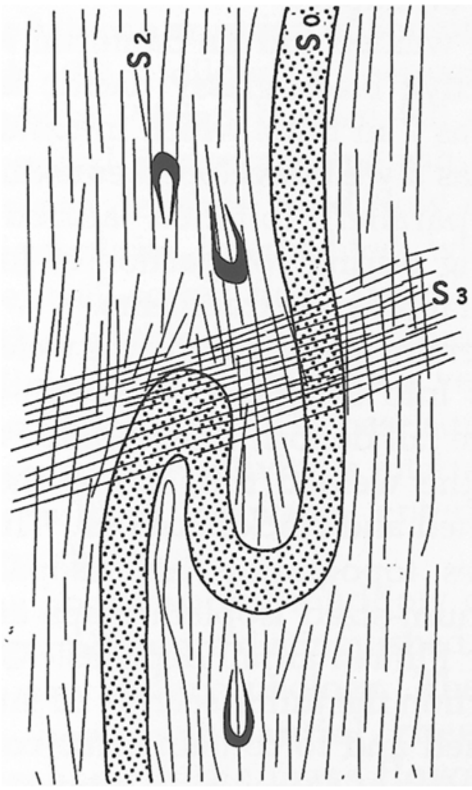


**Figure 3.1** Overprinting relations of the foliation $S_2$ by a crenulation cleavage $S_3$. The asymmetric $F_2$ fold shown has a storngly developed axial planar cleavage, including rootless isoclinal fold hooks

## Welded airfall tuffs

Welded tuffs are common in the geological record and are generally called ignimbrites or ash flow tuffs, implying deposition from a pyroclastic flow. However, welded tuffs produced by airfall are a common volcanic product, and are known to occur on several modern, and many ancient volcanoes. One of the best documented examples is from Santorini volcano.

These tuffs can be distinguished from welded rocks formed from pyroclastic flows by their geometric form, textures and field relations to non-welded counterparts. Their features indicate post-emplacement compaction and welding over a wide area, and cannot simply be ascribed to the agglutination of spatter lumps on impact.

The welded tuff on Santorini forms a distinctive black glassy dacitic layer as much as 7 m thick which in hand specimen has a well developed eutaxitic (bedding parallel) foliation attributed to welding during compaction of formerly vesicular juvenile fragments.

Laterally and vertically the welded tuff passes into a thick, coarse, non-welded pumice fall deposit (the Middle Pumice). Near the welded tuff, this is thermally darkened and black in colour. This layer mantles topography, and isopach and maximum-sized isopleth maps are typical for Plinian airfall deposits. On close inspection the tuff is seen to be internally stratified and to contain some conspicuous layers of coarse pink pumice. Many of these layers are not laterally continuous, and they are thought to have formed by the rapid local accumulation of large pumice bombs.

## THE CORE COMPLEX THAT BECAME A VOLCANO

It is difficult not to conclude that Thera was a core complex before it became a volcano. The Aegean metamorphic core complexes of Ios and Naxos lie immediately to the north, and Ios is immediately adjacent. As is the case in the Colorado River extensional corridor, there is a zone of core complexes in the central Cyclades. The “basement” rocks on Thera are very similar (if not identical) to the rocks in the adjacent core complexes. Therefore, although no direct proof can be offered, we suggest that Thera, like the adjacent core complexes of Ios and Naxos, was once a mountainous schist and gneiss dome, mantled by low-angle normal faults. If we extrapolate data obtained from the adjacent islands, then ~7 MYr after its exposure (by a combination of tectonic and erosional processes) the island was partially annihilated by the sequence of volcanic eruptions described above.

The excursion will commence at the cliff wall in the main township, above the cliff path leading to the old harbour. Descend to the old harbour, and then take a boat to Nea Kameni, examine the recent lava flows, the various active fumaroles, swim in the sulphur springs, and then return to the boat to traverse the caldera wall between the old harbour, and the new harbour of Athinios. Spectacular geology is exposed in the caldera wall along this traverse, including several very graphic exposures of dykes. These will provide text book quality photographs for the able photographer.

Land at the new port of Athinios, and examine basement rocks exposed in the caldera wall on the ascent from Athinios (the new port of Thera). Take extreme care to avoid traffic during the climb to the top of the caldera. With some careful planning ahead of time it is possible to catch a bus to Akrotiri, and then to follow a normal tour through through this spectacular example of a civilisation that “existed with geological consent, subject to change without notice”.

## BASEMENT ROCKS OF THE CALDERA WALL

We will encounter a variety of strongly deformed rocks, and a number of low-angle faults associated with phyllonite zones. There are calcareous conglomerates, chlorite schists, calcareous schists, quartzitic phyllites, and coarse veins.

The dominant fabric is a differentiated crenulation cleavage. As elsewhere in the Aegean, this is a pervasively developed fabric, much modified by later deformation and metamorphism. It is difficult to time the development of this fabric in relation to metamorphism on Thera, because only the latter part of the history seems to have been preserved. The schists are highly deformed, with significant reorientation of all previously formed fabric elements. A stretching lineation has developed with ~N-S trends, and earlier formed lineations and fold axes have been reoriented parallel to this trend.

This traverse begins at the new port of Athinios. The dominant schistosity (S2) can be recognized as a strongly differentiated crenulation cleavage. With a pocket microscope or a good hand lens, it is possible to distinguish well developed spaced cleavage, and occasionally the remnants of earlier fabrics within the microlithons. Occasional overprinting relationships can be distinguished (see Fig. 3.1), where F2 folds are overprinted and/or refolded by later fabrics. As shown in Fig. 3.1, the axial zones of F2 folds are occasionally associated with isoclinally folded elongate quartz lenses. These may have formed during D1, parallel to the earlier fabric S1, and then later they were isoclinally folded during the development of S2.

The dominant fabric (S2) is itself folded, and at least two different styles of refolding can be observed. In the one case there are well-developed axial plane fabrics. These have partially differentiated, and vary from a poorly to well-developed differentiated crenulation cleavage. Near the port itself there are intensely deformed calcareous conglomerates. The stretching direction is ~N-S.

Phyllonites abound, providing evidence of late-stage shearing. The asymmetry of tension gashes suggest some south-directed movement. The calcareous pebbles are highly stretched, with aspect ratios as high as 8:1 in the XY plane. A well-developed crenulation lineation is parallel to the stretching direction.

Some low-angle faults injected by recent dykes may have been related to caldera formation. There are zones of intensely developed phyllonitic fabrics, associated with low-angle faults. These fabrics have formed in late shear zones that shredded the earlier fabrics. In these zones there are also many younger folds. These are not associated with the development of (new) axial planar fabrics. Typically they have box-like or chevron-fold geometries. The zones of phyllonite may be 1-3 m thick. There are also several strongly deformed marble bands. These are planar, with well-developed ribbing lineations. In places the marble is tightly folded. Finally the ascent passes through volcanics that unconformably overlie the basement schists.

# Chapter Four

## The lower plate of the Ios core complex:

### Traverse 1 - Ios chora to the γ4 granite boudin

*Leon Vandenberg, Gordon Lister and Suzanne Baldwin*

## INTRODUCTION

The lower plate of the Ios core complex consists of an augengneiss core and an overlying garnet-mica schist and gneiss mantle. Both core and mantle been strongly deformed during at least five different phases of deformation. Petrological and geochronological data indicate that the lower plate has been subjected to at least three phases of metamorphism.

The first event was a Hercynian (?) M0 amphibolite facies metamorphism, possibly associated with intrusive event that only affected the lower plate (Henje-Kunst & Kreuzer 1982, Andriessen et al. 1987). Keay (in prep) has demonstrated a Hercynian age for the granites that intrude the garnet-mica schist envelope.

Two subsequent phases of Alpine metamorphism have resulted in M1 Eocene (~50 Ma) HP/MT metamorphism and an overprinting M2 Oligo-Miocene (25-14 Ma) greenschist facies metamorphism (Van der Maar 1980, Henjes-Kunst 1980, Henjes-Kunst & Kreuzer 1982, Van der Maar & Jansen 1983, Andriessen et al. 1987, Baldwin & Lister in prep.).

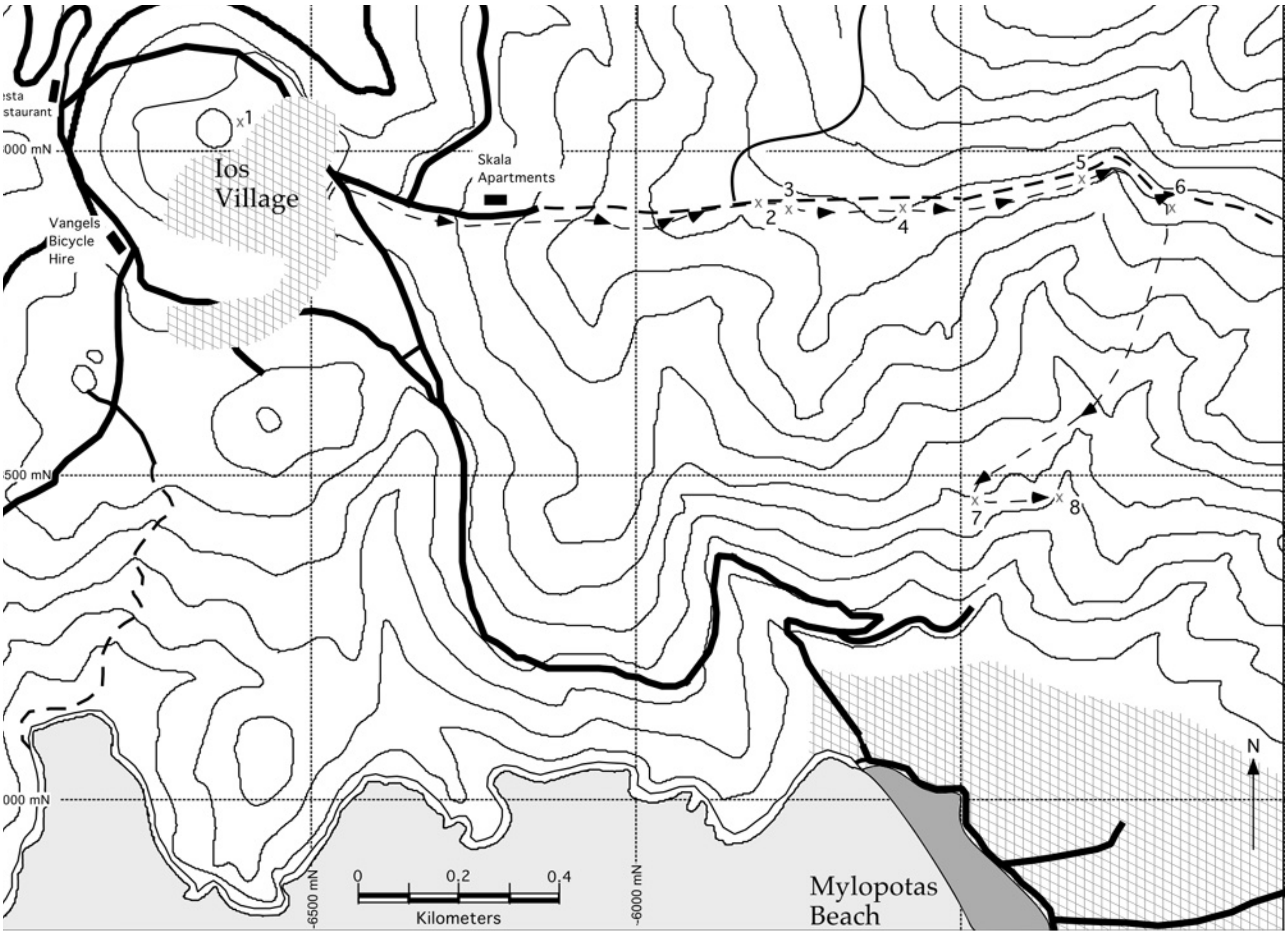


**Figure 4.1** Location map for this traverse

## STRUCTURAL HISTORY

At least five phases of ductile deformation (D1-D5) have been recognised within the lower plate (Vandenberg & Lister 1996). D1 and D2 resulted in the formation of a pervasive schistosity and gneissosity, probably associated with M1 Alpine metamorphism. Later D3 folding has resulted in tight to isoclinal asymmetric fold sets and locally developed crenulation cleavage. Greenschist facies metamorphism has resulted in the static recrystallisation of white-mica grains, and widespread albite blasthesis.

D4 was associated with the development of major shear zones, and the formation of type I and II S-C mylonites, foliation boudinage, discrete shear bands and extensional crenulation cleavages. D4 shearing is associated with further greenschist facies recrystallization. D4 has resulted in the reorientation of most pre-existing structures.

Top-to-the-south D4 shearing in the upper-levels of the Ios lower plate defines the position of the South Cyclades Shear Zone (Banga 1982, Lister et al. 1984). Rare, locally developed D5 folds are upright and open structures with N-S trending fold axes associated with island doming. On Ios (as on Naxos; see Buick 1991a, b, Urai et al. 1990) this generation of deformation was probably responsible for the warping of the carapace shear zone over the island.

The upper levels of the South Cyclades Shear Zone lie in fault contact with the overlying upper plate of the Ios core complex, which is a marble-blueschist "series" (see §6).

## THERMAL HISTORY

A program of 40Ar/39Ar step heating experiments (Baldwin & Lister, in prep.) allows some conclusions to be drawn in respect to the thermal history undergone by this "basement" complex. This traverse is designed to visit many of the sample locations from this study (see Fig. 4.1).

At the end of the traverse we will examine the g4 boudin (see Fig. 4.2). This is a large "augen" or "boudin" of relatively undeformed granite mantled by strongly deformed augengneiss equivalents. It was originally mapped as a young stock (see Van der Maar 1981). However it is clear that this is not the case, for there are no intrusive contacts, and the zone of undeformed granite grades rapidly into the augengneiss that surrounds it.

Baldwin & Lister (in prep.) obtained 40Ar/39Ar apparent ages of 350-500 Ma from strongly kinked unrecrystallized biotites from within the relatively undeformed core of this granitoid augen (Fig. 4.3).

Possibly this age reflects the influence of excess argon in the pore fluid of the rock mass, which has been incorporated into high diffusivity pathways in the biotite. However taking into consideration the structural relationships (Vandenberg & Lister 1996) and that texturally only minor evidence for recrystallization exists, we propose that these results record the effect of biotite growth during or prior to Hercynian amphibolite metamorphism (M0).

**Figure 4.2** View of the $\gamma$4 granite "boudin" from Mylopotas Bay. The relatively undeformed granite forms prominent knolls or hills, overlain and underlain by strongly deformed granite gneiss.

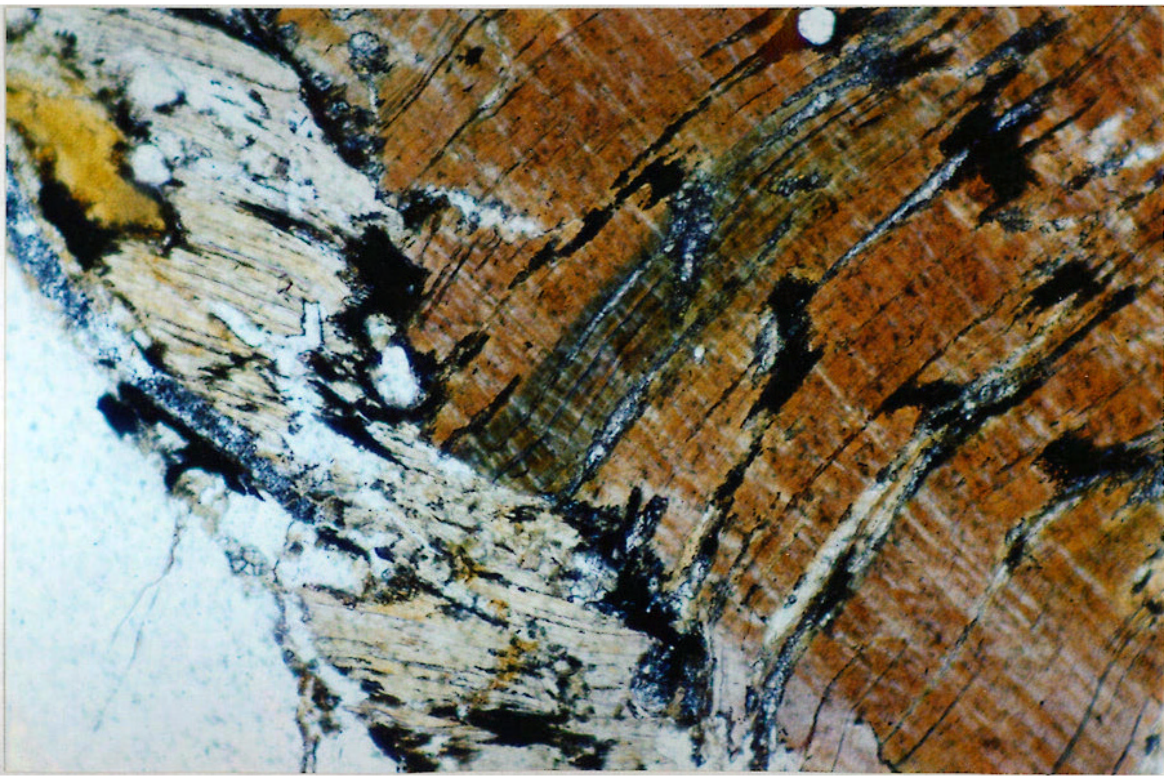

**Figure 4.3** Microphotograph of a kinked Hercynian biotite from g4. Maginification 10X, crossed polarisers. Some recrystallisation occurs in the kinked zone.

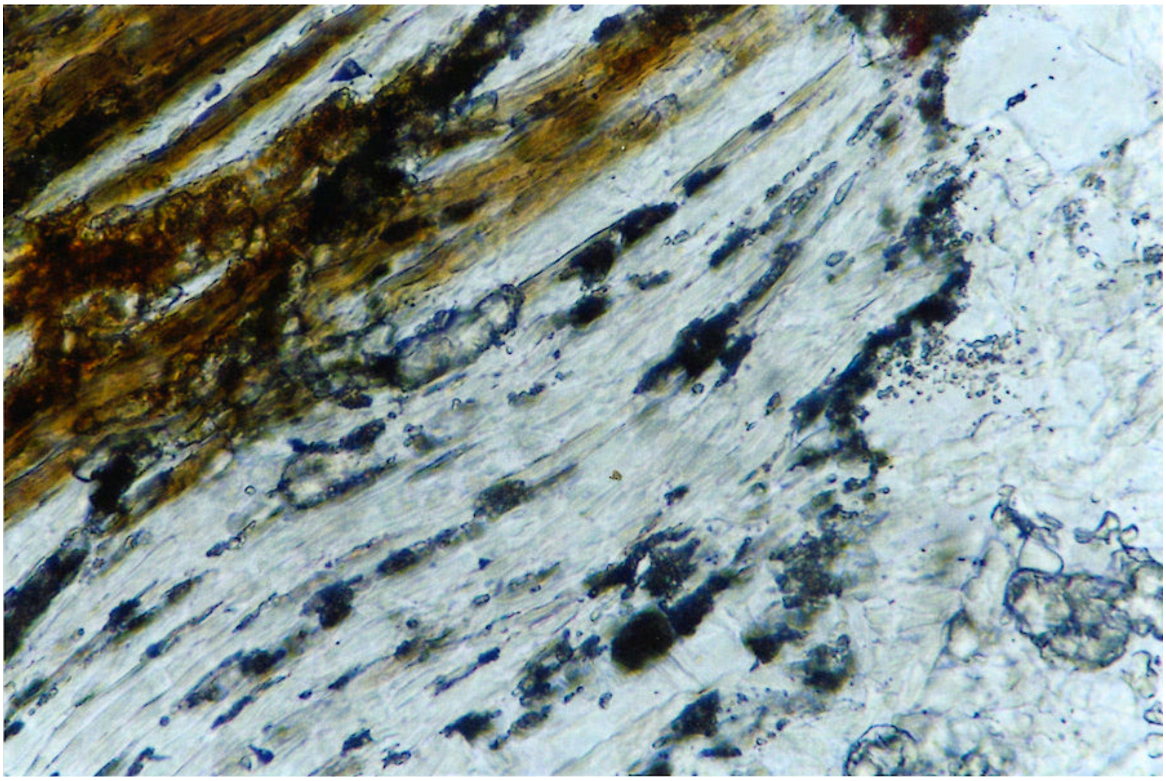

**Figure 4.4** Microphotograph of a Hercynian biotite from g4. Note the replacement fo the biotite by shite mica, and the later rim of white mica and garnet formed during M2.

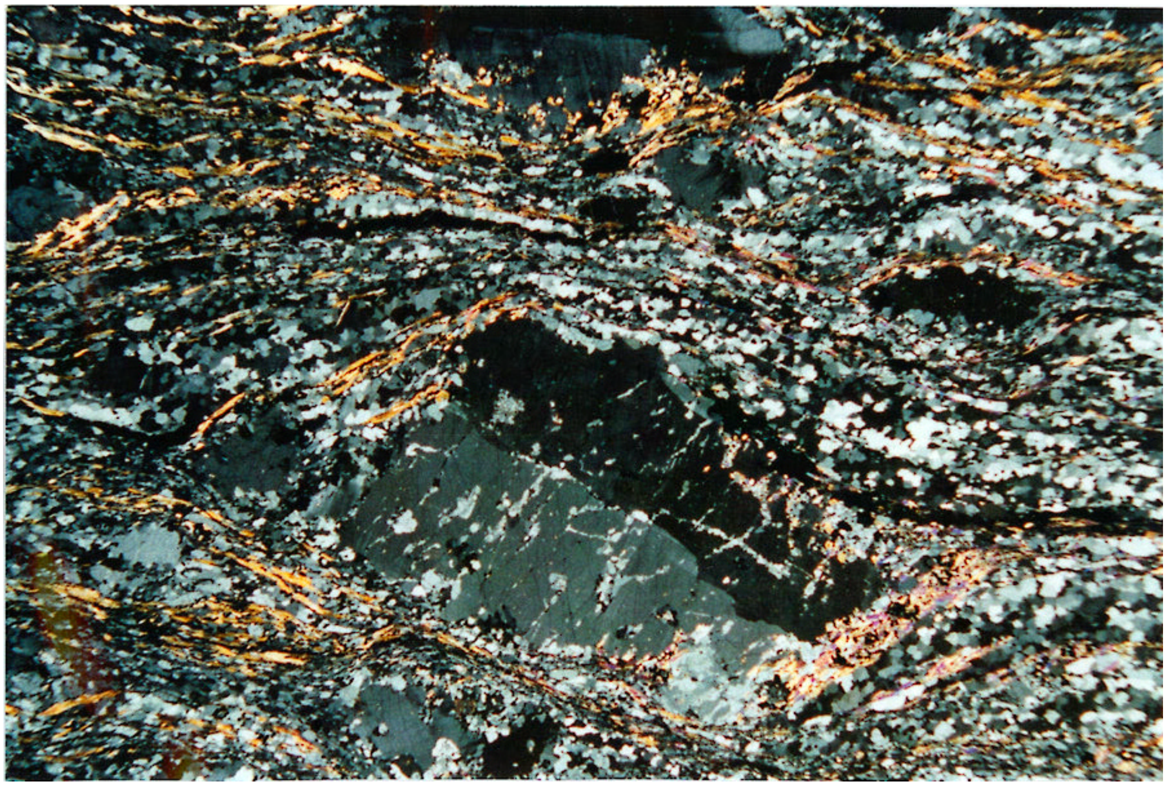

**Figure 4.5** Microphotograph of an S-C mylonite. Note the white mica quartz fabric wrapping an old feldspar porphyroclast.

## How do shear zones operate during the formation of a metamorphic core complex?

The most significant question raised by the Baldwin-Lister study is to ask how it is possible for such old apparent ages to survive both Alpine metamorphism and later Oligo-Miocene greenschist facies overprints.

Baldwin & Lister (in prep.) propose that the central granite gneiss terrain on Ios consisted of a composite terrane of igneous and metamorphic rocks of perhaps different (pre-Alpine) ages. Prior to the onset of the Alpine orogeny these rocks occupied a shallow crustal setting, when they were overridden by Alpine nappes. Pressures increased to ~6-11 kbar and white micas grew (Fig. 4.4) during the Alpine deformation events, with temperature as high as ~400-450°C during metamorphism. However temperature soon returned to <300-350°C, after the periods of metamorphic mineral growth. The rocks were at the crustal level of the so-called argon partial retention/resetting zone during this period (the argon PRZ). The result is that, if the mineral did not recrystallize, old apparent ages were retained in different K-bearing minerals.

During the Miocene thermal pulse, based on the existence of middle greenschist garnet + biotite parageneses, temperatures in the central gneiss terrane reached ~400-450°C. Periods of very rapid deformation ensued when short-lived thermal pulses (caused by the intrusion of Miocene granitoids?) led to increase in temperatures within the South Cyclades Shear Zone. It is difficult to interpret the 40Ar/39Ar apparent ages in any other way except to suggest that a sequence of short-lived thermal pulses occurred, during which metamorphism and intense ductile deformation have taken place.

Cooling subsequent to the Miocene thermal pulse may have involved timescales as short as 10,000 - 100,000 Yr. Yet large strains accumulated in the South Cyclades Shear Zone during the Miocene D4 event. Therefore strain rates must have been very rapid (in the order of 10-9 - 10-11 s-1) while strains involving as much as 70-80% shortening took place. Rapid cooling continued after the Miocene thermal pulse because the core complexes were unroofed due to ongoing extension.

## GEOLOGY OF TRAVERSE ONE

This traverse is a walk along a cross-section through the lower levels of the garnet-mica schists and structurally downwards into the upper levels of the underlying augen-gneiss core (Fig. 4.1). The traverse begins at one of the metamorphosed intrusive bodies found within the garnet-mica schists, at the peak of the Ios chora. From there we walk east through the town square, past the ‘wind mills’ and out along an old walking track for approximately 2.5 km.

After examining the upper levels of the augen-gneiss core, we traverse approximately 1 km SW (across rugged terrain) to inspect an example of the granitic protolith of the augen-gneiss (g4). Along the way please take care not disturb any fences or walls (it may be necessary to cross them) and leave any gates as you might find them. From there we walk approximately 400 metres further southwest to Mylopotas beach.

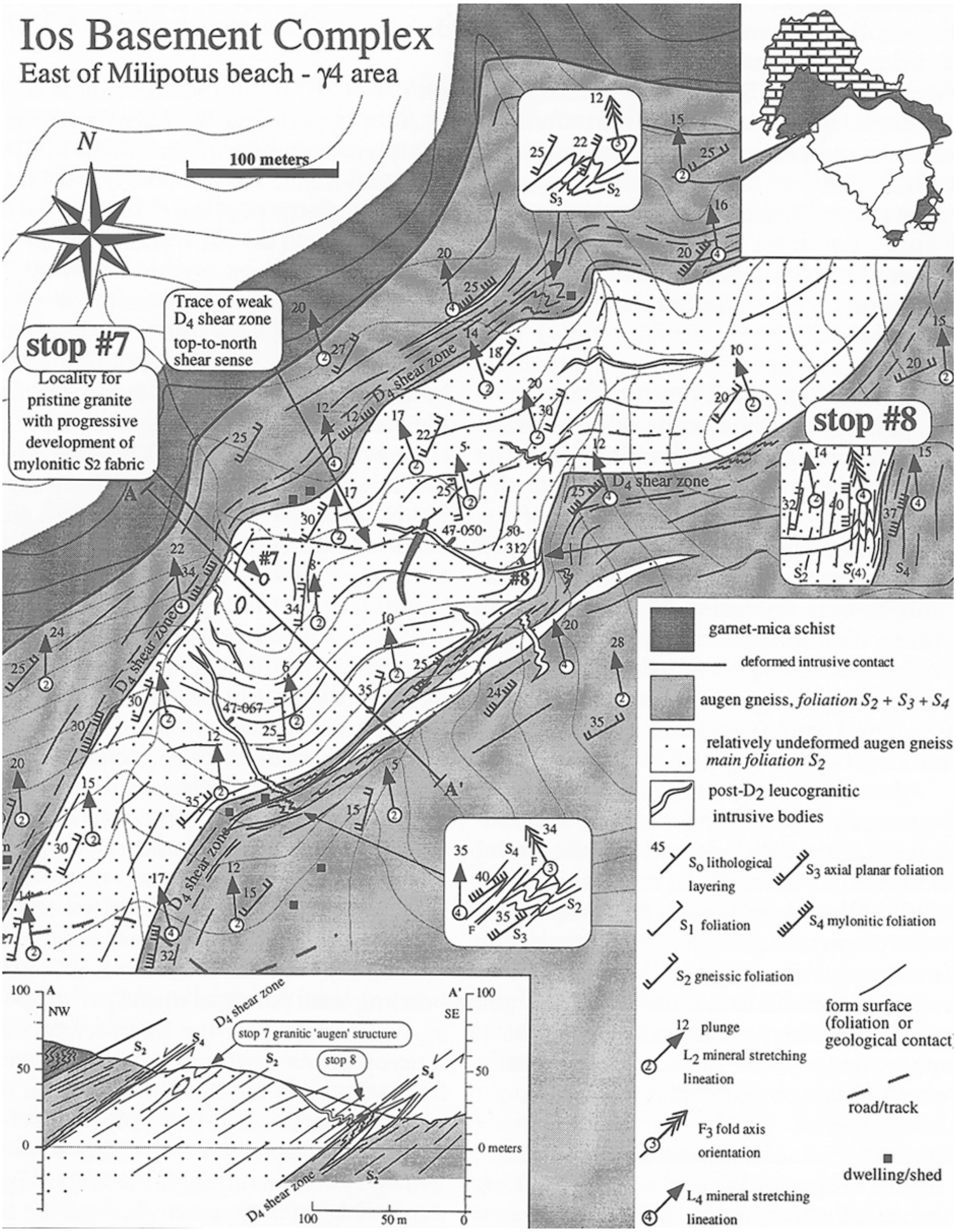


**Figure 4.6** Geology map of the g4 locality, showing the form surfaces for the dominant foliations

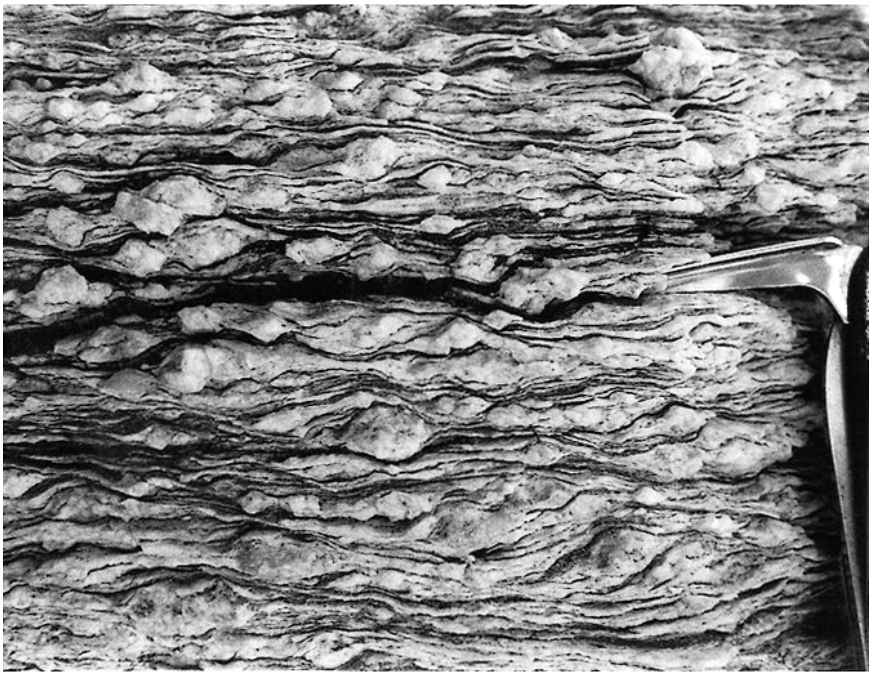

**Figure 4.7** The most spectacular S-C mylonite that you will ever see.

### *Stop #1* Hercynian (?) metagranite

This stop can be reached by walking through the main town of Ios, up towards the main church on the side of the Ios peak. Walk through the churchyard (observing proper decorum, with no use of hammers). Climb up to the main peak. This granite is Hercynian in age (Keay et al. in prep.). It is relatively undeformed, but it is wrapped by the augengneiss of the South Cyclades Shear Zone. This spot affords excellent views of the northern part of the Ios dome, and the Ios Detachment which separates blueschists and marbles of the upper plate from the deformed basement complex.

### *Stop #2* Garnet-mica schist

After negotiating the narrow streets of Ios town, continue up the steep hill past the wind mills. Do not take the Theodoti road. Walk up past the church at the top of the hill onto an old walking track.

Notice the consistent westerly dip of the prominent (S2) schistosity or gneissosity, over this part of the island, and NW to NNW plunging mineral lineation. In general the lineation trends form a N-S pattern over the basement. Over the course of this traverse there are slight deviations away from the westerly dip of S2. D3 folds have axial planes with similar orientations to S2. Significant deviations are probably attributable to a combination of D3 folding and D5 warping.

We pass through several large scale D3 fold-closures during this traverse. F3 fold hinge locations can be determined using the vergence relationships of asymmetric parasitic F3 folds of the S2 schistosity. In general, the overall geometry of F3 folds in this area is inclined (west dipping), NW verging and gently north plunging.

After weaving between three small churches, a branching fork in the track is reached (~300-400 metres east past the last wind mill). Continue on the right branch heading east (straight ahead) to stop #2, several metres past the intersection. The outcrop of interest forms the pavement of the path and is a quartz, white mica, two garnet, epidote-albite (± amphibole) schist. A well developed anastomosing schistosity (S2) envelopes an early generation (pre-Alpine M0) of large almandine garnet porphyroblasts (≤3 cm) with well developed pressure shadows.

Thin sections show a second generation of finer garnets that form fine encrusting rims around the larger garnets. They are also dispersed throughout the foliation and are probably associated with later M1 or M2 Alpine metamorphism.

### *Stop #3* Pegmatite

A pegmatite collected from a few metres from Stop #2 yielded Mesozoic 40Ar/39Ar apparent age spectra.

### *Stop # 4* Granodiorite protolith

Continue east along the track ~400 m. There are many spectacular examples of the large pre-Alpine, pre-S2 garnets in the rocks of the wall material. Several examples also clearly show D3 generation folding of the prominent foliation and ‘garnet strings’. However, please refrain from disturbing the wall rocks. Outcrops either side of the track may provide more appropriate samples.

Stop #4 is a small outcrop of relatively undeformed granite, projecting out onto the track. This is an example of a granitic body in which there is an observable strain decrease relative to surrounding rocks. This granitic body is in the general vicinity of several of the key geochronological and petrological studies of previous workers (e.g., Henjes-Kunst & Kreuzer 1982). These studies first recognized the pre-Alpine intrusive and metamorphic history of these rocks.

Thin-section analysis of selected samples shows the progressive strain of original igneous minerals. Feldspar transformed into a mosaic of white mica and epidote. Biotite formed white mica, rutile, and opaques (during M1) and small encrusting garnet grains and white mica grew during M2, where biotite is in contact with feldspar.

Preferred orientation of elongate and platy metamorphic minerals forms the dominant fabric. This anastomoses around larger pre-deformation garnet porphyroblasts (M0). Later M2 white mica and albite overprint this foliation. Biotite and chlorite have grown in D4 fractures of large garnet porphyroblasts.

### *Stop #5* D3 folds in garnet-mica schist

Continue east along the track for ~200 metres until a small gully is reached. At this locality tight-to-isoclinal, asymmetric D3 folds of the S2 schistosity can be observed. Axial planes dip moderately to the NW and fold hinges plunge north. Significant transposition and overprinting of these D3 folds has also occurred by localised top-to-the north D4 shearing (e.g., shear bands, extensional crenulation cleavages). North directed shearing is common in the areas adjacent to this northern contact with the underlying augengneiss. These fabrics overprint the dominant fabrics of the South Cyclades Shear Zone. Some of the observed folding occurred during D4 shearing.

The effects of post-D3 static M2 metamorphism can be observed in thin-section (white mica recrystallisation and albite blasthesis). These microstructures were subsequently deformed during D4 shearing. The observations suggest a significant phase of static metamorphism between D3 folding and D4 shearing.

### *Stop #6* Granitic augengneiss

Proceed east into the upper levels of the underlying augen-gneiss. The augengneiss shows considerable variation in grain size and foliation development, but the N-S trending mineral stretching lineation remains constant. Spectacular S-C mylonites can be observed (Fig. 4.7).

Grain size is related to the degree of deformation induced recrystallization of quartz, as well as more brittle deformation of feldspar and mica (Fig. 4.5). Feldspar augen generally possess prominent ‘tails’ of recrystallised feldspar and sometimes display ‘core-mantle’ deformation textures. The surrounding anastomosing foliation comprises a mixture of white mica, zoisite, recrystallised poikioblastic feldspar and dynamically recrystallised quartz domains (± grossular garnet). Metamorphic recrystallisation has erased most textural evidence for older fabrics.

Dynamic recrystallization microstructures show that D4 deformation took place during decreasing temperature. Type-I S-C mylonites are commonly observed (Figs. 4.7 and 4.5). Sense of shear, as within the augengneiss is top-to-the-south. Locally however, top-to-the-north shear sense can also be found, particularly within close proximity to the garnet-mica schist contact.

### *Stop #7* The g4 granite boudin

Traverse SW for approximately 1 km towards the g4 granite body across rugged terrain. Several goat tracks head in the general direction.

The g4 body was originally identified by Van der Maar (1980) as a coarse metagranite (+ biotite) body, similar in character to the surrounding augen-gneiss. Subsequent mapping indicates that the extent of outcrop of relatively undeformed granite is somewhat more limited than that indicated by Van der Maar (1980). The g4 body has been delineated as an ‘island’ or ‘augen’ of D2 strain which exhibits limited D4 strain (see Fig. 4.6)

The extent of outcrop with little or no strain is only two to three metres in diameter. An increase in strain can clearly be seen moving away from this outcrop to where the augengneiss foliation and a north plunging lineation begins to develop. Thin sections of this relatively undeformed granite reveal a coarse granitic texture, with strongly kinked biotites (see previous comments on the Baldwin-Lister study). The biotites display an M1 overprint, with white mica overgrowing the biotite, accompanied by growth of sphene, rutile and epidote inclusions (see Fig. 4.4). The M2 overprint is also visible, with the biotites often rimmed by an overgrowth of white mica and garnet, where old biotite grains occur adjacent to plagioclase.

### *Stop # 8* Leucogranite dykes and sills

Proceed east for approximately 150 m until a thin leucogranitic dyke is reached. There are several such dykes which cut across the augengneiss foliation in the vicinity of g4. A progressive increase in fold intensity takes place due to D4 shearing. Access to a clear vantage point in the creek bed can be gained by making your way down the gullies (either side of the peak through which this dyke cuts).

# Chapter Five

## The lower plate of the Ios core complex:

### Traverse 2 - Mylopotas Beach to the south headland

*Gordon Lister and Sue Keay*

## INTRODUCTION

This traverse is designed to allow us to walk from relatively low levels in the South Cyclades Shear Zone towards its upper levels, in particular to the contact with the garnet-mica schist. In this traverse this contact is defined by a north-directed shear zone, with intensely developed fabrics (see Fig. 5.1).

Our structural position will be on the western flank of one of the domes in the Ios basement. The traverse starts from the southern end of Mylopotas Beach, which can be reached by bus, or by foot from Ios central. There is a hotel at the end of the beach. The start of the traverse can be reached by either walking up the side stairs of the hotel, onto the outcrop at the top, or by climbing around from the side of the road that leads up the hill towards Manganari. The traverse follows the southern coastline of Mylopotas Bay, out to its southern headland.

### *Stop #1* [direction to north cape 271°]

This is the Hercynian augengneiss. It was a coarse phenocrystic mafic granite. It appears to be the same mafic granite that is observed elsewhere throughout the Cyclades, for example in northern Paros. Now it is strongly deformed. It has a constant 0-20° trending stretching lineation defined by smeared out mineral grains, and pressure shadows around feldspar porphyroclasts. Similarly it is strongly foliated, with originally anhedral quartz aggregates now smeared out into foliae, and narrow

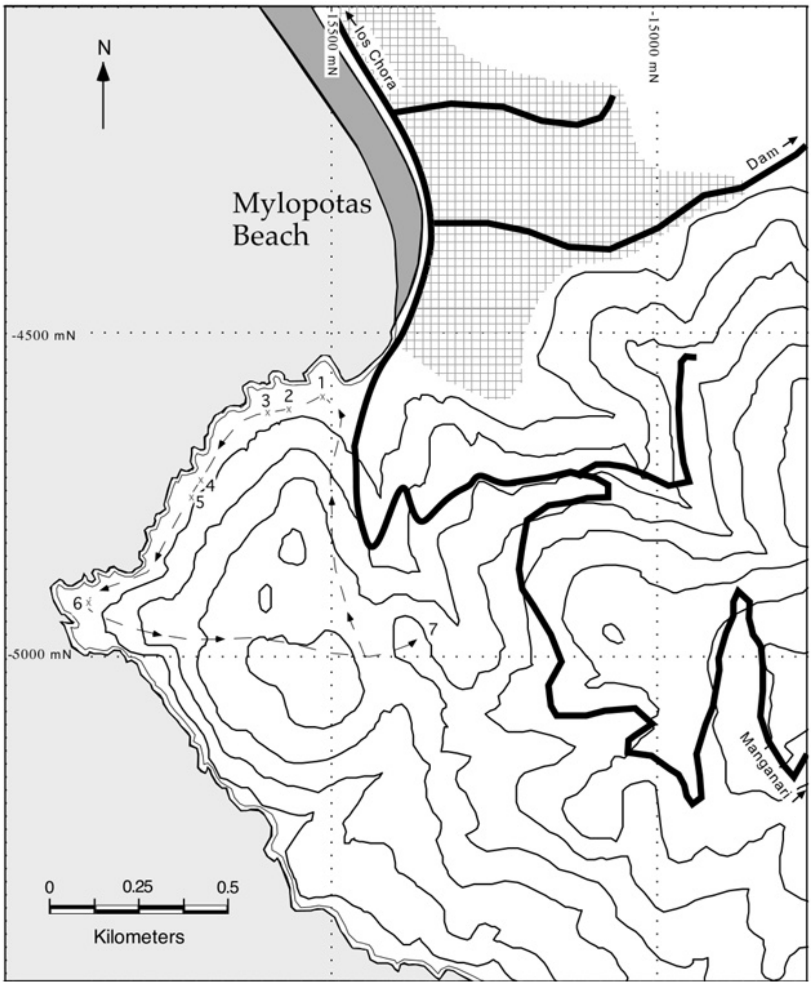


**Figure 5.1** A map showing the location of the traverse from Mylopotas beach to the south headland.

shear bands that have focussed on large biotite aggregates in the original groundmass.

The rock has deformed primarily as the result of crystal plastic processes, with attendant dynamic recrystallization, as well as some cataclasis of the more brittle minerals such as feldspar. It is thus essentially a mylonitic augengneiss. Nevertheless it is still relatively coarse grained, and recrystallized grain size is not so large as to preclude its detection in the field with a pocket microscope. The (south-directed) sense of shear is readily determined as the result of the development of spectacular zones of S-C mylonites (see Fig. 5.2).

The granite is cut by aplite dykes that are locally folded, as the result of the orientation of the dyke in the shortening field of the South Cyclades Shear Zone.

### *Stop #2* [271.8° to north cape]

The coarse augengneiss is intruded by a “sill” of aplite (in fact this is a highly deformed dyke). Above this there is a schist pod (highly deformed) with a north-directed sense of shear defined by S-C fabrics. The schist is so deformed as to resemble a button schist. It appears to have been caught up in a younger (north-directed) shear zone that overprints the main fabric of the South Cyclades Shear Zone (Fig. 5.3). Above the schist pod the augengneiss fabric is considerably comminuted, again in the same (younger) north-sense shear zone.

### *Stop #3* [272° to north cape]

The augengneiss becomes again less deformed and the original phenocrystic texture is clearly more evident. Individual phenocrysts tend to maintain their integrity. Sense of shear is again clearly to the south.

However the outcrop (immediately by the shoreline) reveals a 1m wide north-directed shear zone that overprints the dominant south-directed fabric. Again, this younger shear zone is associated with considerable comminution of the feldspar clasts, and grain size reduction of all minerals is marked. The fabric produced in the older shear zone can be seen curving into the more intensely developed younger fabric at the centre of the shear zone.

This locality is also interesting in that there is a fault that has ductiley shredded these fabrics, and then brecciated them. This fault brings augengneiss into contact with folded garnet-mica schists. The contact between the two units is not fault related in all situations however. There is an apparently intrusive relationship exposed between the augengneiss and the basement garnet-mica schists.

Leucocratic gneisses in the basement schists may be older igneous rocks. Aplites can be seen intruding the augengneiss. These are folded, with the dominant gneissic fabric defining an axial plane foliation. Some shear zones (and folds) have been localized along the intrusive contact between the augengneiss and the older basement schists and gneisses (Fig. 5.4).

### *Stop # 4* [276.2° to north cape]

Xenoliths and enclaves have been observed in the mafic granite.

### *Stop # 5* [276.6° to north cape]

Strain intensity has dropped to a point where the original magmatic texture is clearly evident. The “original” biotite is apparently quite fresh. The protolith is a coarse mafic granite, similar to that found in the g4 boudin (see Traverse 1).

This granitic body is cut by a 0.5-1.0 m wide coarse (5-10 cm) quartz-feldspar pegmatite, with aplitic margins. These margins show evidence of magma assimilation, although they are affected slightly by later deformation. The outcrop is cut by several south-sense, narrow (1-10 cm) ductile shear zones.

Continuing towards the south cape, the traverse will encounter more coarse leucogneiss dykes, and large schist rafts caught up in the granite.

### *Stop # 6* Headland shear zone

The south headland marks the location of a major north-sense ductile shear zone that overprints the south-directed fabric that has been encountered throughout the traverse. This shear zone marks the contact with the garnet-mica schist. All rock types are intensely deformed, and grain size is considerably reduced, as observed in the other north-directed shear zones encountered in this traverse.

There are spectacular examples of foliation boudinage, and other features associated with extreme ductile strain in these rocks. There are numerous folds that have been variably overprinted by the high strain zone. These are overturned west-vergent inclined folds (see Fig. 5.6).

The main question that should be asked at this outcrop is why these younger shear zones are north-directed. This is a particularly interesting question given the existence of major north-directed shear zones on Paros and Naxos (see §2), and in particular given the number of different generations of detachment faults that have been recorded on Ios (see §6).

It appears that there may have been an early generation of south-directed extension, during which the South Cyclades Shear Zone has formed, followed by a younger

**Figure 5.2** Spectacular zones of S-C mylonites in the mylonitic augengneiss, south of Mylopotas Bay. This augengneiss has a Hercynian grranite protolith.

**Figure 5.3** Younger north-directed shear zone cutting fabrics of the South Cyclades Shear Zone. The younger shear zone is associated with considerable grain size reduction.

**Figure 5.4** Fold associated with north-directed shear zone and fault juxtaposing the garnet-mica schist against the mylonitic augengneiss.

**Figure 5.5** West vergent D3 fold on the western flank of the Ios dome in he garnet-mica schist, in the zone effected by the north-directed shear zones.

episode, in which more localized and discrete shear zones formed. This later generation of shear zones involved very high strains.

Note that there are at least two periods of greenschist metamorphism that have been detected in the microstructure, and inferred from the 40Ar/39Ar apparent age spectra. These episodes may be coincident with the two generations of extension-related shear zones that have been recorded.

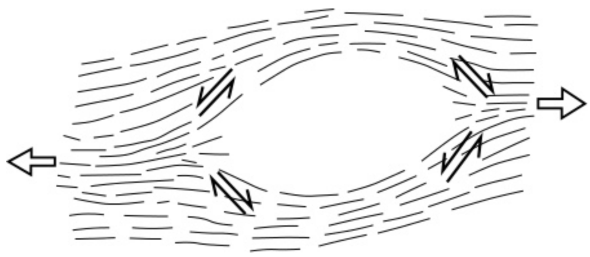

**Figure 5.6** Variation of the sense of shear around an undeformed 'augen'or 'boudin'in the South Cyclades Shear Zone.

### *Stop #7* Granite boudin

The traverse continues, by climbing the hill, on a poorly marked path, making our way towards the crest, and back towards the Mylopotas Road. At the main crest, the "basement" augen-gneisses are variably deformed, and large boudins begin to be observed.

These "boudins" or "augen" are in fact less deformed ellipsoidal zones in the sheared matrix. Similar features were mapped by the original workers on Ios as younger granitic stocks, and these were identified as g1, g2, ... g5. All of these structures have now been shown to be zones of low strain in which the original protolith is relatively well-preserved. They are surrounded by anastomosing zones of highly deformed augengneiss (see Fig. 5.6). The particular example that has been chosen is a Hercynian intrusion. A U-Pb age of ~300 Ma has been obtained by Keay et al (in prep.). The 3-D structure of the "boudin" or "augen" is clearly visible, due to its small size (a few metres across) and the 3-D nature of the outcrop.

The sense of shear varies according to the structural position around the boudin as shown (see Fig. 5.6). The change in sense of shear suggests that the rock mass was subject to coaxial stretching. Yet the outcrop occurs adjacent to or within a major ductile shear zone.

Such observations are not uncommon in major shear zones (e.g., Garcia-Celma (1983) observed similar variation in sense-of-shear around boudins, while working in mylonitic shear zones in the Cap de Creus, in the axial zone of the Pyrenees).

# Chapter Six

## Detachment fault systems on Ios

### Traverse 3 - Tower Hill

*Marnie Forster and Gordon Lister*

## INTRODUCTION

Ios is transected by at least two systems of low angle normal faults. It appears that both of these fault systems accomplish significant relative movement. These fault systems have therefore been referred to as detachment faults (following the usage of Davis & Lister 1988).

Other authors have suggested that detachment faults do exist in the Aegean (Lee & Lister 1992, Gautier et al 1993) but these faults (e.g., on Naxos, Paros, and Mykonos) separate non-metamorphic rocks from the underlying metamorphic tectonites.

The low-angle normal faults that separate non-metamorphic rocks from underlying metamorphic tectonites may be a distinct late generation of detachment faults responsible for late stage exhumation of the Aegean core complexes.

Faults of this character have not been discovered on Ios. The detachment fault systems on Ios are structurally deeper and suspected to be earlier generations of detachment faults than those reported on Naxos and Paros. On Ios the detachment faults separate slices of metamorphic tectonites from different crustal levels.

## IOS DETACHMENT SYSTEM

The first recognised generation of detachment faults separates the upper-plate (the so-called “series”) from the underlying “basement” (lower-plate) schists and gneisses. This complex array of anastomosing normal faults has been termed the Ios Detachment Fault system.

## COASTAL DETACHMENT SYSTEM

The second generation of detachment faults is found along the north-west coastline of Ios. The upper-plate of this fault system is generally defined by brecciated non-foliated and non-lineated marbles. These outcrop as marble peninsulas, and as klippen on topographically elevated areas. It is believed these marbles (in the upper-plate to the Coastal Fault system) have come from relatively shallow crustal levels. They did not undergo the ductile deformation evident in rocks that were once deeper in the crust, as in the lower-plate of the Coastal Fault system.

This traverse is designed to pass through the South Cyclades Shear Zone and the Ios Detachment Fault system (see Fig. 6.3).

## ACCESS

By foot from the Port Beach, walk towards the base of ridge below the highest peak, then make your way up the spur to the base of Tower Hill (see Fig. 6.1)

### *Stop #1* Ios Detachment System

View from the Fiesta Restaurant on road between the port and Ios central (Fig. 6.4). The Ios Detachment is clearly discernable where it truncates the cream marble bands at the structurally lowest level of the upper plate. This fault outcrops just below the ridge crest. Observe the ramp geometry of the Ios detachment at the base of Tower Hill.

We suspect that another fault occurs at the base of the hillside where there are sharp demarcations defined by the nature of the outcrop. Above this fault, outcrop is well defined, while below the fault there is a break in slope and bedding is considerably less well-defined.

Your present location (in the Fiesta Restaurant) is approximately in the middle of the South Cyclades Shear Zone. This shear zone is a major (top to the south) shear zone up to one kilometre thick, which occurs at the structurally higher levels of the lower plate of the Ios core complex. The shear zone is domed over the island, dipping towards the north at this location.

### *Stop #2* Granite

At the base of the spur below Tower Hill, walk up through deformed granite and observe the variations in mineralogy and intensity in deformation. Mylonitic stretching lineations typically trend between 0-20°N, and these are strongly developed. This deformed granite is part of the g1 granite originally mapped by Van der Maar (1980).

Potassium feldspar porphyroclasts display prominent ‘tails’ of recrystallised feldspar debris. The surrounding fabric is an anastomosing foliation defined by white mica (now decussately recrystallised), zoisite, minor garnet and albite. The initial development of this fabric is probably associated with Eocene collision (S2). However, the fabric now defines the ‘S’-plane of S-C mylonites (associated with the South Cyclades Shear Zone) and display prominent dynamically recrystallised quartz and feldspar microstructures. Microshear bands formed through decussately recrystallised white mica bands (M2?) are also observed (with incipient recrystallisation), together with M2 biotite grown in dilatant sites (i.e., shearing under greenschist facies conditions).

These mylonites vary in their intensity with prominent zones of intense shear fabrics. The sense of shear in the field can be clearly seen to be south directed (Fig. 6.2). The protolith is a Hercynian granite (Keay et al., in prep.).

### *Stop #3* Metabasite

At approximately seventy-two metres altitude there is a deformed metabasite sill with relict green phenocrysts (probably hornblende). Van der Maar (1980) suggests this to be the metabasite (with actinolite megacrysts) and infers the existence of an old ophiolite sheet and the approximate position of the ‘Basement-Series’contact.

### *Stop #4* Granite/Garnet-mica schist

The contact between granite and garnet-mica-schist may be a fault or a deformed intrusive contact. To the east, on the next spur, looking north-east, one can see that the axial planar (S3) foliation of the schists and the mylonitic augen-gneiss foliation of the deformed granite are conformable (?) across this contact. This contact is defined by a sharp boundary and it is not associated with breccia or fault rock of any kind.

Where the contact is observed lower down, at the waters edge to the southwest, the boundary has localised post-D4 shearing, late fault.

### *Stop #5* Graphitic quartzite

The graphitic quartzite in the garnet-mica-schist varies from an impure graphitic quartzite to an almost pure graphite. These layers can be spectacularly folded by

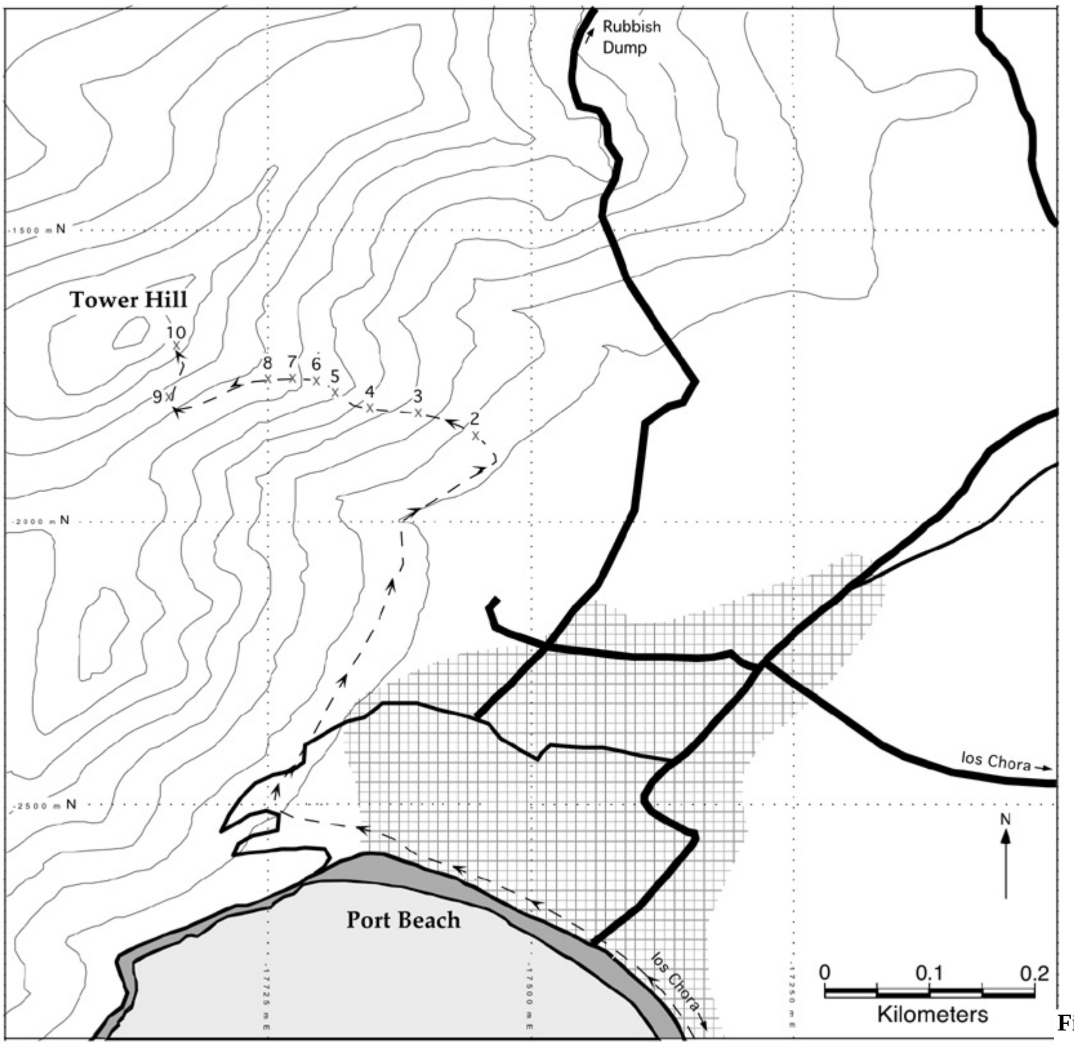


**Figure 6.1** Locality map.

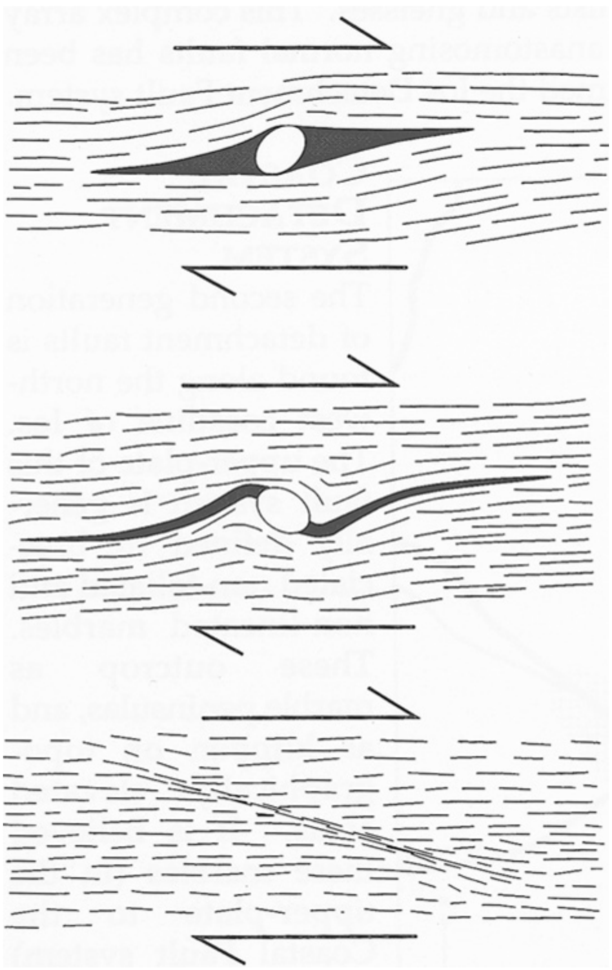

**Figure 6.2** Example of porphyroclasts showing asymmetry of pressure shados and shear bands showing sense of shear.

several generations of folding events, and non-cylindrical sheath folds are common. Lineations associated with the mylonitic shear zone are also folded, suggesting that progressive deformation may have taken place. Some folds have axial plane differentiated crenulation cleavages, and these also are rotated into adjacent shear zones. Again this suggests that progressive deformation has taken place.

### *Stop #6* Garnet-mica schist

In the garnet-mica schist unit a variation in mineralogy occurs, which includes a garnet+biotite schist and graphitic schist. There are several generations of garnet porphyroblasts, including those grown during the Hercynian amphibolite facies metamorphism. These have well developed quartz pressure shadows and relict differentiated crenulation cleavage (S2), intensely deformed during operation of the South Cyclades Shear Zone (S4).

At approximately 136 metres altitude fine bands of graphite-rich assemblages occur in the garnet-mica schist slice. These graphitic bands increase in width and number towards the Ios Detachment. These softer graphitic bands have accommodated more strain.

### *Stop #7* Graphitic schist

Immediately below the Ios Detachment (approximately 140 metres altitude) a zone of graphitic schist occurs. This contains well developed south-directed shear bands. We suggest this slice is fault bounded. The fault at the structurally higher contact is the Ios Detachment, however the contact at the base may represent a gradational variation into the garnet-mica schist.

### *Stop #8* Ios detachment

Cream marble bands in the structurally lower levels of the upper-plate are truncated by the Ios Detachment. In places the cream marble bands dip at ~40°-60°W and are truncated by the Ios detachment which is dips at ~20° to the northwest. This can be seen by climbing to the east side of the outcrop and looking westward.

At this point you should be able to observe the opposite spur, where several low-angle faults can be seen, and the truncation of the cream marble beds with a ramp geometry. Some of these faults are associated with spectacular breccias (Fig. 6.5).

### *Stop #9* Blueschist to greenschist

Walk across the saddle (~170 metres altitude) observing partial transformation of the blueschist facies assemblages into greenschist facies assemblages, where chlorite-albite button schists have developed. The development of these chlorite assemblages represent retrogression from a greenschist facies assemblage either from continuing exhumation or in association with the Coastal Detachment system (see §7).

### *Stop # 10* Coastal Detachment system

The grey marble unit which outcrops immediately above this point is suggested to have been emplaced by a fault structurally higher than the Ios Detachment, the Andre Fault (Forster & Lister, in press).

Halfway up this grey marble band, and structurally higher than the Andre Fault, there is a ledge marked by undifferentiated schist. (On previous years this has been the home to a snake family, take care.) This ledge appears to mark a fault plane of the Coastal Fault array.

## End of traverse

Return to Ios either by the same route, or by descending another spur. It is also worthwhile to walk westward along ridge crest to join Traverse 4 and to observe the Coastal Fault array from that point.

**Figure 6.3** A schematic map of the upper-plate of the Ios core complex, showing the location of the Ios detachment fault system and the Coastal low-angle normal Fault array (Forster, 1996).

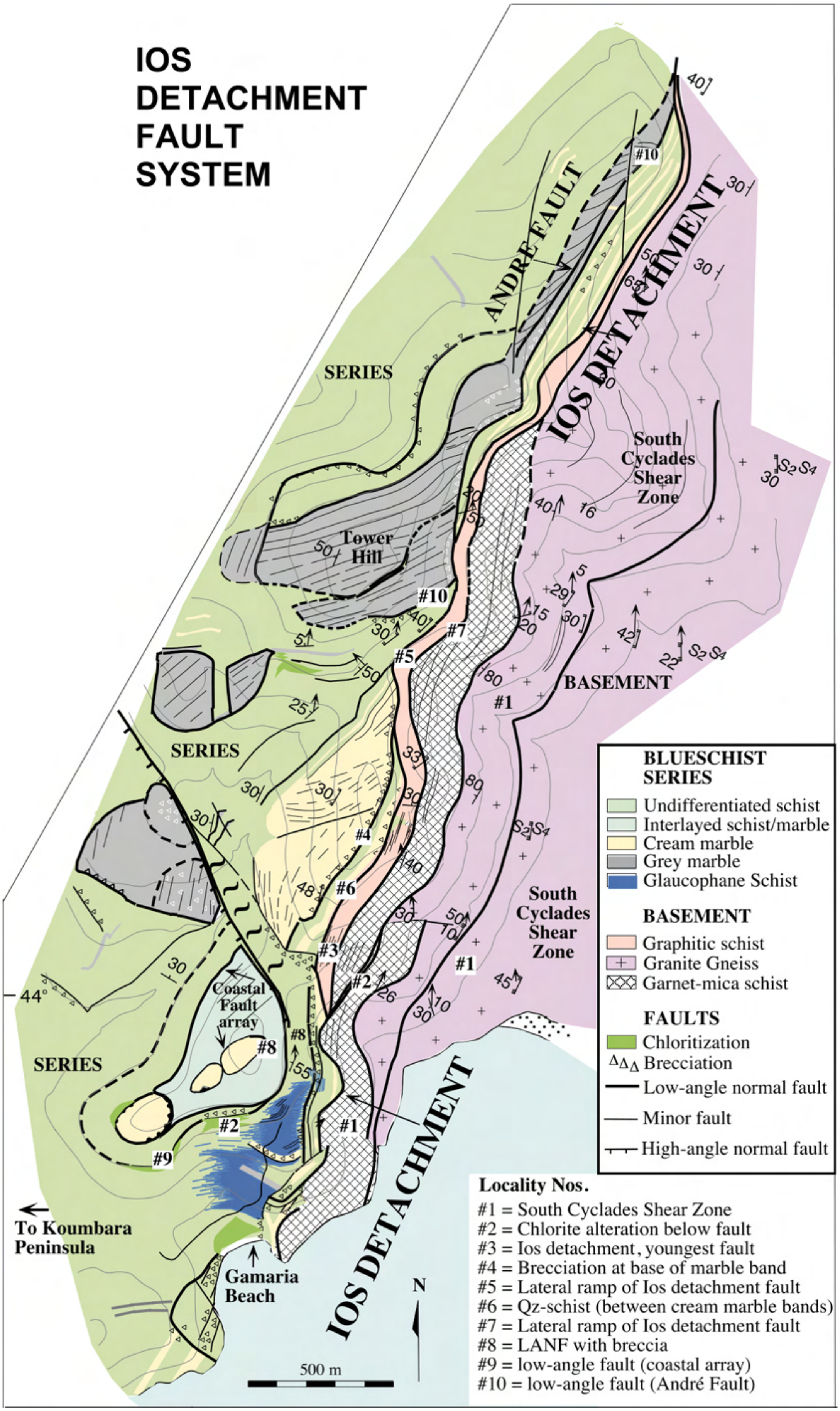

**Figure 6.4** Photograph of the contact between the upper- and lower-plates of the Ios detachment fault system. This shows the array of faults that can be observed.

**Figure 6.5** The marble breccia that defines one of the anastomosing faults of the Ios detachment fault system.

# Chapter Seven

## Detachment fault systems on Ios

### Traverse 4 - Port Beach shear zone to Koumbara Peninsula

*Marnie Forster and Gordon Lister*

## INTRODUCTION

This traverse begins in the lower plate at the northwestern end of the Port Beach, cutting obliquely through the South Cyclades Shear Zone and on to Gamaria Beach and the contact of the upper plate (Fig. 7.1). The traverse then continues northwest to the top of the ridge and west to Koumbara Peninsula. This second part of the traverse displays slices from different structural levels of the upper plate that have been segmented by the Coastal Detachment system (Figs. 7.2 and 7.3).

Access is gained by bus or by a pleasant walk from Ios village down the "Donkey Trail" to the Port Beach. Continue along the Port Beach to the NW end of the beach. Begin the traverse on the outcrop at the waters edge, heading in a southwesterly direction.

### *Stop #1* [36° 43.70'N 25° 16.13'E]

Deformed granite in the South Cyclades Shear Zone. D4 is intensely deformed with well developed shear bands. The protolith is generally, but not always, recognisable.

### *Stop #2* [36° 43.66'N 25° 16.09'E]

Xenoliths of garnet mica-schist in the deformed granite can be observed here. At least two sorts of granite that can also be discerned. In the granite schist the feldspar clasts are relict from the original coarse phenocrysts that can be observed at deeper structural levels in the basement, beneath the South Cyclades Shear Zone. There has been

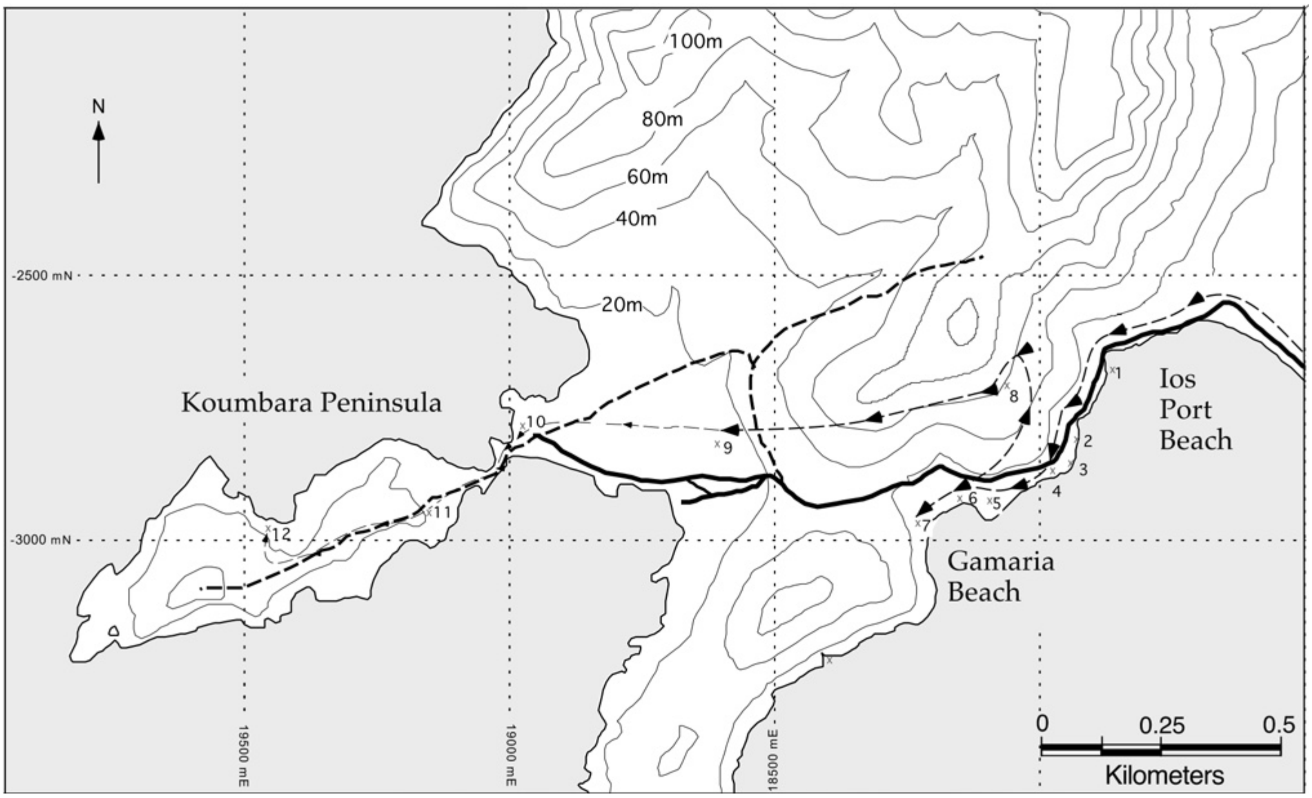


**Figure 7.1** A map of the route followed by this traverse.

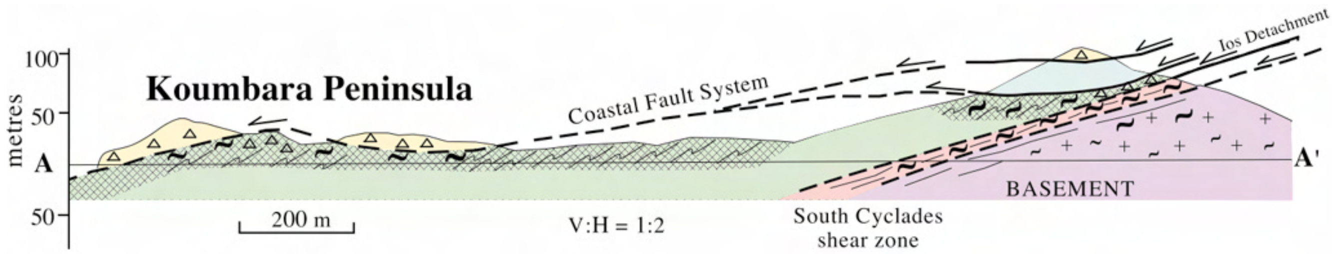


**Figure 7.2** Cross-section of the low angle Coastal Fault array through the Koumbara Peninsula (Forster 1996).

considerable grain size reduction, however sense of shear (south-directed) can be readily determined by the asymmetry of pressure shadows.

### *Stop #3* [36° 43.66'N 25° 16.09'E]

Along this section the garnet-mica schist and granite contact are observed to be faulted against one another.

### *Stop #4* [36° 43.66'N 25° 16.09'E]

A variety of schists occur in this garnet-mica schist zone. Mylonitized quartz veins can be found isoclinally folded into rootless fold hooks. These isoclinal folds are themselves refolded by west vergent parasitic folds with a weakly developed axial planar cleavage. The isoclinal folds have the dominant fabric (S2) as their axial plane.

### *Stop #5* Graphitic lens

At the structurally highest levels of the garnet-mica schist a slice of graphitic-rich bands occur. These graphitic-rich bands are immediately below the fault contact with the cream marble beds of the upper plate.

Quartz veins also occur in this section which display mylonitic textures, and are often isoclinally folded, with their fold axes parallel to the stretching lineation (see Figs. 7.6 & 7.7). Some schists display aligned needles (~0.5mm by <3 mm) of altered (?) amphibole.

### *Stop #6* Gamaria Beach

Both the upper and lower plate in Gamaria Beach area display complex structural geology. The fault juxtaposing the upper and lower plates has been cut by younger faults, making it difficult to ascertain the character of the juxtaposition. A fault can be observed at the base of the structurally lowest cream marble bandand is by a band of marble breccia, suspected to be the Ios Detachment Fault.

### *Stop #7* Breccia bands at Gamaria

A breccia defined fault(~3 metres thick) runs subparallel to the Ios Detachment Fault but this occurs only in the upper plate (Fig. 6.5).Observe breccia on adjacent headland. Cross beach, and look at this breccia close at hand. These breccia bands are distinct from the Ios detachment and mark other faults structurally higher in the Ios Detachment array (Fig. 6.5).

### *Stop #8* Coastal Detachment system

Climb hill above Gamaria beach, observing the different deformational styles above and below the cream marble bands. The fault slices at the top of the hill are klippen related to the Coastal Detachment Fault system in the Ios upper plate.

### *Stop #9* Koumbara Isthmus

Walking down the hill, in what should be a structually higher region, we will encounter material from a deeper crustal level in the Ios upper plate. These grey marble rocks have been ductilely deformed with well developed foliations and lineations, a direct contrast to the marbles at the top of the hill at Stop #8 and Koumbara Peninsula. This suggests several slices of material from different structural levels (Figs. 7.2 and 7.3).

### *Stop #10* Koumbara Peninsula

Walk down hill towards Koumbara peninsula (Fig. 7.4). The outcrop at the isthmus contains chlorite-epidote-quartz rock (Fig. 7.5). These rocks are typical of the footwall of the Coastal Fault array, and can be intensely foliated and lineated. Lineations typically trend from ~40° to 90°. The dip of the fault plane at Koumbara is sub-horizontal (Fig. 7.2).

### *Stop #11* Koumbara Peninsula

Continue walking out on the southern part of the Koumbara peninsula, until we encounter low-angle faults (Fig. 7.4) separating brecciated marbles in the hangingwall from ductilely deformed schists in the footwall. This is the same fault system observed at Stop #8 (Fig. 7.2).

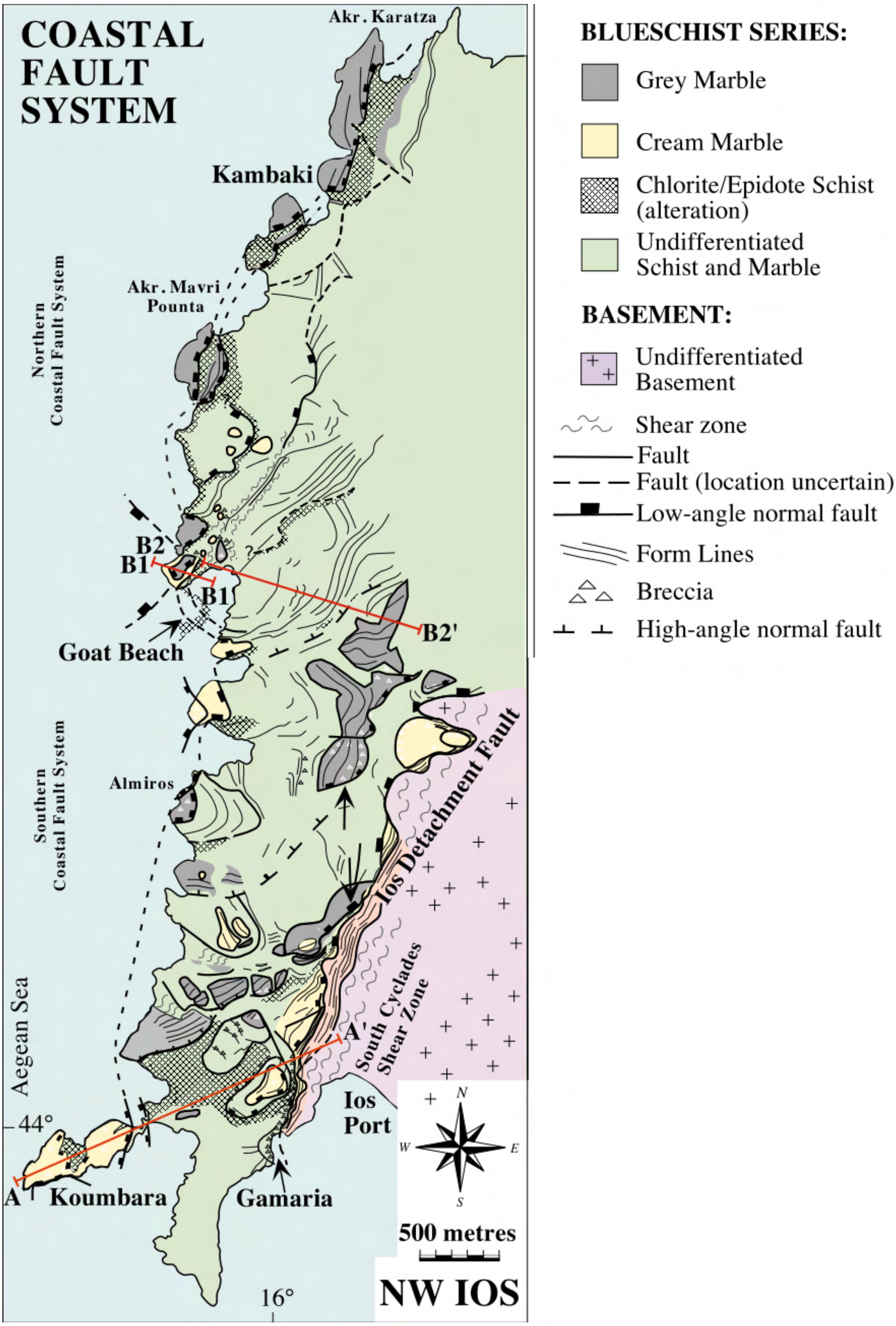


**Figure 7.3** Map of the Coastal Detachment Fault array on Ios (from Forster 1996).

**Figure 7.4** Overview of the Koumbara Peninsula, showing the higher structural levels of the coastal fault array. The actual trace of one of the low-angle faults can be discerned.

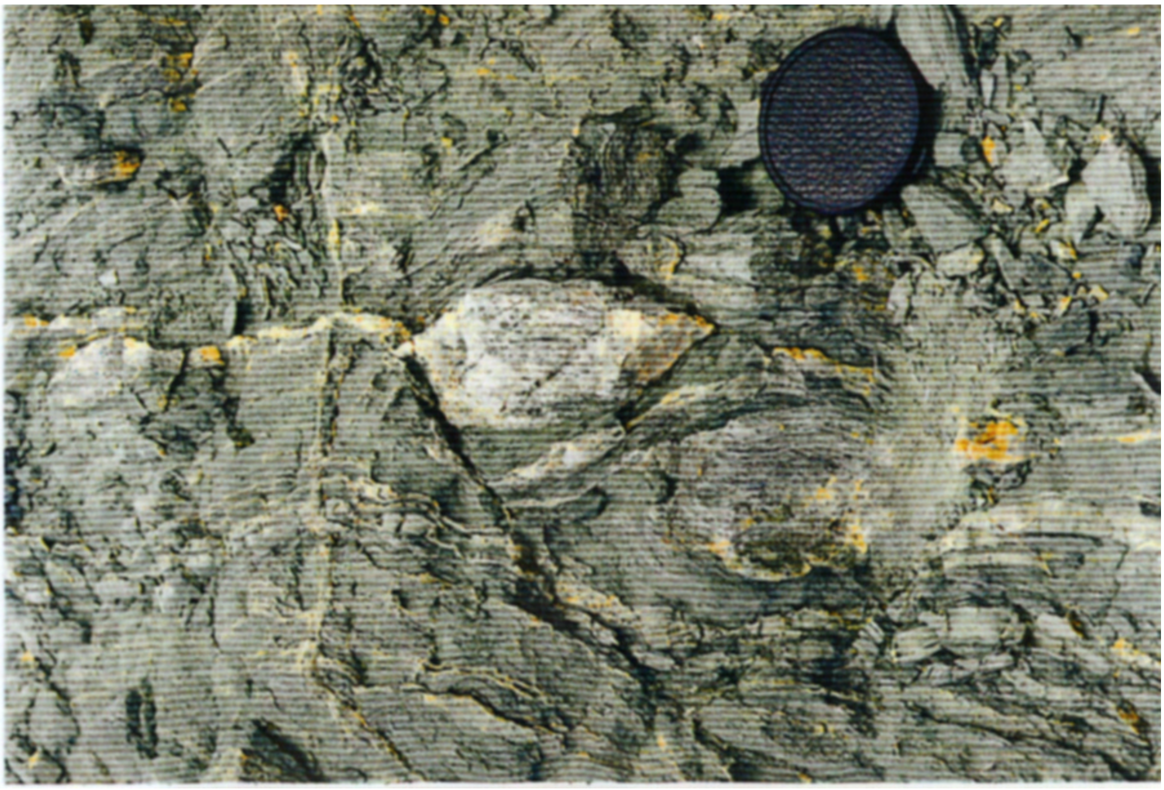

**Figure 7.5** Chlorite epidote quartz rock associated with the footwall of the coastal fault array, displaying boudinage and small scale late folding.

### *Stop #12* Metabasic volcanics

Chloritized outcrops of metabasic volcanics have intruded the detachment fault system, and may provide a constraint on the timing of these faults. The brecciated volcanic layer occurs along a low-angle normal fault, between a cream marble and schist layer. These rocks display volcanic textures with laths of plagioclase phenocrysts occurring in a felted groundmass of plagioclase, with chlorite and minor rutile, sericite and epidote.

Chloritic alteration and brecciation has taken place but no major ductile deformation or metamorphic effects on textures and minerals is apparent in this rock.

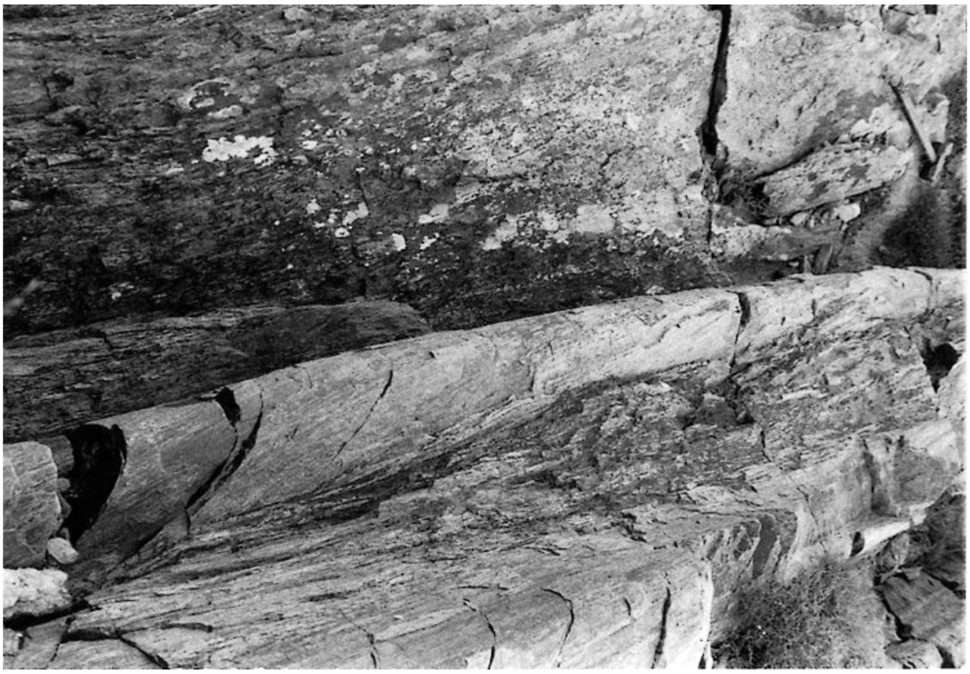

**Figure 7.6** Refolded folds in the graphitic quartzites, in the garnet-mica schist outcrops above the Port Beach. These folds are aligned with their fold axes trending N-S, but a mineral stretching lineation is folded around the hinge. These are probably D3 folds refolding L2 lineations, reoriented in the South Cyclades Shear Zone.

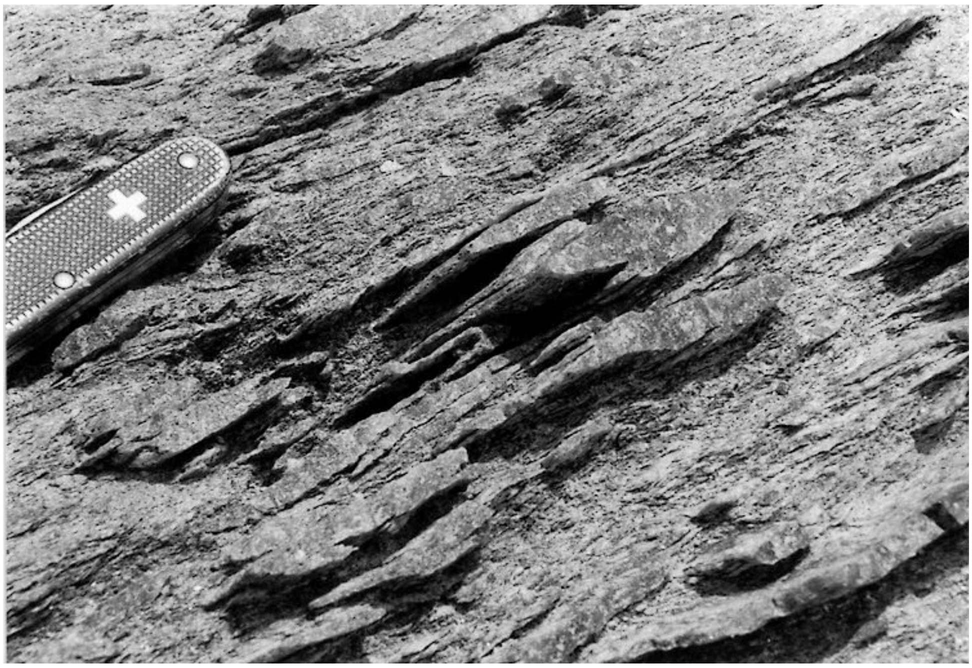

**Figure 7.7** Strongly attenuated quartz veins and quartz lenses that have been isoclinally folded, and intensely stretched. As a result, rootless fold hinges have developed. This photo was taken near stop #4. These are D3 folds that have been stretched subsequent to their formation, in the South Cyclades Shear Zone.

# Chapter Eight

## Evolution of the Ios upper plate

### Traverse 5 - Varvara Bouding to "Goat Beach"

*Marnie Forster and Gordon Lister*

## INTRODUCTION

The Ios core complex is located in a HP-LT blueschist belt in the Aegean Sea. However, this broad classification as a 'blueschist belt' disguises an array of assemblages ranging from eclogite facies assemblages to chlorite schist, produced from different protoliths which at times are difficult to determine. The upper plate consists of deformed and metamorphosed neritic carbonates, psammites, pelites, basic and acid volcanics, which are suggested to have been initially deposited during the Mesozoic (Van der Maar 1980). Deposition took place in a shallow marine environment on a continental margin (Boronkay & Doutsos 1994).

Previous workers (e.g., Van der Maar 1980) have described the upper plate as a "series", a layer-cake stratigraphy defined by an alternation of marble units and schists - where only some of the contacts are tectonic. However detailed mapping (Forster 1996) shows that the lower boundary of the massive marble units (not the narrow marble belt layers), where they come into contact with the underlying blueschist units, are always tectonic and defined by low angle extensional faults (Figs 7.2, 7.3, 8.5 and 8.6).

## MARBLE UNITS

The massive marble units display a lateral variations in both thickness and appearance. They are located at the outer edge of peninsulas along the west coast of the island, flanking the Ios dome, and on the high points on hills (Fig. 7.3). These larger units can range in thickness from

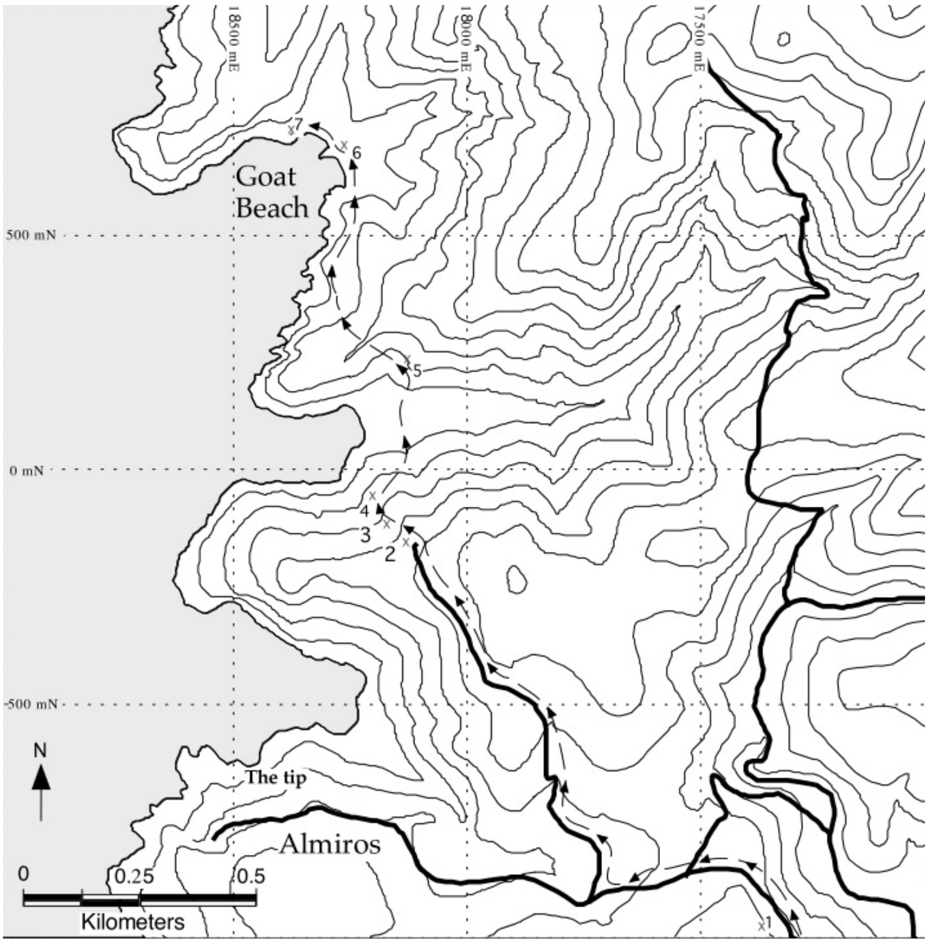


**Figure 8.1** Locality map of Traverse 5 - Varva Boudin to the "Goat Beach"

approximately 20 metres to at least 100 metres. The original thickness of these units is not known as the inferred basal contacts are always faults, while the upper contacts are eroded.

Narrow marble beds/layers are interbedded in the blueschist units and occur throughout the upper plate with no particular spatial pattern to the surrounding schist units. The marble beds display radically different deformational characteristics compared to the larger units, possibly due to the finer layering, but more likely due to substantially different P-T conditions during deformation. We suggest the blueschist units, with the interlayer marble beds, to have been exhumed beneath detachment faults, from substantially deeper levels.

The composition of the marble units and beds range from grey and cream calcitic to dolomitic marbles with local variations occurring, such as micaceous lenses, haematitic lenses, and haematite/limonite pseudomorphs after pyrite.

## BLUESCHIST UNITS

The blueschist units are dominated by rock displaying a schistose fabric. Minor intercalations of more massive lenses of a variety of different rock types, including metabasites, and marbles are present.

The blueschist units are characterised by chlorite schist, actinolite schist, glaucophanitic schist and quartz-mica schist (Van der Maar 1980) as well as narrow beds of dolomitic and calcitic marbles.

The rocks with a more massive appearance are albite-rich bands, glaucophanite lenses, eclogite lenses, magnetite and/or haematite lenses, and small lenses of ultrabasic material. These lenses have a more massive character compared to the more common schistose fabric observed in the blueschist units. Van der Maar & Jansen (1983) suggest that some of these different lenses within the blueschist units mark old tectonic contacts, simply due to the diverse origin of the different rock types.

The chlorite schist develops as a result of the retrogression of higher grade assemblages, the relict minerals being rarely preserved. They have a distinctive green colour and are often interlayered with epidote and albite/quartz-rich layers. Albite/quartz-rich layers typically display both micro-boudinage and micro-folding at the one site.

Large areas of chloritization occur below major faults and associated with fluid influx along these paths. It is also common for chlorite to occur as layers (≤ millimetres to several centimetres thick) in glaucophanitic or actinolite schists, representing the effect of fluid ingress along microscale joints, fractures and shear zones.

The actinolite schist is associated with greenschist facies overprinting of calc-schist or metabasics. Depending on original bulk composition, differing degrees of albite porphyroblastic growth takes place, producing layers of actinolite-rich and albite-rich assemblages. Actinolite schist can also be associated with the metasomatism of layers of glaucophanitic schists. Retrogression from glaucophanitic schists produces an assemblage dominated by actinolite with minor chlorite and epidote.

The presence of glaucophanitic schistwithin rocks of Ios characterises the regional blueschist belt and lead to the question of how they were preserved and exhumed. Glaucophanitic schists occur with a variety of mineral assemblages. These layers vary from glaucophane dominant layers (<20 centimetres thick), to fine layers with varying proportions of white mica and garnet porphyroblasts, or with varying amounts of clinozoisite and white mica. These rocks have been subject to varying degrees of greenschist facies overprinting and/or retrogression.

## METABASICS

Metamorphic assemblages derived from basaltic to ultramafic protoliths are preserved as eclogite boudins and minor glaucophane-rich assemblages.

Eclogite assemblages are typically preserved lenses within the blueschists. These lenses are important as they preserve an earlier history than the surrounding blueschist assemblages. The narrower eclogite lenses (<~1 m) are overprinted by later deformation and retrograde metamorphism. The larger boudins (<~10 m) preserve pristine eclogite assemblages (omphacite-garnet). These boudins occur within one kilometre of one another on the southwest coast of the area.

Massive Na-amphibole bands and lenses occur in close proximity to the eclogite boudins. Like the eclogite boudins, these Na-amphibole assemblages occur as isolated pockets and are relatively uncommon. They can contain garnet-rich layers with large Na-amphiboles (≤ 1 centimetre in length) with a typically more massive appearance than the surrounding blueschists. They may be derived from the eclogite boudins as the result of a second high pressure blueschist metamorphic event, subsequent to the eclogite facies metamorphism.

## ACCESS

This traverse cuts across the South Cyclades Shear Zone, the Ios detachment and the lower levels of the Ios upper plate. It ends at the headland north of “Goat Beach” where several faults of the Coastal Detachment array are exposed.

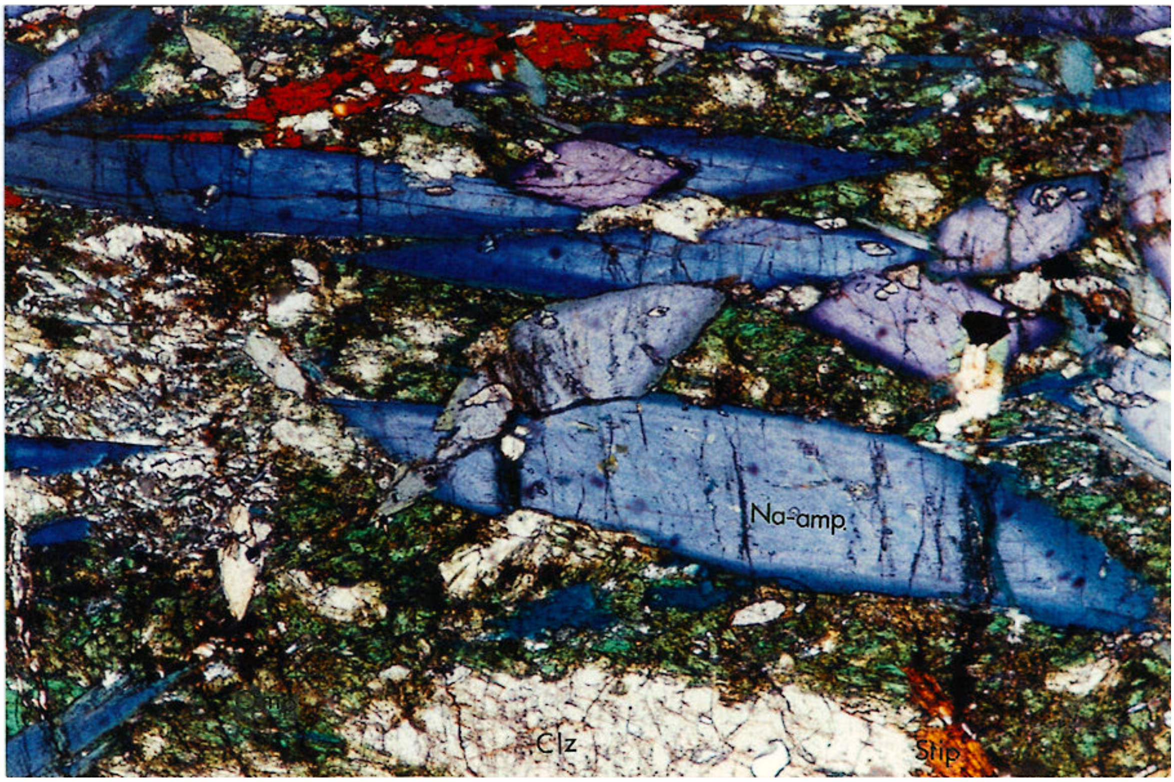


**Figure 8.2** Photomicrograph of M1c sodic-amphiboles overprinting M1b omphacite-garnet assemblage. Photo taken at 10X magnification under crossed-polarisers.

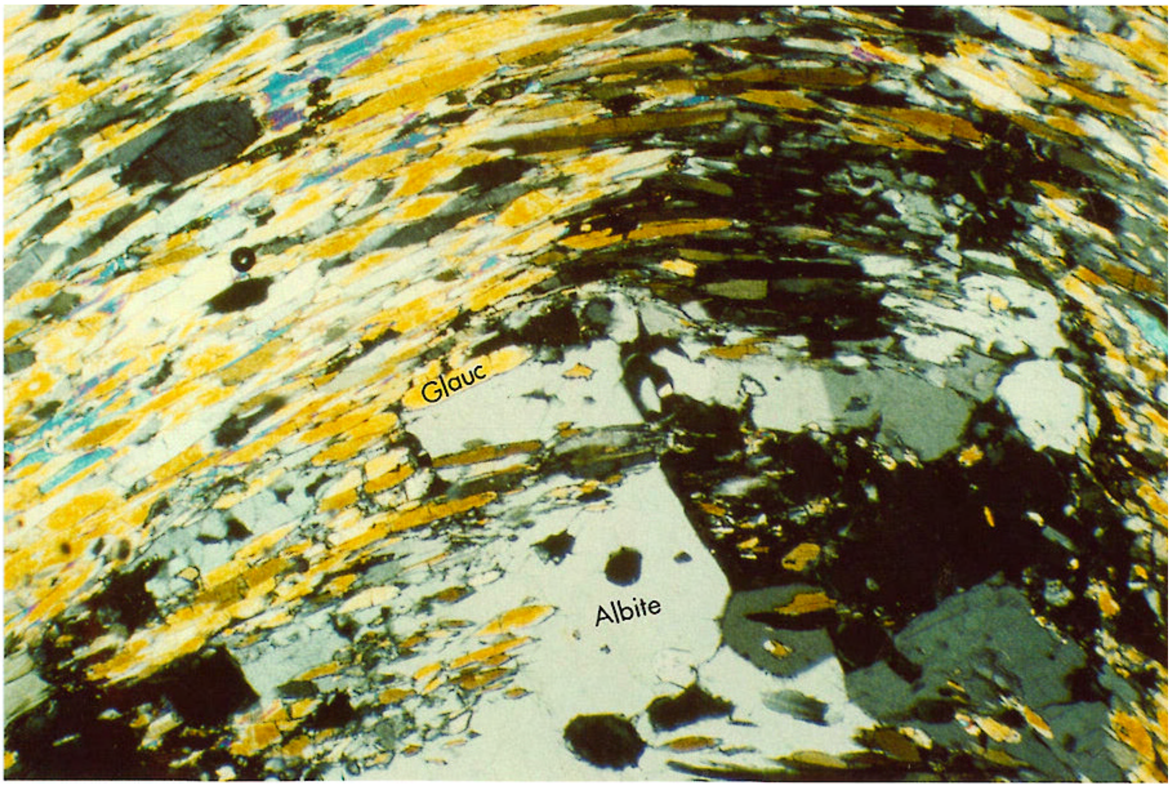


**Figure 8.3**. Photomicrograph of M2 albite porphyroblasts overgrowing M1c glaucophane assemblage. Photo taken at 10X magnification under crossed-polarisers.

Access is via the road to Almiros (the local tip). Follow the road to the right where it forks at the top of the first hill. Continue on this road to Varvara Beach, where the road descends steeply in a sequence of tight S-bends. The traverse continues on foot along a coastal path to “Goat Beach”, and on to the following headland where the Coastal Fault array is exposed. This is the end of the traverse (Fig. 8.1).

### *Stop #1* Leucogranite

On the ‘Rubbish Tip’road, immediately prior to the Ios detachment, 100 metres below the fault contact in the lower plate. This is an intensely deformed leucogranite schist mapped as a young stock (g1) by Van der Maar & Jansen (1983).

### *Stop #2* Phengite-rich zone

Note the phengite-rich rocks, of the upper plate, in the road cutting above the Varvara Boudin.

### *Stop #3* Varvara Boudin

This is the Varvara Boudin. It was narrowly missed by the new road down to the beach. It is found immediately beneath the first S-bend on the descent. PLEASE do not use hammers on this outcrop. It is not a large body of rock and it is rare to find even partially preserved eclogite in the boudins on Ios.

The eclogite boudin developed during an early period of metamorphism, M1b. This involved (see Forster 1996) the growth of omphacite and garnet over an earlier blueschist assemblage (M1a). The earlier assemblage can only be detected in inclusion trails within the porphyroblastic garnets.

Although the omphacite-garnet assemblage is preserved only within the core of the boudin, there is no reason to suppose that it was not more pervasively developed through the rock mass of the upper plate.

The boudin is mantled by a skin of sodic amphibole. This grew during a second period of high pressure blur-schist facies metamorphism (M1c), which was associated with blastic growth of sodic amphibole, white mica, and zoisite. The M1c blueschist assemblages overprint the M1b omphacite-garnet (eclogite) assemblage (Fig. 8.2).

The sodic amphibole progressively becomes more intensely lineated towards the outer skin of the boudin. The lineation trend (NW) is typical of glaucophane mineral lineations observed in this part of Ios. The lineations appear to have formed during the second penetrative deformation (D2), during which the dominant differentiated crenulation cleavage formed.The boudin is cut by numerous veins, infilled by monomineralic assemblages of sodic-amphibole or epidote.

### *Stop #4* Reoriented mineral lineations

Descend ~10 m to observe tight parasitic (east vergent) folds, and white mica, albite, carbonate and sodic

**Figure 8.4** Spectacular folds at “Goat Beach”.

**Figure 8.5** The peninsula northwest of “Goat Beach” showing multiple faults of the Coastal Detachment system.

amphibole porphyroblasts. On the fold limbs the sodic-amphiboles define a northwest mineral lineation, whereas in the hinge the prisms are reoriented in a north-south direction.

### *Stop #5* Massive glaucophanites

Descend the hill and climb ~40 metres up the opposite hill, on the other side of the beach, to a site where massive glaucophanitic assemblages can be found.

These massive glaucophanites are thought to be from the same protolith as the Varvara Boudin eclogites, however the M1c blueschist overprint has been more pervasive. Note the trend of the sodic-amphibole lineation in the glaucophanites is the same as in the Varvara Boudin eclogites (~northwest-southeast).

### *Stop #6* “Goat Beach”

Continue walking northward on the donkey trail along the coast to “Goat Beach”. The outcrop at the centre of the beach displays spectacular tight folds (D3?) in marbles and schists, adjacent to a shear zone in chloritized albite-phengite schist (Fig. 8.4). We will examine this fold closely, but as there are several features of interest at this outcrop we should walk around a little before focussing on anything in particular.

There is a lens of ultramafic rock exposed in the central gully. This may mark the location of a significant fault, possibly one that formed early in the geological history. Several lenses of ultramafic rock have been reported on Ios, as well as on other Cycladic islands. These are reported as marking older tectonic contacts (e.g., Feenstra 1985), for example thrusts that have juxtaposed ultramafic material (of mantle origin) against metasediments.

If such an old fault does exist, it will have been stretched and/or folded during later deformation events. Talc schists below the adjacent fold closure may support this hypothesis. The talc schist may have been derived from the ultramafic rocks, and folded along with the overthrust metasediments.

The synformal closure to the southeast of the ultramafic lens refolds the dominant fabric (S2), and thus is a fold that is either D3 or D4 in age (or an interference structure formed during both folding episodes). Some evidence exists to support the latter possibility. For example, some of the axial planes of the parasitic folds are themselves folded. Over-printed older folds can be found in the axial plane region, in the talc schist. These are rare. Please do not sample them!

Adjacent to these D3 folds (towards the northwest) a younger shear zone has deformed albite-mica schists (leading to the development of S-C fabrics), and mylonitized the adjacent marble beds (further to the northwest). This shear zone is only a few metres wide, but illustrates the effect of later deformations on older fabrics, and it demonstrates the linkage that exists between these shear zones and adjacent (earlier-formed) fold closures.

The schists have undergone early high pressure metamorphism (M1c), subsequent to which the (dominant) differentiated crenulation cleavage (S2) was imposed (during D2). Later greenschist facies metamorphism (M2) led to the widespread growth of albite porphyroblasts, and these in many cases statically overgrew the S2 fabric (Fig.

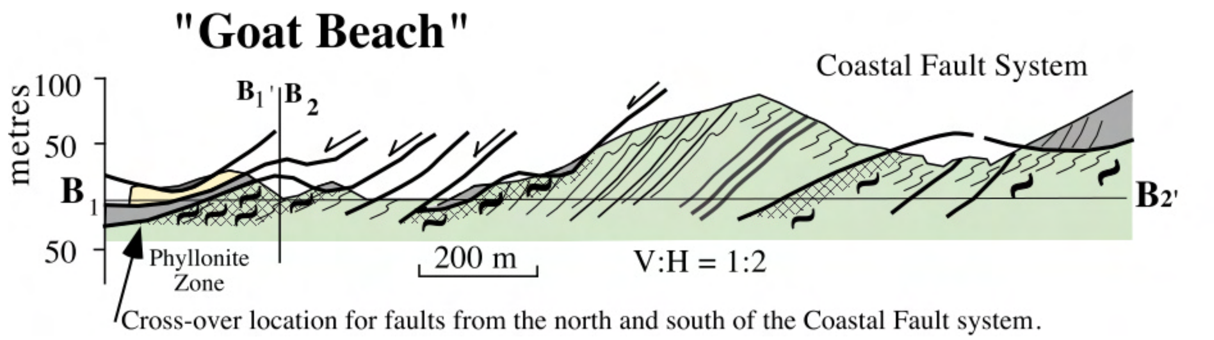


**Figure 8.6** Cross-section B of peninsula NW of the "Goat Beach" showing multiple faults of the Coastal Detachment Fault array.

8.3). Thereafter, during the period in which the South Cyclades Shear Zone formed (D4), the rock mass was stretched and sheared, and the earlier formed fabrics and microstructures were substantially modified.

In this outcrop, the effects of this later shearing are evident, with foliation planes wrapping around albite porphyroblasts, as well as well-defined S-C fabrics. These are south-directed at this locality. Lineations trend approximately north-south, both in the phengite schist and in the adjacent carbonates, although the actual attitude of the foliations is moderate to steeply inclined. This occurs due to their location on the dome flank, where foliations have been thrown into steeply-dipping orientations by later east-west shortening during dome formation.

At the northwest end of this outcrop (which can be reached by walking around the outcrop, or ascending the gully that contains the ultramafic lens) the marbles display lineations that are again northwest oriented. These are formed in the earlier period of shearing that affected these rocks (D2), during which the dominant fabric (S2) developed, and lineations (at least on Ios) formed with a NW-trend.

## *Stop #7* Coastal Detachment system

Climb the hill to the peninsula to the NW of "Goat Beach". This peninsula is sliced by multiple faults from the Coastal Fault array (Fig. 8.5). The structurally higher fault slices are defined by alternating massive grey, cream and grey marble units, underlain by a structurally lower schist unit (Fig. 8.6). The structurally lower grey marble slice is pinched out beneath the cream marble as a result of deformation associated with the emplacement of the cream marble.

The footwall of the lower grey marble slice is characterised by chloritized phyllonites produced by intense alteration of former glaucophane-bearing assemblages. A variation from purple to green alteration of these schists is due to the influences of oxidizing and reducing fluids.

The mylonitized chlorite schist located in the cliff face displays a NE-SW to E-W trending relative movement. These faults are associated with the Coastal Detachment Fault array, which thus shows a change in kinematics from the older N-S trending extension that characterizes the Ios Detachment Fault system. This intensely mylonitized chlorite schist occurs in a shear zone below a band of finely brecciated material in the fault zone.

## *Stop #8* Phyllonites

An additional stop for the enthusiastic participant is to continue northward up the hill to a site of fine grained interlayered green and silver phyllitic material (chloritized and graphitic). These phyllites occur in the footwall of the next structurally deeper slice of the Coastal Fault array. The hanging wall immediately above this fault contact displays what appears to be pencil structures occurring in the schist unit. Any suggestions or opinions on these structure will be most welcome.

# Naxos

# population ~21000

The Temple of Apollo was begun in 530 BC by the tyrant of Naxos, Lygdamis, on Palatia island. Of this 30 m temple, which was never completed, only the huge Portara remains. The portal was constructed to face towards the sacred island of Delos.

When the Venetian Marco Sanudos landed his boats on the SW corner of Naxos his band of mercenaries took one look at the island's fortifications and decided they weren't interested in fighting. To force his hired guns into action Marco Sanudi burnt his boats off the beach of Agiassos so there was no possibility of a return to Venice. The mercenaries laid siege to the castle of Apalirou for 6 months until the inhabitants' water supply ran out and they were forced to surrender, marking the beginning of Venetian dominance in the Aegean. The temple of Apollo at Naxos was constructed by the tyrant Lygdamis in 530 BC.

# Chapter Nine

## Evolution of the Naxos Core Complex

### Traverse 6 - Ano Potamia to Moutsouna

*Sue Keay and Gordon Lister*

## INTRODUCTION

Naxos was one of the first metamorphic core complexes recognised in the Aegean. Initially it was suggested that Naxos resembled metamorphic core complexes found throughout the North American Cordillera (see Lister et al. 1984). However, detailed work in the intervening decade (e.g., Urai et al. 1990, Buick 1991a, b) has made it clear that Naxos has several quite distinctive characteristics. The geology in many aspects bears little resemblance to that of U.S. style core complexes, although there are still many points of correspondence (see §2). There is more in common with the sillimanite-cored mantled gneiss domes reported from the Seward Peninsular (Miller et al. 1992). A schematic illustration of the geology of Naxos is shown in Fig. 9.1 (modified from Jansen & Schuiling 1976).

## GEOLOGY OF NAXOS

Naxos is a mountainous island with a rugged interior defined by a deeply eroded N-S trending elongate structural dome. We will examine a profile of the eroded dome from the vantage point offered by Stellida, in the NW of the island (see Figs 9.1, 9.2 and §11).

Like Ios, Naxos consists of a variegated sequence of deformed and metamorphosed Mesozoic platform sediments (Dürr et al. 1978) which are underlain by Hercynian basement gneisses (Andriessen et al. 1987). The entire metamorphic complex is overlain by relatively undeformed Mio-Pliocene sediments (Roesler 1978). The non-metamorphic cover is separated from the metamorphic complex by low angle normal faults (Lister et al. 1984). Conglomerates from the eroding dome were shed onto the dome flanks, and overlie all of these rocks unconformably.

The rocks comprising the lower plate have undergone at least two Alpine regional metamorphic events. Eocene high pressure, low temperature metamorphism (Van der Maar & Jansen 1983, Ridley 1982) took place early in the Alpine history, followed by an Oligo-Miocene medium pressure, high temperature event. This regional greenschist facies Barrovian metamorphic event has reached amphibolite facies grade on Naxos. Because of widespread replacement by younger metamorphic minerals, Alpine high pressure mineral assemblages are only preserved in the south-eastern corner of the island.

A relatively large I-type granodiorite has intruded in the western part of the island, associated with minor contact metamorphism. In the north a number of small bodies of granitoid have intruded before, during and subsequent to Barrovian metamorphism. A larger granite body may exist in the subsurface, associated with swarms of aplite and pegmatite dykes (see §10).

## LITHOLOGIES

Mesozoic Units - these consist dominantly of marble (especially in southern Naxos) intercalated with dolomite. They contain lenses of metabauxite, and are presumed to be Jurassic in age (Feenstra 1985). Other units include metapelites and psammites, amphibolites, ultrabasic pods, calc-silicates, felsic metavolcanics, graphitic quartzites and rare orthogneisses.

Hercynian Basement - this is comprised of a range of orthogneisses restricted to the migmatitic core of the Naxos dome. These gneisses show remarkable similarity to the basement of Ios (Andriessen et al. 1987). The orthogneisses show a varying degree of migmatisation, increasing towards the central portion of the core.

Naxos Granodiorite - in the west of Naxos there is extensive outcrop of a medium to coarse-grained granodiorite/quartz monzonite. This consists of plagioclase, quartz, green hornblende, biotite and sphene, interspersed with large phenocrysts of K-feldspar. It contains numerous microgranular enclaves (Didier 1973, Didier & Barbarin 1991).

Other Intrusives - mainly S-type granites (including biotite, garnet-tourmaline, and garnet-two mica types). Some fractionated I-type granites have been identified by the appearance of sphene, and by virtue of their uncomplicated zircon populations (Keay, unpubl. data).

Non-metamorphic sediments and remnants of the Cycladic ophiolite nappe - these consist of serpentinites and non-metamorphic sediments ranging from Upper Permian to Pliocene (Roesler 1978).

## METAMORPHISM

Four main periods of metamorphism were distinguished by previous workers:

M1 - Alpine high pressure, low temperature metamorphism, assigned a minimum age by Rb-Sr and K-Ar dating of white micas from Zones 1 & 2 (see below), at 45 ± 5 Ma (Middle Eocene). As noted on Ios, there is excellent evidence that more than one episode of high pressure metamorphism took place.

M2 - medium pressure, high temperature Barrovian metamorphism, dated by Rb-Sr and K-Ar analysis of a range of minerals from Zones 3 to 6 (see below), at 25 ± 5 Ma (Late Oligocene/Early Miocene). Estimated ages appear to decrease according to increasing metamorphic grade. The youngest ages were thought to signify prolonged cooling after peak metamorphism until 11 Ma (Late Miocene), according to biotite K-Ar ages obtained from Zone 6.

M3 - the age of contact metamorphism initiated by intrusion of the western granodiorite of Naxos, with a minimum age of 11.1 ± 0.7 Ma determined from a Rb-Sr whole rock isochron. This isochron was derived from aplitic and pegmatitic dykes that cut the main granodiorite body.

M4 - a retrograde metamorphism supposedly recorded by a K-Ar date from a pseudotachylite veinlet, as 10 Ma. A similar age is also seen in four mineral dates from other areas of Naxos.

## THE NAXOS DOME

The Naxos dome was originally described as a thermal dome (see Jansen & Schuiling 1976). However the domal structure of the island reveals itself in the orientation of gneissic fabrics in a major ductile shear zone that acts as the carapace to the central migmatite core. This shear zone appears to have been bowed up relatively late in the history of deformation and metamorphism, so essentially, the Naxos dome is structural in its origin.

A series of apparent ‘isograd’ surfaces are detailed in Fig. 9.1 (modified after Jansen 1973a&b, Jansen & Schuiling 1976). This zonal pattern of increasing grade of metamorphism corresponds with increasing structural depth, with maximum crustal depth (and highest metamorphic grade) being reached in the core of the Naxos dome. Yet these ‘isograd’ surfaces are parallel to the carapace shear zone that bounds the central migmatite core, and they appear to have been deformed by it. A traverse across the Naxos dome therefore may represent a considerably attenuated section of the Earth’s crust.

A complete Barrovian facies sequence is exposed on Naxos, involving progressive metamorphism ranging in temperature from ~380 to ~700°C (Jansen & Schuiling 1976, Buick & Holland 1989, 1991). Peak metamorphic conditions in the migmatite core have been estimated to have risen from ~600°C (at 8-10 kbar) to ~670°C (at 6-8 kbar) (Buick & Holland 1989). This implies a temperature rise while significant decompression took place, and led Buick & Holland (1989) to conclude that “the entire history of M2 deformation and metamorphism on Naxos occurred during active extension”.

## THE METAMORPHIC ‘ISOGRADS’

Pelitic and bauxitic units have been used to determine the reaction isograds (Jansen 1973a,b, Jansen & Schuiling 1976).

In Zone 1 (diaspore) the pelites show greenschist assemblages (albite-quartz-chlorite-sericite) while meta-bauxites contain diaspore-chloritoid-hematite. Mafic metavolcanics are largely composed of glaucophane relict from the earlier (Eocene) period of high pressure metamorphism.

In Zone 2 (chlorite-sericite) diaspore in the metabauxites has reacted with water to form corundum. These rocks have the assemblage corundum-chloritoid-haematite.

Zone 3 (biotite-chloritoid) is defined by the consistent appearance of biotite in pelites and disappearance of the chlorite-muscovite assemblage. This represents the transition from greenschist to amphibolite facies conditions. Margarite and chloritoid commonly occur in the bauxites.

Zone 4 (kyanite) is defined by the disappearance of chloritoid in both pelites and metabauxites. This zone is also noted for the appearance of staurolite in the metabauxites, and kyanite and staurolite in the pelites.

Zone 5a (kyanite-sillimanite transition) is marked by the first appearance of sillimanite in pelites and the disappearance of staurolite. Staurolite remains stable in the rare meta-bauxite lens in this zone.

Zone 5b (sillimanite) is delineated by the disappearance of kyanite, although this does not represent a true isograd surface. In fact the zone contains several kyanite-bearing pelites! These have only relatively recently been recognised (Buick & Holland 1989). Primary margarite has disappeared from metabauxite assemblages which reach their highest grade in this zone.

Zone 6 (the migmatite core) is marked by the beginning of anatexis. This zone contains only isolated “rafts” of presumably Mesozoic marbles and pelites. A granitic melt appears in the pelitic units which are generally sillimanite-rich, although kyanite has not entirely disappeared from

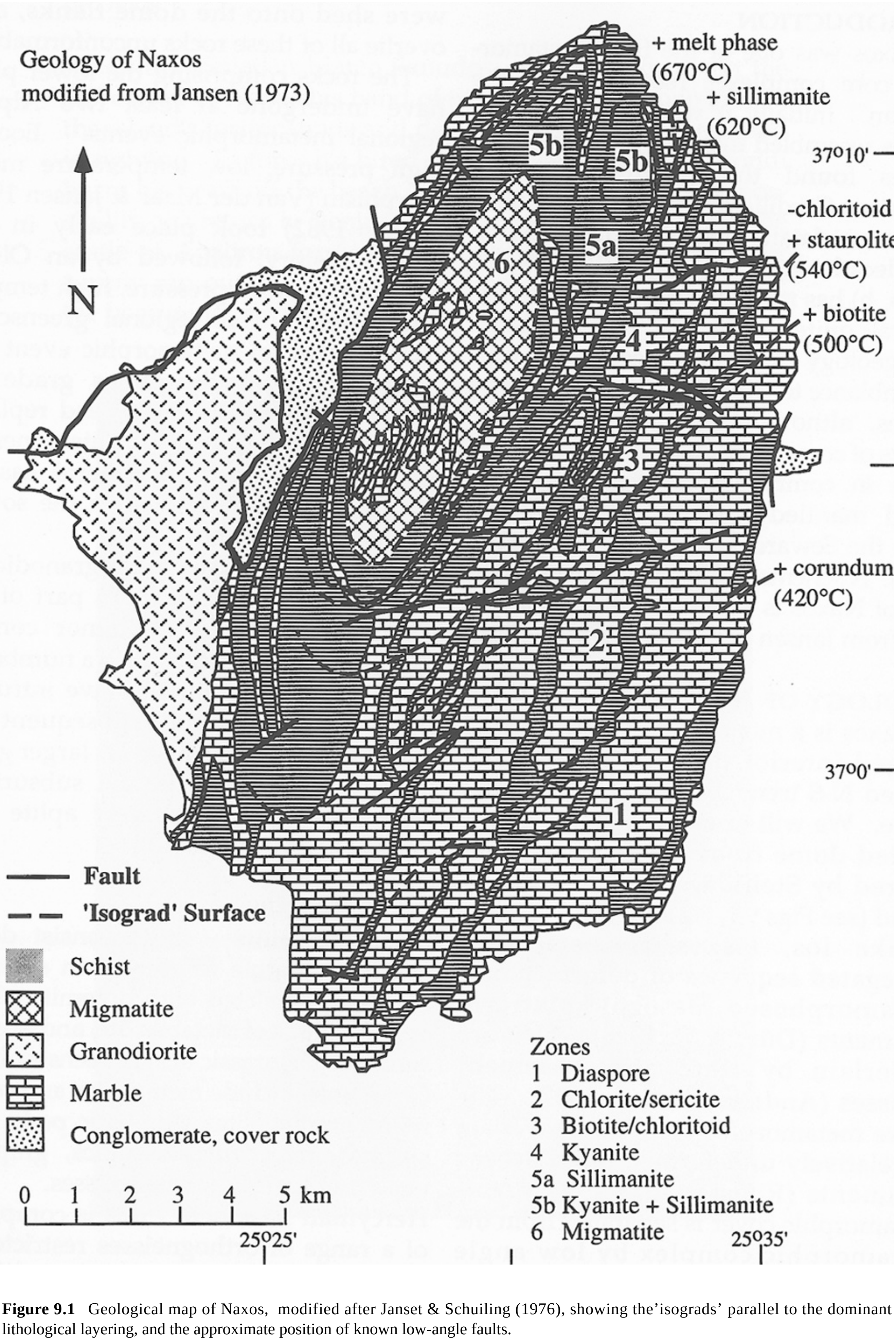


**Figure 9.1** Geological map of Naxos, modified after Janset & Schuiling (1976), showing the'isograds' parallel to the dominant lithological layering, and the approximate position of known low-angle faults.

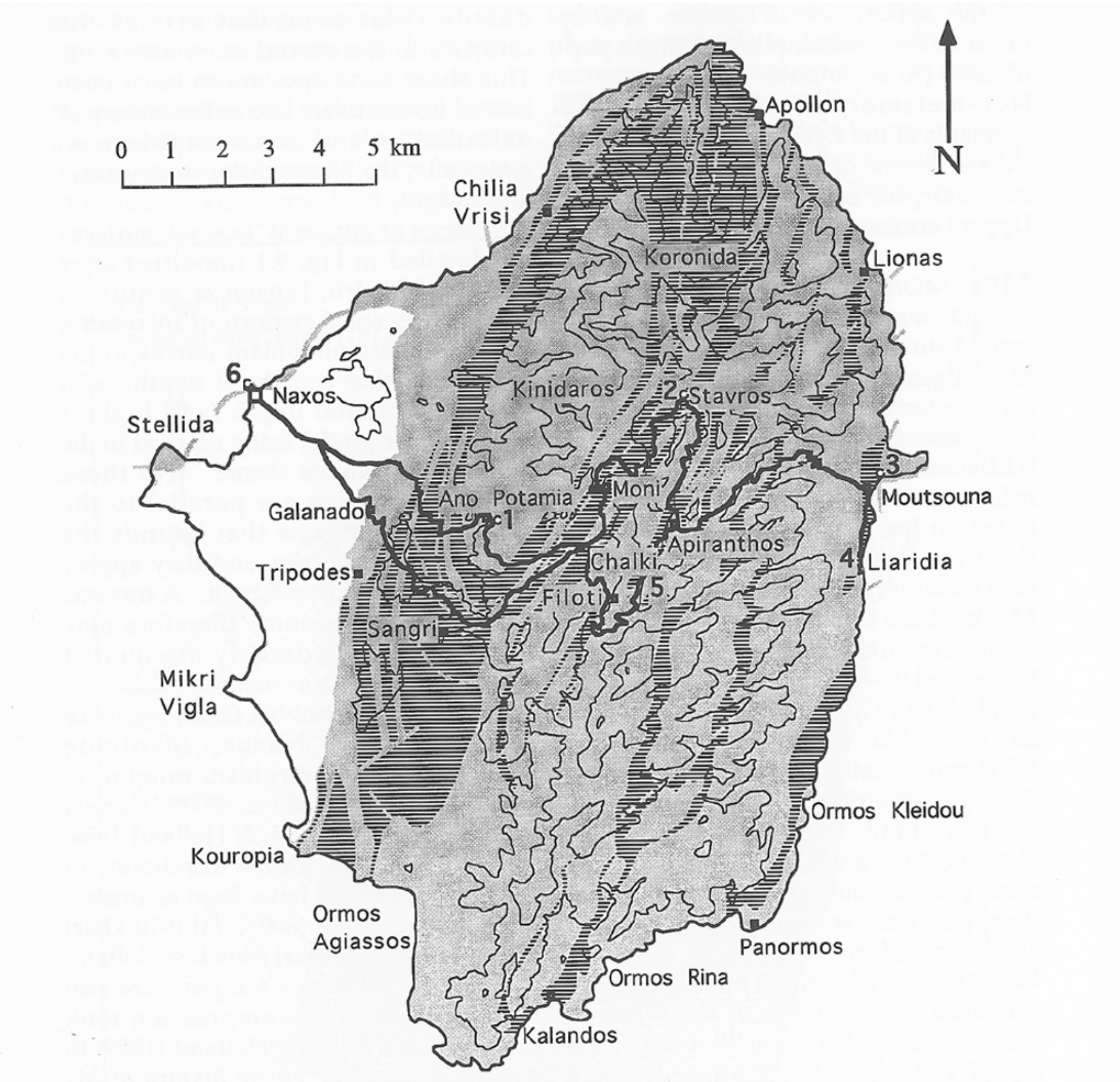


**Figure 9.2** The route followed by this transect, and different localities and stops that will be visited.

the pelites, even at this grade (Buick & Holland 1989, 1991). The marble shows a marked increase in grain size, improving the marble quality for commercial exploitation.

## GEOCHRONOLOGY

Until isotopic studies of the Cyclades were undertaken (e.g., Andriessen 1978), little was known about the temporal evolution of the region except from rare palaeontological identifications, and dubious correlations with other Alpine terranes. On Naxos, both Permian limestones (Marks & Schuiling 1965 in Jansen & Schuiling 1976) and lower Pliocene sediments (Roesler 1978) were identified in upper plate rocks, while Triassic algae were tentatively identified in the lower plate marbles (Dürr et al. 1978).

Andriessen (1978) and Andriessen et al. (1979) provided a com-prehensive geochronological frame-work for the geology of Naxos from extensive K-Ar and Rb-Sr age dating. Andriessen's data for M1 is consistent with dating from Sifnos (Altherr et al. 1979) where M1 assemblages have undergone minimal M2 overprinting. These give 41-48 Ma ages from K-Ar dating of phengites.

Altherr et al. (1982) obtain a seemingly incongruous K-Ar age of 14.7 ± 0.3 Ma for a hornblende from the high grade portion of Naxos, an age they attribute to possible impurities in the sample. The same workers also measured a fission track apatite age from the main granodiorite at 8.2 Ma, which they suggest records the time of cooling below 120˚C.

The basal unit of Naxos shows similar characteristics to basement rocks exposed on nearby Ios, known to be pre-Alpine in age (Henjes-Kunst & Kreuzer 1982, Van der Maar & Jansen 1983). A Rb-Sr and U-Pb study of the Ios basement revealed a Hercynian age, and was thought to chronicle the metamorphism of the orthogneisses. An age of 300-305 Ma was obtained by conventional U-Pb zircon, while a 500 Ma Rb-Sr whole rock isochron was obtained for relict intermediate intrusions. Since these intrusions had largely escaped polyphase deformation, this age was interpreted as an original igneous emplacement older age (Henjes-Kunst et al. 1982).

Conventional U-Pb zircon work on the migmatite on Naxos has confirmed the existence of pre-Alpine basement on Naxos, yielding a zircon crystallisation age of 372 Ma (+28/-24) after coarse zircon fractions were removed to minimise the effects of inherited radiogenic Pb (Andriessen et al. 1987). Another attempt to conventionally date zircon from Naxos was not successful, with Henjes-Kunst et al. (1988) finding they could not obtain a meaningful age of emplacement for the Naxos granodiorite from 7 multi-grain zircon and uranothorite separates. They concluded that the zircons had undergone partial Pb loss without being influenced by any thermal overprint.

More recent dating has utilised 40Ar/39Ar age spectrum analysis. The application of this technique to evaluating timing relationships on Naxos revealed ambiguous ages thought to result from mixing of at least two separate white mica populations in the multigrain analyses (Wijbrans & McDougall 1988). Further work suggested that M1 occurred before 50 Ma, using the age of white micas from Zone 1.

We will return to other issues in relation to geochronology at various points during the excursion.

## ACCESS

Naxos is the largest island of the Cyclades (21 by 18 km2) with a good, if somewhat complex and changeable road system. Transport around Naxos will be by bus for all three traverses on this island. Most of the locations are either along road-cuts or a short walk from the nearest road. Each traverse starts from and returns to the town of Naxos. The location of this traverse and the main stops are shown in Fig. 9.2. This first traverse across Naxos will allow us to view the carapace shear zone that mantles the migmatite core of the Naxos dome (at its southern end). We will then view what has been suggested to be one of the major detachment faults in the Cyclades, at Moutsouna, and the intense zone of shearing that lies immediately beneath this late brittle fault.

## STRUCTURE

The structural development of Naxos is not well understood. Gautier & Brun (1994) use cartoons based on models developed for Basin and Range geology which implicitly address the question as to how the particular detachment faults form. These authors have opted for a model based on progressive rotation of high-angle normal faults. However, even in the U.S. core complexes, where much of the debate as to the nature and origin of detachment faults has been centred, this type of model may have little validity (e.g., see Scott & Lister 1992). There are no strongly rotated tilt blocks reported on Naxos or Ios, as is required by the model of Gautier & Brun (1994), and disruption of the upper-plate by sequences of highly rotated tilt blocks is not a feature of the Aegean core complexes. Contrary to the cross-section of Naxos produced by Gautier et al. (1993), there is no data to support the existence of a domed foliation in the western granodiorite of Naxos.

There is a zone of mylonitization and chloritization beneath the Naxos detachment, but this is confined to a domain a few hundred metres thick, below the northward dipping low-angle normal fault that bounds the northern coastline. As on Ios, there are likely to be several generations of detachment faults, operating under the influences of different kinematic frameworks.

Alternative (but still schematic) cross-sections of Naxos are illustrated in Figs. 9.7 & 9.8, based on reports prepared by students from Columbia University (Lamont-Doherty Geological Observatory) during a six week field excursion in 1986. Some modifications have been made, based on subsequent field work. Figure 9.3 shows a schematic N-S cross-section through the Naxos dome, with the central migmatite core and its carapace shear zone.

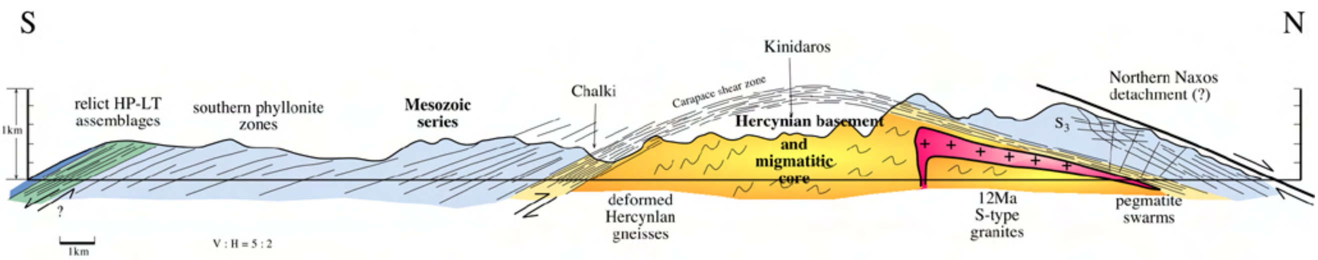


**Figure 9.3** A schematic N-S cross-section through Naxos emphasizing the main structural features. The Hercynian core is exposed at the core of an elongate structural dome, and has been subjected to the highest grade of M2 Barrovian facies metamorphism. Partial melting took place and migmatites developed. The sillimanite cored gneiss dome of Naxos resembles those described by Miller et al. (1992). No data exists for sense-of-shear in the phyllonite zones recognized in the south of the island. The carapace shear zone of the Naxos gneiss dome has been folded during (later) E-W crustal shortening. The sense-of-shear is invariably north-directed.

### *Stop #1* Ano Potamia

**Naxos grid [-2810E, -20930N]**
**Map 7642.3F Zone 6**

Following the road east from the village of Kato (Lower) Potamia to Tsikalaria, the transition from the "Series" rocks into the migmatite core can be traced along the road cutting as we travel across the southern edge of the Naxos dome. Strongly lineated layers of marble, pelite and amphibolite make up the "Series" rocks while layered leucogneisses, strongly foliated, isoclinally folded and cut by open folded pegmatites and S-type "dykes" cutting at an angle to the foliation, comprise the core.

The similarity between the core on Naxos and the Hercynian basement recognised on Ios has led many workers to suggest that the core of the Naxos gneiss dome is also Hercynian (see previous). SHRIMP U-Pb dates from this area confirm this idea and show a remarkable similarity between the ages of the granite protoliths of Ios and Naxos (Keay et al., in prep.).

We will first stop just before Mesi (Middle) Potamia to view the southern portion of the dome and trace the transition from Series rocks to core from west to east.

Our main stop will be SE of Ano (Upper) Potamia to examine the carapace shear zone of the migmatitic core of the Naxos gneiss dome (see Figs. 9.3 & 9.4). The degree of mylonitization is variable. We will be able to examine the range of rock-types in the core, many of which have begun to undergo partial anatexis.

The timing of the migmatisation has been poorly constrained but SHRIMP U-Pb dating of fine new growth rims on zircon grains suggests that migmatisation occurred at 17-18 Ma (Keay et al., in prep). The gneisses consist of a variegated sequence of K-feldspar to plagioclase-rich gneisses and rare "rafts" of pelite.

### *Stop #2* Stavros

**Naxos grid reference [5055E -16130N]**
**Map 7633.7D Zone 4**

The pass at Stavros is the highest point on Naxos allowing an unobstructed view to both the east and west coasts of the island. To the west one looks across the migmatite core, over the western edge of the Naxos dome, into the plains atop the Naxos granodiorite. To the east, across the marble dominated eastern rim of the gneiss dome, the view towards Moutsouna reveals the major detachment fault we are about to visit. In the distance on the coast the contact between the marble/schist sequence of the lower plate and the essentially unmetamorphosed sediments of the upper plate can be distinguished. The upper plate can be seen forming the easternmost tip of the coastline, forming a prominent headland, dark brown in colour (see Fig. 9.5).

### *Stop #3* Moutsouna

**Naxos grid [10500E -19500N]**
**Map 7643.3E Zone 2**

Within the Aegean core complexes of Naxos, Mykonos and Paros, there is a late generation of low-angle normal faults that might be equivalent to the spectacular detachment faults observed in the North American Cordillera. These faults have been responsible for the juxtaposition of remnants of the so-called Cyclades ophiolite nappe against the metamorphic tectonites of the lower plate.

Walking north following the coastline from the small fishing village and emery port of Moutsouna, we cross over one of the major detachment faults in the Cyclades. A flat plane of marble and schist forming the lower plate can be seen juxtaposed against a melange of upper plate sediments (see Fig. 9.6).

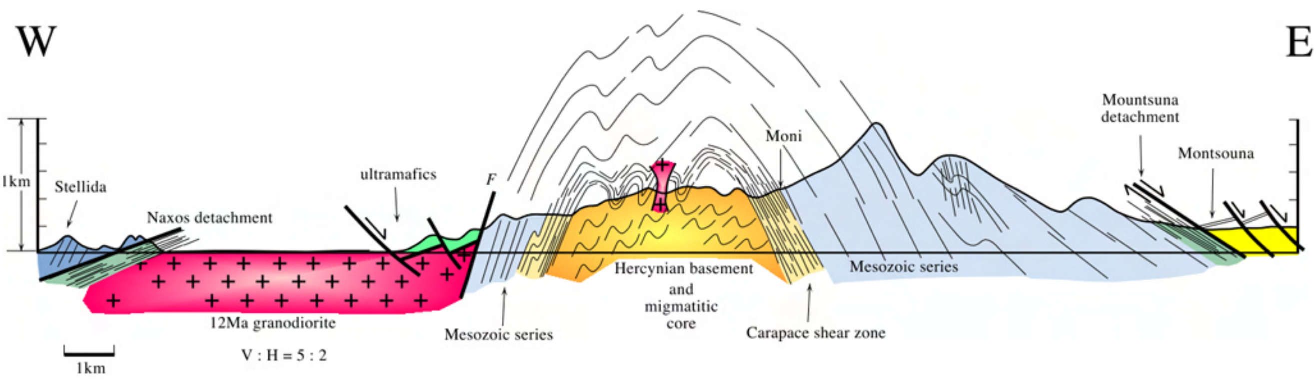


**Figure 9.4** A schematic E-Wcross-section through Naxos emphasizing the main structural features. The Hercynian core contains 'rafts' of Mesozoic marbles and schists subject to the highest grade of M2 metamorphism. The core is dominated by upright folds, and these may also affect the carapace shear zone. The extent of E-W crustal shortening during Miocene extension has been greatly underestimated. The mylonites on the dome flanks are often steeply dipping, in particular on the western flank. The sense-of-shear is invariably north-directed, on both sides of the dome.

**Figure 9.5** Deformed Hercynian granites, south of the main road to Chalki. These intensely deformed granite schists define the carapace shear zone of the migmatite core of the Naxos gneiss dome.

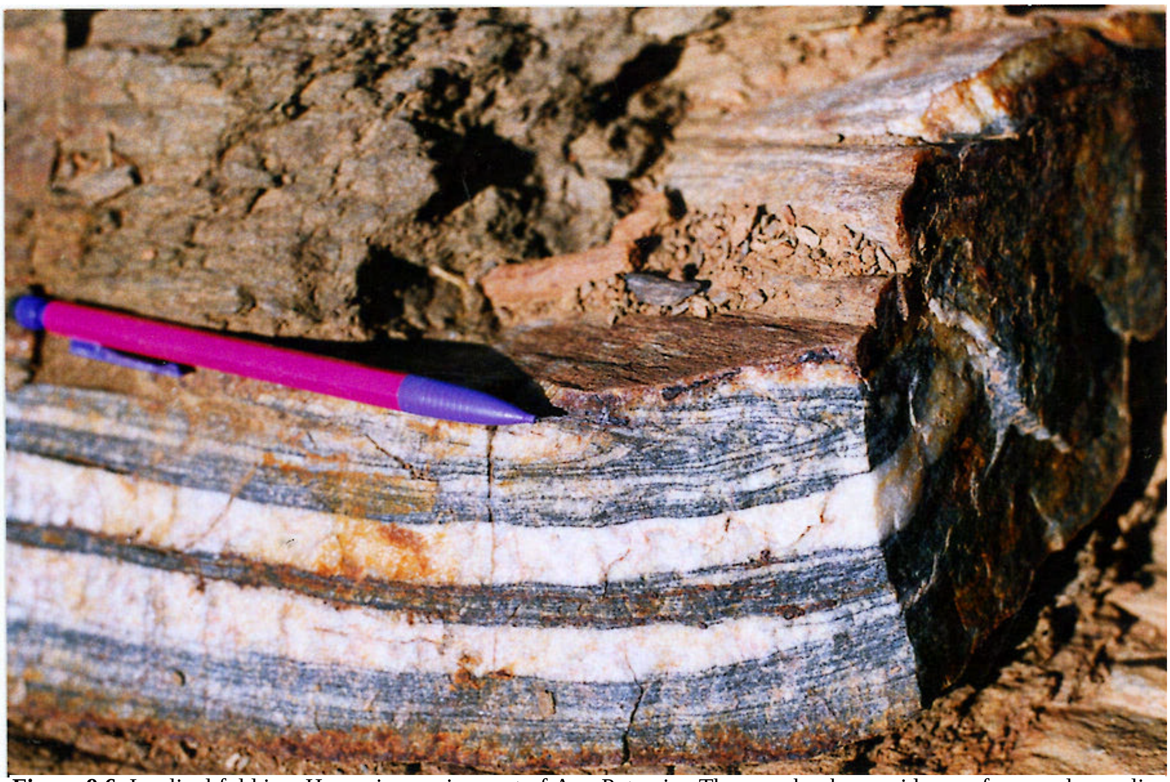

**Figure 9.6** Isoclinal fold in a Hercynian gneiss, east of Ano Potamia. These rocks show evidence of a complex earlier history, but are still caught up in the (north-directed) carapace shear zone of the Naxos dome.

The upper plate consists of Early-Mid Miocene marine sediments, age determined from foraminifera and molluscs (Roesler 1978), associated with ophiolites. Coarser paralic and fluvial conglomerate deposits also occur with pebbles of ophiolite and non-metamorphic rocks predominating (Fig. 9.9), ranging in age from Oligocene to Palaeozoic (Roesler 1978). These have undergone only prehnite-pumpellyite metamorphism. Apatite fission track analysis (Dumitru, unpubl. data) indicates a cooling age of ~50 Ma for some pebbles. Pebbles include ultramafics, chert and gabbro, that may have been shed from an ophiolite sheet (the Cyclades ophiolite nappe, Dürr et al. 1978). On the hillside above this location there is a large lens of serpentinite.

The "ophiolite" nappe is named because there is a collection of different rock types that are typical of an ophiolite sequence. These overlie low-angle faults, and are exposed at many different localities throughout the Cyclades. At first these low-angle faults were identified as thrusts. There was considerable mystery associated with the fact that the rocks above the low-angle faults were so highly faulted and disrupted, and only rarely were thicknesses in excess of 100 metres of any stratigraphic succession preserved. It is has become recently evident that they are low-angle faults that juxtapose rocks that have been formed at vastly different crustal levels.

The rocks of the upper-plate are oftentimes unconsolidated sediments, for example consisting of well-rounded boulders and pebbles of a provenance that is completely unrelated to the metamorphic tectonites of the lower plate. Pebbles include cherts, as well as other elements of an ophiolite provenance, as we will see at Moutsouna.

The Moutsouna "detachment fault" is quite different in its character to its counterparts in the Colorado River extensional corridor. Yet there are some characteristics that are similar. The low angle fault at Moutsouna does not have a microbreccia ledge, but it does cut through the underlying schists and carbonate lenses knife-sharp on a single surface, at a low intersection angle. There is no evidence of extensive metasomatic alteration of the upper plate, and the potash and iron metasomatism that is so characteristic in the U.S. core complexes is absent.

It is difficult to explain the existence of this single fracture surface which has allowed considerable movement on a low-angle fault in an extensional situation. There has been insufficient friction to allow any disruption of the underlying material and the juxtaposition of upper- and lower-plate occurs on a single surface. Even on a scale of centimetres, the fault has not disrupted the schistosity of gentle undulations in the footwall fabrics. These are cut sharply and cleanly, with no evidence of "reactivation".

Perhaps the only way to explain the existence of such faults is to suppose they were initially tension mode fractures that were filled with fluid during the movements that allowed their formation?

Note also at this locality the later conglomerates that shed from the Naxos dome, while it was being eroded during the last stages of its geological evolution.

**Figure 9.7** View of the non-metamorphic rocks in the upper-plate of the Naxos core complex, exposed above a N-S trending normal fault near Moutsouna, eastern Naxos.

**Figure 9.8** The low-angle normal fault north of Moutsouna is overlain by poorly consolidated conglomerate containing clasts of chert, and limestone. It is also overlain by a massive serpentinite lens. Note the essentially planar nature of this fault, which cuts through a folded schist and carbonate sequence with complete disregard for the orientation of existing layering.

Note also the intensity of ductile deformation in the schists and carbonate lenses below the Moutsouna "detachment". These fabrics, while relatively youthful, appear to have nothing to do with the later brittle low-angle fault.

### *Stop #4* [37°03.85'N 25°35.11'E]

### Naxos grid [10330E -20960N]
### Map 7643.4F Zone 2

Follow the concrete steps down into the protected beach at Liaridia, south of Moutsouna. Abroken fold in the marble is a good example of the E-W compression which accompanied exhumation of the Naxos dome (see Fig. 9.10). The sequence consists mainly of marble interbedded with some dolomite and mica schist. Astrong lineation in mica schists (22 __> 193) has developed. Under the cliff there are spectacular examples of transposition in a young shear zone (see Fig. 9.11). The lithological layering is completely disrupted, and there are numerous examples of isoclinal fold hooks.

Dolomite in marble forms boudins showing a north-directed sense of shear. Marble itself forms chocolate tablet boudinage structures in the schist. Numerous isoclinal fold hooks defined by quartz veins in the schist are visible, but S0 traces are harder to decipher. The dominant cleavage in the pelite is a crenulation cleavage which is in turn weakly crenulated to form a weak spaced cleavage parallel to jointing surfaces. Follow the cliff around to find examples of dolomite clasts with asymmetric tails (revealing a north-directed sense of shear).

### *Stop #5* Filoti lookout

### Naxos grid [3550E, -21650N]
### Map 7642.4F Zone 4

On the road from Apiranthos to Filoti, stop at the lookout for a bird's eye view of the southern portion of the Naxos dome looking west. We can trace the route we took from our first stop across the core and into the mountains. The flat plains of Livadia, formed on the Naxos granodiorite are also visible. The stop is located in metasediments on the eastern flank of the Naxos dome.

### *Stop #6* Temple of Apollo

### Naxos grid [-8500E, -15600N]
### Map 7631.8D

Walking from the Paralia (in Naxos town) across a narrow isthmus to the small islet of Palatia, we come to the most noticeable of Naxos's landmarks. Resting on a thick sequence of conglomerate is the imposing marble-pillared portal to the Temple of Apollo (600 BC?), aligned to face towards the sacred island of Delos.

In contrast to the conglomerate at Moutsouna, the pebbles in this sequence are primarily derived from the metamorphic basement, shed from the imposing heights of the Naxos dome as it eroded. Freshwater gastropods date the conglomerate as Upper Pliocene (Roesler 1978). The formation of the conglomerate probably indicates the emergence of the metamorphic core complex above sea-level approximately 2 million years ago.

This huge alluvial fan deposit eroded from the dome of Naxos contains a variety of rounded clasts up to 1 metre in diameter in a coarse sand matrix. Close to the granodiorite the upper plate is cut by numerous quartz veins - honeycomb style weathering makes the quartz veins more prominent. (If you wait long enough, rumour has it that when the Byzantine capital of Greece, Constantinople, once again becomes Greek territory the gates of the portal will close).

**Figure 9.9** Upper-plate conglomerate containing pebbles and boulders up to 10 cm diameter consisting of chert, neritic limestone, serpentinite fragments, and gabbro.

**Figure 9.10** Late-stage E-W shortening was associated with the formation of island-scale doming, producing parasitic folds and locally, small reverse faults. This fold, and associated reverse fault, is exposed on the southern side of Liaridia beach.

**Figure 9.11** Isoclinally folded quartz lenses in a greenschist facies ductile shear zone immediately below the Moutsouna "detachment fault". D4 shearing has transposed existing layering.

**Figure 9.12** Dolomite clasts in a sheared calcitic marble matrix develop asymmetric 'tails'that indicate a north-directed sense-of-shear.

# Chapter Ten

# Inside the Dome of the Naxos Core Complex

## Traverse 7 - Kourounochori to Apollon

*Sue Keay and Gordon Lister*

## INTRODUCTION

The excursion now winds its way though the central gneiss dome of Naxos (Fig 10.1). We begin by examining deformed metasediments on the western flank of the dome, and then proceed deeper into the dome, where an old tectonic contact can be seen, marked by ultramafic lenses. This boundary apparently separates the Mesozoic "series" from the partly Hercynian core of the Naxos dome (Keay et al., in prep.).

We will examine rocks in the migmatitic core zone, and then lunch at Moni, on the eastern flank of the Naxos dome. A short traverse will allow rocks in the kyanite-sillimanite zone to be examined, on the eastern flank of the dome, before descending into Keramoti, to cross once more into the core zone.

We will then take a bus ride to Apollon, though spectacularly rough terrain, descending a steep valley, into the NE flank of the dome. An old emery deposit will be visited, before descending finally to Apollon. Here we will examine a key locality at which the structural and metamorphic history is at least in part visible, before returning towards Naxos along the northern cliffs of the Naxos dome.

This final part of the route will take us across the northern axis of the median antiform of the Naxos dome. The abrupt change in orientation across the dome axis will be observed. We also plan to stop briefly to examine aplite and pegmatite dyke swarms which may emanate from a buried pluton. These dykes have been caught up in the general N-S extension, but are generally relatively little deformed in comparison to the surrounding rocks.

The main issues that we intend to deal with in this traverse are the nature and origin of the M2 metamorphism, the migmatite core of the Naxos dome, and the structural and metamorphic history. Figure 10.1 shows the location of the traverse and the stops that we will make.

## M2 METAMORPHISM

The M2 metamorphism may in fact have involved several distinct thermal and/or fluid pulses, some of which may have been quite short in duration. At least four different time periods have been identified in which episodes of (continuing?) metamorphic growth may have taken place.

Apparent 40Ar/39Ar ages for M2 vary according to metamorphic grade, with older hornblende ages in lower grade zones, ranging from 19.8 ± 0.1 Ma to 15.0 ± 0.1 Ma. This data has previously been interpreted as indicating the range of age during which the peak of M2 metamorphism took place (Wijbrans & McDougall 1986, 1988). Younger ages of 11.8 ± 0.1 Ma for muscovite and 11.4 ± 0.1 Ma for biotite from Zone 6 have been regarded as representing rapid cooling from peak M2 conditions.

An alternative explanation is that there may have been at least two or three or even four separate phases of Miocene metamorphic mineral growth, the last of which may have been indirectly associated with the magmatic event that resulted in the intrusion of the granodiorite on western Naxos.

The geochronological data can be reinterpreted in support of several separate thermal and/or fluid events, as can the microstructural information that constrains the relative timing of deformation and metamorphism.

Supporting evidence for timing the peak M2 metamorphism at ~20 Ma can be derived from tourmalines from syntectonic pegmatites and laccoliths on Naxos which record K-Ar ages of 18-22 Ma (Andriessen et al. 1991). This is older than corresponding hornblende ages for the migmatite and suggests that tourmaline has a higher closure temperature. The corresponding K-Ar dates for muscovites from these samples range from 11.4-12.7 Ma which also corresponds to the cooling ages of Wijbrans & McDougall (1988).

Another study of a syntectonic monzo-granite revealed a Rb-Sr whole rock isochron of 19-20 Ma, with younger Rb-Sr muscovite (13 Ma) and apatite fission track (10 Ma) ages (Andriessen & Jansen 1990). It is thus possible that there has been more than one Barrovian metamorphic episode. Andriessen & Jansen (1990) have subdivided the M2 event on Naxos into two separate events, M2a (at 23 Ma) representing regional Barrovian greenschist facies metamorphism (dated by Rb-Sr and K-Ar of low grade muscovite), and M2b (at 19-20 Ma) representing the higher grade thermal overprint.

Support for an event at 19-20 Ma has been derived from SHRIMP U-Pb zircon dating of new growth rims of zircon found in samples from the migmatite core which place the timing of anatexis at approximately 18 Ma (Keay, unpubl. data).

An additional period of zircon growth has also been identified from SHRIMP U-Pb ages of new growth rims of zircon from a calc-silicate in the amphibolite-facies shear zone enveloping the migmatite core. This gave ages of ~14 Ma, supporting Buick (1991a) who suggested that an M2c event was associated with new mineral growth during uplift under mid-amphibolite to greenschist conditions, at 15-16 Ma, based on the geochronology of Wijbrans & McDougall (1986, 1988).

On the return journey to Naxos, on the northern cliffs of the Naxos dome, the excursion will be able to observe some of the relatively undeformed dyke swarms that may have emanated from an intrusion at depth under the central gneiss dome of Naxos (see Figs. 10.2). Such plutons may have been responsible for a thermal pulse at ~12 Ma rejuvenating K-Ar mineral ages. Alternatively, the current explanation may be valid, and rapid unroofing of the Naxos metamorphic core complex at that time may have been responsible for the period of rapid cooling recorded in the argon data.

## HERCYNIAN BASEMENT IN THE CORE OF THE NAXOS DOME

The original interpretation of pre-Alpine basement on Ios suggested a Hercynian age of metamorphism for the orthogneisses comprising the basement (300-305 Ma by conventional U-Pb zircon) while a 500 Ma Rb-Sr whole rock isochron for relatively undeformed intermediate intrusions was interpreted as an original igneous emplacement age (Henjes-Kunst & Kreuzer 1982).

SHRIMP U-Pb zircon ages ranging from 300-330 Ma were derived from orthogneisses comprising the basement of Ios, including a small number of zircons from an undeformed granite boudin within one of the orthogneiss zones. Deformation seems to have had very little effect on zircon crystallisation and zircons from the deformed granite are generally smaller in size than those from the undeformed boudin, suggesting zircon may have dissolved during Alpine deformation rather than precipitating. These ages correlate with the Hercynian ages previously reported by Henjes-Kunst & Kreuzer (1982).

Zircons from both deformed and undeformed samples have inherited cores which range in age from 460-1400 Ma. The fact that both deformed and undeformed samples produce ages in the range 300-330 Ma suggests this is more likely to represent the age of intrusion of the granite protoliths rather than metamorphism. This is contrary to the interpretation made by Henjes-Kunst & Kreuzer (1982).

Dating of zircons from an orthogneiss from the core of Naxos was undertaken to confirm whether the core was pre-Alpine basement as suggested by previous workers (Henjes-Kunst & Kreuzer 1982, Van der Maar & Jansen 1983, Andriessen et al. 1987).

A SHRIMP U-Pb age of approx 310 Ma correlates with the SHRIMP ages from Ios, suggesting the basement is the same age. Two inherited grains were also found with ages of 480 Ma and 520 Ma correlating with the 500 Ma Rb-Sr age from Ios of Henjes-Kunst & Kreuzer (1982).

While these zircon ages correlate well with age data from Ios, they conflict with the conventional U-Pb zircon work of Andriessen et al. (1987) which suggests an emplacement age of 372 Ma (+28/-24) for the Naxos basement.

It is possible that this age represents mixing of a 500 Ma inherited age component with a younger (310 Ma) crystallisation age. Andriessen & Jansen (1990) report that the eight zircon fractions analysed fall between 515 Ma and 316 Ma clustering around 375 Ma, adding weight to the hypothesis of age mixing, a common problem where multiple whole grain samples are used.

## DEFORMATION AND METAMORPHISM

It has become increasingly evident that the Aegean has been subject to a complex history of deformation and meta-morphism (see §1). Naxos is not a good place to study the early history of deformation and metamorphism, because of the intensity of relatively late deformation, and because a high grade of metamorphism has been achieved in the most youthful part of its thermal history. It is an excellent place to study the effects of a relatively recent Barrovian facies metamorphism, particularly from the point of view of the timing and duration of possible metamorphic ‘pulses’ and their relation to ongoing extensional tectonism.

Urai et al. (1990) published some of the first detailed structural work on Naxos, suggesting two main deformation events could be recognised, associated with compression and extension respectively. They identified three separate (but temporally overlapping) generations of structures. The first two fold generations (B1 & B2) produced tight to isoclinal folds, and have been related to the compressional part of the orogenic cycle. The third generation (B3) has been associated with extensional tectonism, although it produced upright open structures. Some mylonites are locally folded by B3 folds, and yet the same zones cut B1 and B2 structures. Urai et al. (1990) suggested this simple structural pattern was due to reactivation and transposition of older structures during ongoing deformation in a long-lived zone of movement.

There is some evidence that several generations of isoclinal folds with similar orientations are developed during M1 on other islands (e.g., Avigad et al. 1988). Interpreting structures in the migmatite core is complicated by the presence of earlier fabrics in the Hercynian basement rocks, for example as found in the basement on Ios (Henjes-Kunst & Kreuzer 1982).

Buick (1991a) produced a different chronology for the structural history of Naxos, but he may have identified different generations of folds in the high grade core. B1 and B2 may both have occurred during extension and M2 metamorphism. The two generations of isoclinal folding visible in the high grade core of Naxos display fabrics defined by characteristic high grade mineral assemblages. These structures are transected by mylonitic fabrics which occur after the peak of M2b metamorphism. This was followed by the development of B3 structures, and formation of the Naxos dome structure.

Both of these interpretations have important implications for the M2 isograd pattern. This has traditionally been interpreted as a static thermal overprint on an earlier structural dome (Schuiling & Kreulen 1979, but see also Buick 1991b). However B3 occurs after the peak M2b metamorphism. The isograd surfaces have already formed by this time, so therefore the pattern of isograds must represent the effect of folding (Buick 1991b).

Our work on Naxos suggests an even more complex history of deformation and metamorphism. A similar pattern of deformation and metamorphism can be seen on Naxos as can be seen on other islands in the Aegean, for example as on Ios, immediately to the south. There are at least five distinct generations of folding and/or fabric formation.

In the central high grade zone, because ongoing deformation took place during later high grade metamorphism, earlier formed folds were stretched, and new minerals grew in their axial planes. Correlation with fold events outside the migmatite core might thus be difficult and in some cases it could be misleading. But if such correlation is possible, the earlier folding events can be related to deformation prior to Miocene high grade metamorphism.

Outside of the high grade core zone at least two fabric forming events can be recognized (D1 and D2). These have been affected by a recumbent folding event (D3), locally associated with the development of axial-plane cleavage, but more commonly an intense crenulation develops. This folding may have been synchronous with or prior to the onset of Barrovian facies metamorphism.

D4 shear zones are folded by moderate to open upright folds. But, as is the case on Ios, there may be more than one generation of shear zones that has formed. It is possible that each thermal event triggered continued operation of different shear zones, albeit under different conditions of pressure and temperature for each episode of movement. Deformation (at least in D4 shear zones) outlasted high grade metamorphism, and in many localities a progressive sequence of retrograde reactions can be discerned in such shear zones.

Island-scale doming (D5) folded these D3 (?) and D4 shear zones. Unlike in the Basin and Range, where considerable uncertainty surrounds the origin of transverse warps or folds of the mylonitic foliation, the origin of these folds can definitely be related to crustal shortening. There is ample evidence that the mylonitic foliation was in the

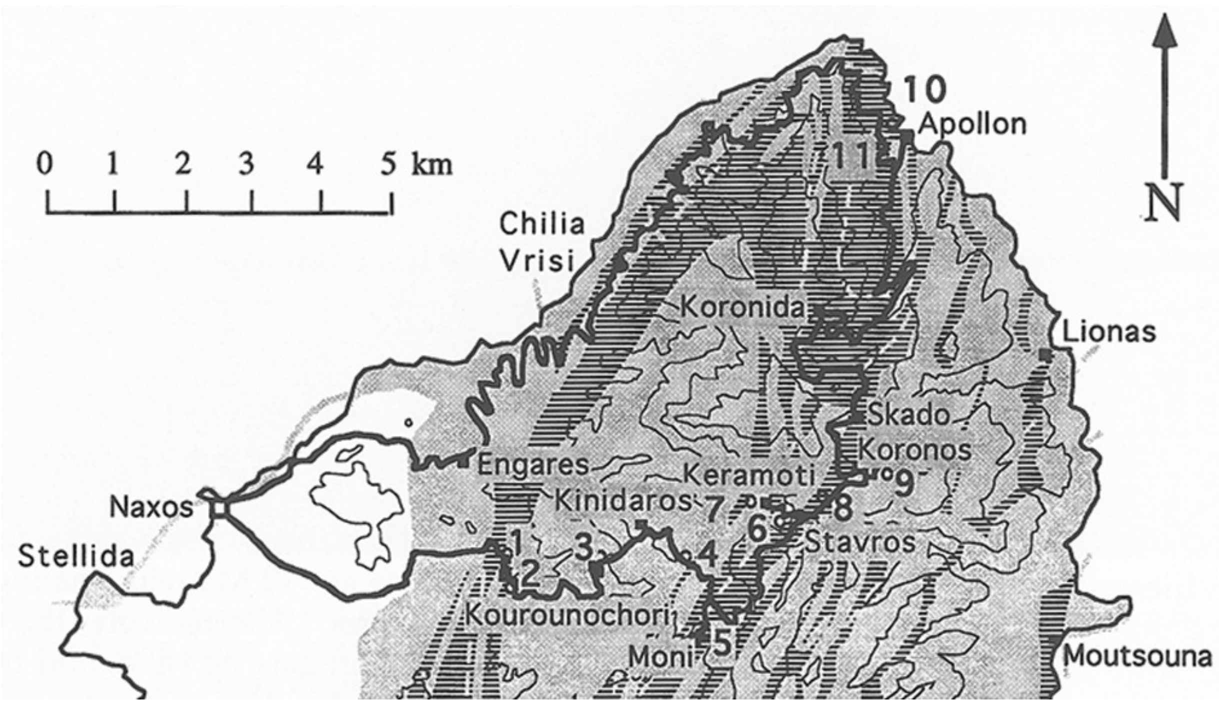


**Figure 10.1** Route followed by this traverse and location of stops.

shortening field (along EW cross-sections), and many upright parasitic folds have developed that attest to this fact (see Fig. 10.3). In places, reverse faults associated with chevron-like folds overprint the mylonitic fabrics (see §9), so island scale doming may have taken place under a variety of metamorphic conditions.

Doming may have taken place during continued N-S extension, because although upright folds formed in the mylonitic fabrics, these have fold axes parallel to the well developed stretching lineations.

## GEOLOGY OF TRAVERSE

Today's traverse will once again take us across the melt phase isograd into the migmatitic core (see Fig. 10.2), tracing the progression from unmelted rocks through to migmatite, and also from marbles and schists presumably of Mesozoic origin through to orthogneisses forming a Hercynian basement.

### *Stop #1* [37°05.86'N, 25° 26.63' E]

### Naxos grid [-2210E, -17170N]
### Map 7642.1E Zone 5

Stop at a road cutting between the Melanes turnoff and Kourounochori on the U-bend below the cafe/bar (altitude ~178 metres). At this locality a series of metasediments intruded by granitic dykes, aplites and/or pegmatites are exposed. These have been caught up in a major ductile shear zone on the western flank of the Naxos dome.

Tight to isoclinal (D2) folds are defined by interlayered psammites, pelites and leucocratic gneisses, with an axial planar foliation parallel to the dominant fabric (S2). These isoclinal folds are refolded by later inclined asymmetric folds that are parasitic to the main dome structure (with vergence to the east). Later chevron folds can also be found. Several important overprinting relationships can be discerned.

In fresh outcrops one can see cleavage refracted in the pelite. The sequence is cut by small (10 centimetres wide) tourmaline-bearing pegmatite dykes which have been warped by E-W compression.

There is some evidence that the psammitic units in this sequence are derived from an immature volcanogenic source. Zircons extracted from these rocks are generally elongate, prismatic grains showing little abrasion, suggesting they have not undergone a protracted sedimentary cycle. In addition the zircon population consists almost entirely of grains of mid to late Triassic age, indicating the age of the protolith and, assuming the grains are in fact volcanic, restricting the timing of sedimentation for the "Series" rocks to Late Triassic or younger.

### *Stop #2* [37° 05.59' N, 25° 26.85 E]

### Naxos grid [ -1815E, -17650N]
### Map 7642.1E Zone 6

On the roadside immediately east of the cemetery above Kourounochori still on the western edge of the Naxos dome, interbedded augengneiss, sillimanite schists and pelites are isoclinally folded and cut by veins of pegmatite. At least two generations of pegmatite are visible, one layer parallel and boudinaged, the other cross-cutting all structures. A weakly developed lineation (6__>182) is developed in the gneisses (this is a mineral elongation defined by biotite).

Approaching the ultramafic body, a more mafic gneiss is encountered, possibly a metatonalite (Buick, pers comm.). Towards the cemetery an elongated lens of ultramafic material outcrops. It has been suggested (Jansen & Schuiling 1976) that this represents a disrupted ophiolite sequence delineating the detachment between pre-Alpine basement and the Mesozoic Upper Palaeozoic marble-schist series. This hypothesis has been tested by dating zircons from the metatonalite which confirms that the gniesses represent Hercynian basement. According to the field guide of Dixon & Ridley (1987) the ultramafic unit consists of enstatite and olivine with minor clino-chlore, amphibole and spinel. Several metasomatic reaction rims are developed, commonly monomineralic, ranging from anthophyllite, actinolite to phlogopite with increasing distance from the core of the lens.

### *Stop #3* [37° 05.85' N, 25° 28.27' E]

### Naxos grid [0090E, -17230N]
### Map 7642.2E Zone 6

Stop at the top of the hairpin bends on the road from Mili to Kinidaros. Since the village of Mili we have been travelling through the migmatitic core of the Naxos dome. Intercalated marble and schist form largely unmelted "rafts" in the migmatite.

Some of the large marble quarries in these rafts are now clearly visible. The extent of the migmatite is partly delineated by the exploitation of marble. Marble quarries are mainly restricted to the core of the dome which has experienced the highest temperatures, producing the best quality coarse-grained marble.

The marble units in the outcrop define tight upright folds interspersed by bands of mafic and felsic schist (and calc-silicate) in which pegmatite veins are boudinaged. No obvious axial plane foliations are found in these upright structures, and they may be folds formed quite late in the structural history (e.g., during D3 or D4).

**Figure 10.2** View of the Naxos dome, looking towards Keramoti. The steeply east dipping marbles on the eastern flank of the dome are clearly visible. The metamorphic grade rises abruptly over a few hundred metres, until the zone of migmatites and S-type granites is encountered.

**Figure 10.3** Moderate to tight, inclined to upright folds in metasediments on the eastern flank of the Naxos dome. These folds are D3 folds or younger. They are parasitic to the median antiform of the Naxos dome.

**Figure 10.4** Refolded quartz lenses define rootless isoclinal fold hooks, at an outcrop near Apollon. These are twice refolded, once by D2 when the dominant foliation was formed, and again about gently north-dipping S3 planes. They are cut by D4 shear bands (see text).

**Figure 10.5** Spectacular 'sheath'folds on the north road between Apollon and Engares, recently bulldozed into non-existence. These folds had S3 as a shallow-dipping axial-plane fabric, and highly non-cylindrical fold axes. Layering at this locality dips moderately steeply to the north, and is significantly divergent (on a large scale) from the orientation of S3.

The folded gneissic layering is cut by a younger granitic dyke. The older gneissic fabric is preserved, with zones of coarse biotite bordering individual layers. There are amphibolite boudins in the sequence, adjacent to tightly folded coarse marble layers. Some interesting metamorphic reactions occur in the contact zone.

Figure 10.6 shows a cross-section of the outcrop. Most of the section is dominated by tight asymmetric folds, that are overturned and east vergent. Late shear zones have tight isoclinal folds in them. These may be appressed versions of folds observed outside the shear zone. At the western end of this section, some of these folds are overprinted by yet another generation of folds (see Fig. 10.6) perhaps related to late faulting.

### *Stop # 4* Marble offcut dump

### Naxos grid [2010E, -17120N]
### Map 7642.2E Zone 6

On the roadside opposite a marble cutting facility east of Kinidaros is a marble dump where marble offcuts are thrown away. Coarse-grained marble of high commercial grade is exploited in the core of Naxos for use in building materials (mainly tiles). This marble has been mined since at least 500 BC and commercial exploitation of this resource was restarted some years ago. The marble is mined as large blocks (~1 x 1 x 1.5 m3) and extracted from the rock face by the use of large drills and explosives. These blocks are then either shipped to Athens or cut at a number of marble cutting facilities on Naxos and used locally, or exported from the island.

### *Stop #5* Moni kyanites

### Naxos grid [2550E, -18675N]
### Map 7642.2E Zone 5

After lunch at Moni we will walk up the road towards the west, observing features in the outcrop beside the road. Kyanite porphyroblasts (5-30 mm in size) can be seen in the large boulder at the entrance to Moni. These have overgrown S2, and then have been rotated towards the plane of the foliation by ongoing deformation (e.g., during D3). This suggests that N-S extension was initiated during or shortly after the peak of M2 metamorphism. Kyanite is found in pelitic rocks in zones 4 and 5a, above the -chloritoid/+staurolite isograd, representing temperatures >540°C. Kyanite is also reported from zones 5b and 6 (Buick 1991b) which are supposedly above the kyanite-out isograd.

The section that we are examining is in the zone in which kyanite and sillimanite (metastably) coexist. The metasediments dip steeply to the east, on the eastern flank

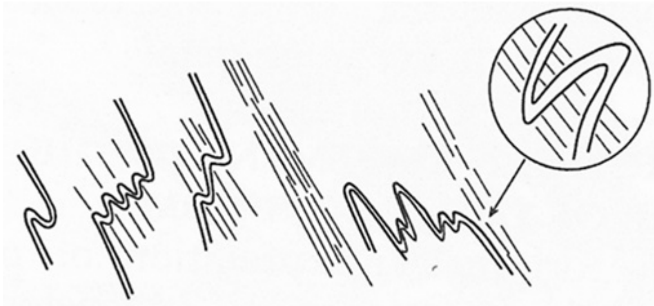

**Figure 10.6** Schematic cross-section of the section at stop #3, in the migmatite core. The upright folds define an antiformal closure. Some overprinting relations are also discernible, and younger shear zones.

of the Naxos dome. They are strongly lineated, with mineral lineations trending N-S.

In a quarry part of the way along the road there are late veins which cause coarsening and new growth in the reaction haloes that surround them.

### Stop #6 [37° 06.34'N, 25° 31.26' E]

### Naxos grid [4700E, -16450N]
### Map 7633.7D Zone 5

Following the road from Stavros down to Keramoti, stop at the first hairpin bend and walk south through the thorn bushes to a small outcrop of boulders (at ~630 m altitude). The rocks here display kyanite crystals up to 2.5 cm long, overgrowing the dominant foliation (S2) and rotating into it as the result of later deformation. Garnet, kyanite and staurolite coexist, suggesting metamorphic temperatures of 600-620°C. Yet, structurally, we are less than a few hundred metres from the migmatitic core where the same rocks have begun to melt.

This points to the fact that there has been considerable ductile elongation of the rock mass, and the attenuation of the apparent geotherm that results is responsible for these remarkable 'gradients'. Figure 10.2 shows the view towards Keramoti, including the deformed marbles and schists on the eastern flank of the Naxos dome, and granite in the interior.

### Stop #7 Keramoti traverse [25°30.83'E, 37°06.80'N]

### Naxos grid [4100E, -15650N]
### Map 7632.8D Zone 5-6

Follow the path through the village of Keramoti, down the steps following the aqueduct, across the bridge and continue following the marble pathway west along the wall of the valley. The path follows the transition from Series rocks on the eastern flank of the dome into the migmatite

**Figure 10.7** A considerable variety of deformed granitic dykes can be discerned. These vary from intensely deformed dykes parallel to the dominant fabrics in young shear zones, or relatively undeformed dykes, also parallel to the dominant fabric. This photo shows strongly deformed dykes, more or less parallel to lithological layering.

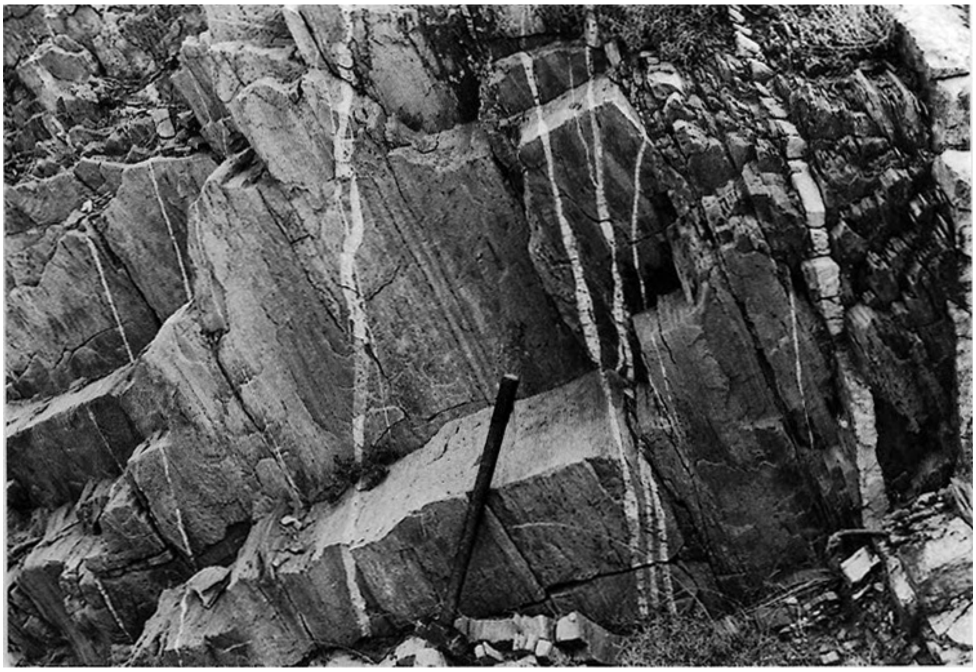

**Figure 10.8** Granitic and aplitic dykes cross-cut intensely foliated and lineated tectonites. They intruded late in the deformation history, so that they are relatively undeformed. These dykes cross-cut intensely foliated and lineated tectonites on the flank of the Naxos dome. Their orientation suggests these dykes intruded relatively late in the history of dome formation.

core. Heading westward, sillimanite-bearing pelitic schists begin to show evidence of partial melting. Eventually we cross a boundary between the partially molten pelite and the migmatite proper.

### *Stop #8* Folds beside road

### Naxos grid [5540E, -15665N]
### Map 7633.7D Zone 4

Approximately 400 m past the church at Stavros on the road towards Koronos, large scale folds are well exposed (see Fig. 10.3). Individual units of marble, calc-silicates, psammites and pelites are pinched out due to isoclinal folding. Pelitic schists are strongly crenulated while psammites preserve a more spaced cleavage. A strong lineation trending 14__>191 is defined by mineral elongation. Careful examination will reveal overprinting relationships, allowing these folds to be timed as D3 or later.

### *Stop #9* Emery lenses

### Naxos grid [6250E, -15100N]
### Map7633.7D Zone 4

About 100 m along the road to the fishing village of Lionas, lenses of emery are exposed. Unless the emery trucks have collected them, the site is marked by a pile of emery blocks on the side of the road. These roughly pyramidal shaped piles are formed by the local emery miners who still work the corundum-rich rocks of Naxos today.

Emery has been mined on Naxos for several centuries. While global demand for emery has decreased since the manufacture of synthetic corundum, the Greek government subsidises the industry to try and stem the depopulation of the inland villages of Naxos. When emery mining was at its peak a company decided to build an amazing funicular system of aerial buckets to carry emery down to the port of Moutsouna. The system now lies defunct, and emery is transported by truck to Moutsouna and is exported to Athens by boat several times a year. Due to the harsh conditions, emery mining ceases during the summer months.

Naxos is a typical example of emery deposits formed by regional metamorphism of karst bauxites, a rare occurrence on a global scale (Feenstra 1985, Bardossy 1982). Metabauxite deposits are found, interspersed in the marble sequences in all areas of the island except the migmatite core. Most deposits form part of discontinuous stratigraphic horizons, which can be traced over several kilometres.

They form lenticular shapes ranging up to 8 m in size with an average thickness of 2-4 m (Feenstra 1985). In the south-eastern corner of Naxos in Zone 1 the metabauxites are diasporites while north-west of the corundum-in isograd these gradually change into emeries, with corundum associated with haematite at low grades and with magnetite at higher grades.

The age of the bauxites is difficult to constrain, but Feenstra (1985) showed that they had similar chemical characteristics to Jurassic karst bauxites of the Balkan region and these are inferred to be of similar age.

### *Stop #10* Koronos-Koronida

View of the steeply sided valley descending to Apollon. One of the shallow dipping isograds is intersected by this valley, allowing exposure once more of deeper crustal levels in the sillimanite zone.

### *Stop #11*

### Naxos grid [7100E, -7550N]
### Map 7633.1 Zone 5

Following the road out of Apollon and past the sign for the “kouros”, the first turn to the right takes us down into the houses of northern Apollon until we reach a cul-de-sac. Walk down the pathway to the boulder beach behind which is a small outcrop of schist. The schist at this locality displays overprinting relations between several generations of structures.

The dominant foliation (S2) is defined by a differentiated crenulation cleavage. This is axial plane to isoclinal rootless fold hooks (see Fig. 10.4), defined by elongate quartz veins formed in an earlier generation of deformation. These elongate quartz lenses probably formed parallel to S1, implying the potential existence of D1 shear zones at this locality.

The isoclinally folded quartz lenses are themselves refolded by subhorizontal fabrics, with weakly differentiated axial-plane crenulation cleavages. All of these fabrics are transected by D4 shear bands, that align the previously grown metamorphic minerals. The shear bands have a north-directed sense-of-shear. Fold axes of earlier formed folds are also N-S trending, parallel to the mineral stretching lineation. Shear bands thus transect these fold structures.

Careful examination of the outcrop will reveal both kyanite porphyroblasts, and clumps of aligned ‘fibrolite’ (sillimanite clusters). This is a rare outcrop, so please do not remove pieces of it.

**Figure 10.9** A swarm of granitic, aplitic and pegmatitic dykes intersects the north road. These are relatively undeformed in comparison to the surrounding rocks, and have been little affected by the ongoing processes of N-S extension. It is suggested that they intruded late in the extensional history, and that they may be synchronous with the emplacement of the 12 Ma pluton in western Naxos.

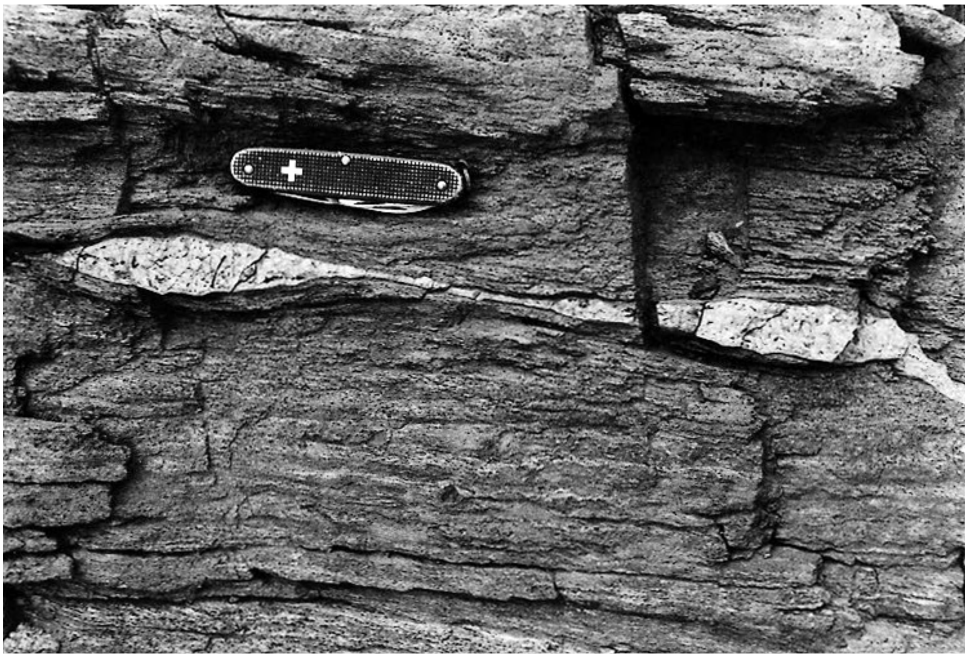

**Figure 10.10** Photo shows 'pinch and swell'structures that are either related to localized development of shear bands, or the emplacement of magma parallel to shear discontinuities during ongoing deformation, accentuating the development of mesoscopic dilatancy.

### *Tourist stop* Kouros

### Naxos grid [7150E, -7959N] Map 7633.1 Zone 5

Follow the steps from the sign on the main road to the quarry housing the colossal (10 m) Kouros of Apollonas (7th century BC), left lying on its side, unfinished due to the development of a large crack. Kouros means young man, and the figure has been interpreted as a representation of Dionysius. It seems likely that this statue was carved as a votive offering for the huge sanctuary of Apollo on Delos. Ashort distance into the bush, but difficult to locate, are some carved words in the marble saying “here is the boundary of the realm of Apollo”.

### *Stop #12*

The return journey will be via the north road, along the sea cliffs, from Apollon to Engares. There are several notable aspects, e.g., we will cross the median antiform of the Naxos gneiss dome, marked by a sharp change in the orientation of the dominant layering.

Further along the road, we will come to the remnants of an outcrop that used to display remarkable sheath folds (Fig. 10.5). These were formed by the interaction of D3 with pre-existing structure. The orientation of S3 is quite shallow, in contrast to the orientation of the lithological layering which dips quite steeply at this locality.

Still further along the road, we will encounter swarms of granite, aplite and pegmatite dykes (Figs. 10.7-10.11). These dykes may be the same age as the Naxos granodiorite and may emanate from a buried pluton. The dykes exhibit remarkably little internal deformation, which is not consistent with the current view that they formed synchronously with the peak of M2 metamorphism.

SHRIMP U-Pb dating of one of the S-type granites from the north-west coast yields an age of approximately 12 Ma from monazite dating while a fractionated I-type body from the north-eastern tip of Naxos is also 12 Ma, from both sphene and zircon, identical to the age for the Naxos granodiorite (Keay, unpubl. data). No other reports of dating of these S-type granites on Naxos have been made, and these results force considerable revision of the geology.

These ages are significantly younger than the presumed timing of syntectonic granite emplacement suggested to be 19-20 Ma from Rb-Sr whole rock, 15-19.8 Ma from K-Ar dates on tourmaline, with younger ages of 13 Ma from Rb-Sr muscovite, 11.4-12.7 Ma from K-Ar muscovite, and 10 Ma from apatite fission track dating (Andriessen et al. 1991; Andriessen & Jansen 1990).

There are numerous other stops that can be made along the north road, for example at the site of the sheath folds (see Fig. 10.5), or numerous locations where the complexity of the deformation history is evident in the roadside outcrop (e.g,. see Fig. 10.11).

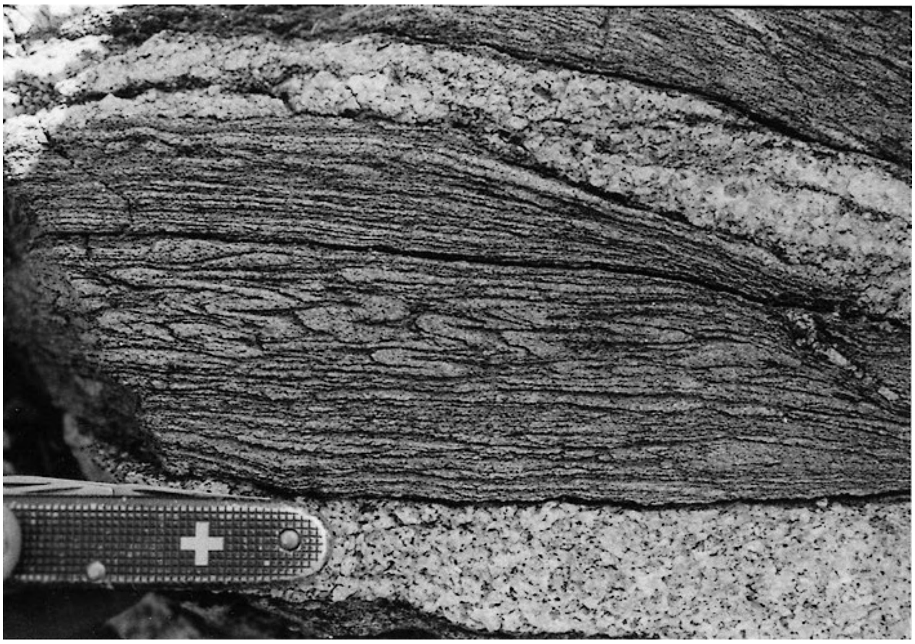

**Figure 10.11** Photo shows how transposition associated with development of the dominant fabric (S2) hides a complex history. These tight isoclinal folds have the dominant fabric parallel to their axial planes. Note that relatively undeformed granitic dykes have intruded subparallel to S2.

# Chapter Eleven

## The Naxos Detachment Fault

### Traverse 8 - Stellida to Naxos chora

*Sue Keay and Gordon Lister*

## INTRODUCTION

Traverse 8 will take us to the prominent headland visible west of Naxos town, commonly called Stellida. It is past the airport on the way to Agia Anna (see Fig. 11.1). This traverse will allow us to examine the granodiorite that outcrops over much of western Naxos, and the effects of the Naxos Detachment Fault.

## THE AGE OF THE WESTERN GRANODIORITE OF NAXOS

Wijbrans & McDougall (1988) refined the age for the granodiorite intrusion of western Naxos, obtaining K-Ar ages of 12.1 to 13.6 Ma (based on hornblende) and 11.4 Ma (based on biotite), while a disturbed 40Ar/39Ar age spectra suggested a hornblende age of 12.2 Ma. Note that the inferred Tc for the minerals dated are: hornblende 525°C, muscovite 300°C and biotite 280°C.

Despite numerous attempts over the last fifteen years to define the emplacement age of the granodiorite on Naxos, workers in the area are still forced to admit that the age is not well constrained (Wijbrans & McDougall 1988). A minimum age for the intrusion was obtained by Andriessen et al. (1979) who determined a Rb-Sr whole rock age of 11.1 ± 0.7 Ma for aplitic dykes cutting the main granodiorite body. The granodiorite itself does not define an isochron (Altherr et al. 1988).

K/Ar ages from the granodiorite of 12.1 to 13.6 Ma (hornblende) and 11.4 Ma (biotite) have been obtained along with a poorly defined 40Ar/39Ar apparent age plateau at 12.2 Ma (hornblende) (Wijbrans & McDougall 1988). A fission track apatite age from the main granodiorite of 8.2 Ma (Altherr et al. 1988) is thought to record cooling below 120˚C.

An attempt to date the granodiorite using conventional U-Pb techniques was unsuccessful (Henjes-Kunst et al. 1988), yielding discordant ages attributed to partial Pb loss from both zircons and uranothorites. This interpretation was strongly influenced by the use of a two component Pb model with inheritance of 1100 Ma assumed, and also by the use of multi-grain samples where the choice of pristine zircon grains is not assured, producing a wide scatter in results.

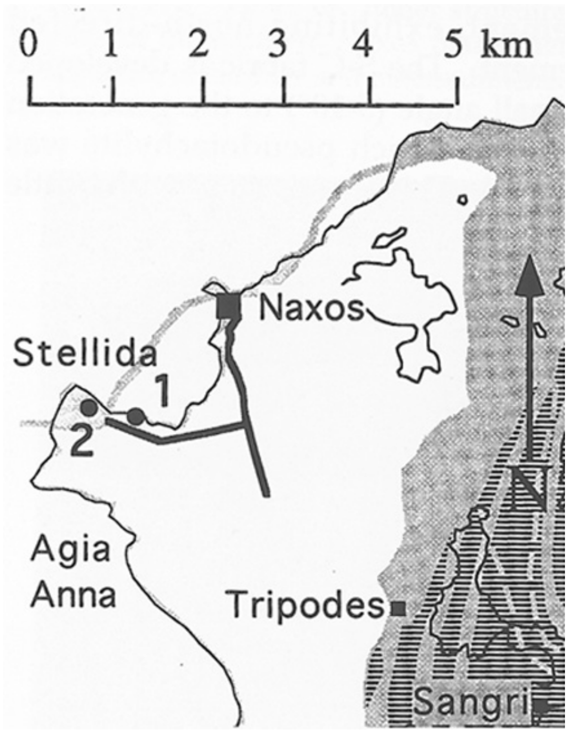


**Figure 11.1** Location svisited in this traverse.

U-Pb in zircons analysed using SHRIMP show little evidence of Pb loss, having only small variations in U/Pb ratios compared to those reported by Henjes-Kunst et al. (1988). No inheritance in any zircon grains was identified using SHRIMP and the results indicate a time of emplacement for the granodiorite of approximately 12 Ma. Analyses of sphene from the same sample also yield an age of approximately 12 Ma.

### *Stop #1* Pseudotachylites

### Naxos grid [-10105E, -18005N]
### Map 7641.1E

Chloritic breccias do not in general underlie the supposed detachment faults of the Aegean core complexes. On Ios, Forster (1996) discovered that the Coastal Detachment Fault system is associated with chloritic alteration, and a variable degree of retrogression to chlorite and epidote bearing assemblages. These produce spectacular phyllonites that vary from purple to green, depending on

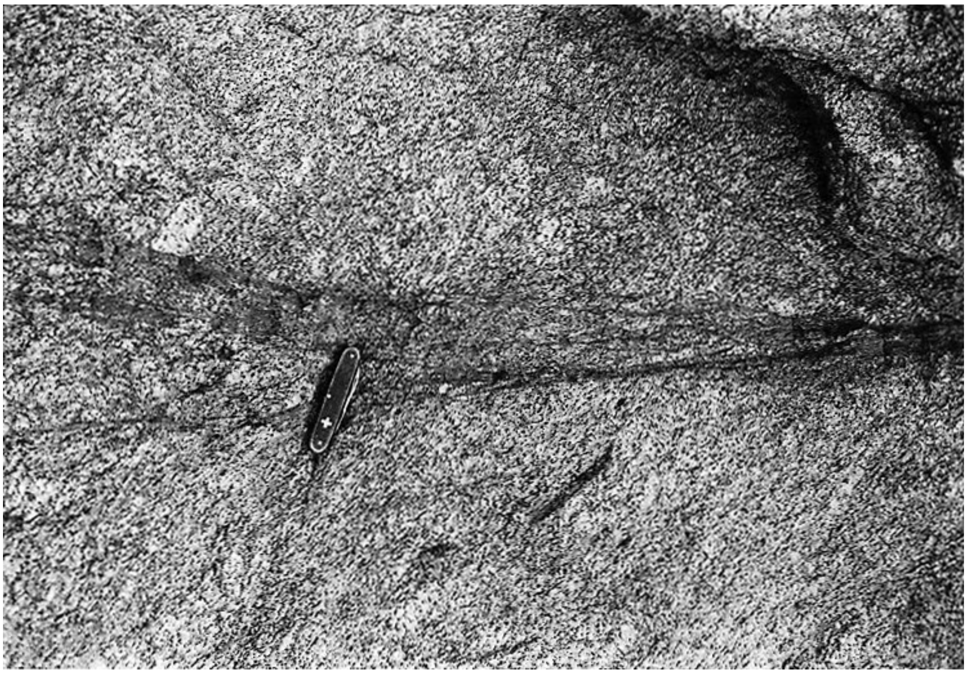

**Figure 11.2** The Naxos granodiorite was first deformed in a ~500 m thick ductile shear zone, and then fault activity led to the formation of pseudotachylites. Photo shows a generation surface that produced pseudotachylite during seismic activity on the northern Naxos detachment. Injection veins were filled with pseudotachylite after the melt was generated, as it fractured and penetrated the adjacent rock mass.

**Figure 11.3** Photo of "finger structures" in the hydrothermal cinter at Stellida, in the upper plate of the northern Naxos detachment, where almost complete silicification of an original sequence of marbles and metasediments has occurred.

**Figure 11.4** Replacement of gypsum crystals has taken place, but the original morphology remains. Extensive silicification has taken place associated with cinter activity.

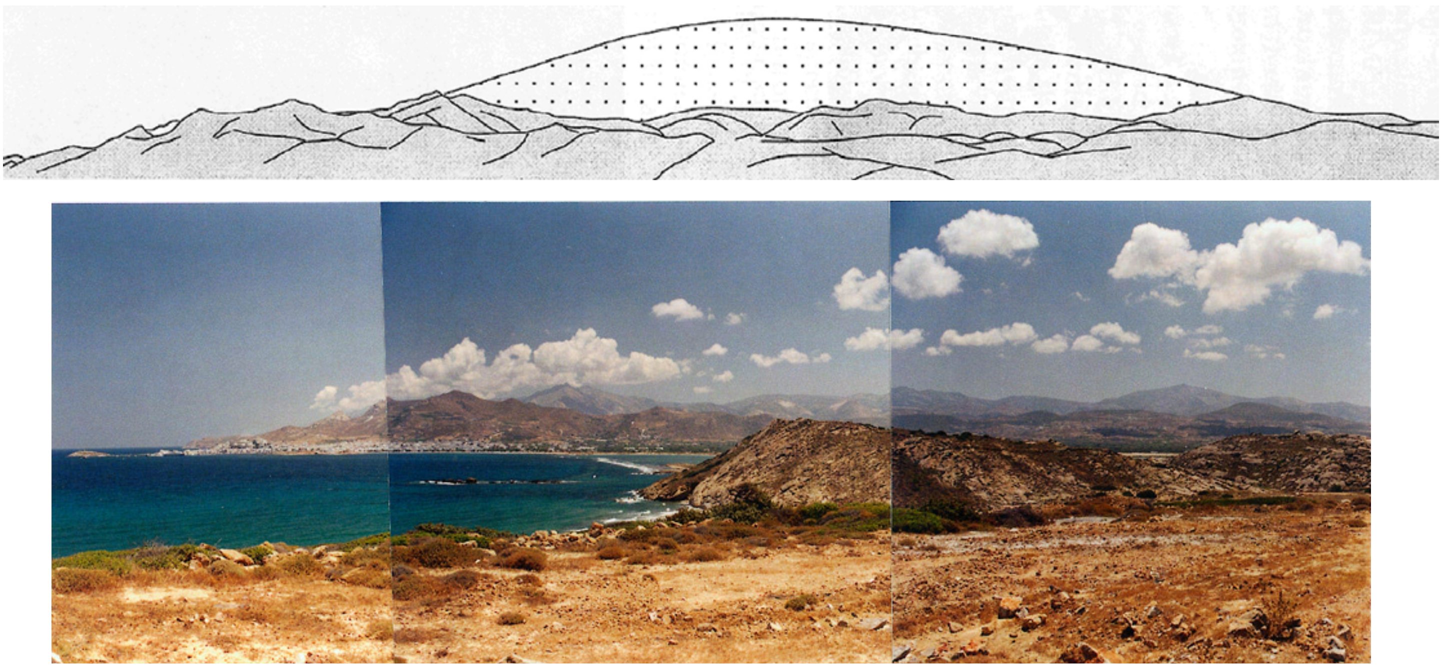

**Figure 11.5** The Naxos dome can be regarded in profile from this vantage point. The sketch above the photo shows the probable extent of the sillimanite cored Naxos gneiss dome prior to the extensive erosion that has removed its inner core. If this is true, the original dome may have risen out of the Aegean Sea by a distance of ~2-3 km, in a similar fashion, and with similar morphology to the giant gneiss domes that characterize the metamorphic core complexes of the Solomon Sea (Hill et al. 1992). The sediments that were shed from the flanks of the Naxos dome as it eroded are still partially preserved, as pediments and alluvial fans (e.g., near Engares). These often take the form of boulder conglomerates that overlie both upper plate and lower plate unconformably.

the degree of retrogression of glaucophane bearing assemblages.

In some cases it is clear that there is a temporal and a spatial relationship between ductile and brittle fabrics, for example in the northern low-angle faults on Naxos, where they cut the 12 Ma granodiorite that outcrops in the western region of Naxos. At this location there are mylonitic fabrics with well-developed shear bands, cut in turn by pseudotachylites (see Fig. 11.2). The position of the fault can be constrained by the geology, but the actual fault does not outcrop unfortunately.

This location is on the sea cliffs on a small headland directly east of Stellida, in an outcrop of the Naxos granodiorite. From the end of the road to the beach, walk to the right to the nearest outcrop. Here S-C mylonites and pseudotachylites are developed in proximity to a large normal fault forming a complicated detachment between upper and lower plate rocks. The upper plate rocks are not visible at this location.

S-C mylonites show a normal sense of movement, exhibiting north-directed movement. The S-C fabric is developed at a small angle (5-10°) to the generation surfaces on which pseudotachylite was developed. This is consistent with brittle movement associated with pseudotachylite generation taking place under the same kinematic constraints as the formation of S-C mylonites.

The formation of pseudotachylites is generally assumed to be associated with seismic activity. Rapid movement on the generation surfaces leads to the development of a super-heated cataclasite, which melts (not because of slow equilibrium reactions, but because individual minerals fuse). Once melting has taken place, the “pseudotachylite” (which has the same composition as the adjacent rocks) injects violently into the surrounding rock mass. It is possible to find several examples of generation surfaces, and branching veins that lead at high angles from the generation surface, where melt injection has occurred.

Generation surfaces are usually planar, and no more than a few millimetres of pseudotachylite remains on them. The greatest volume of fault melt is to be found in the adjacent injection veins.

In this area the granodiorite shows a distinct tectonic foliation that overprints a magmatic foliation, preserved further south near Mikri Vigla (Gautier et al., 1993).

The granodiorite is a typical I-type granitoid (Chappell & White, 1974), consisting dominantly of plagioclase with hornblende, biotite and sphene. It contains numerous microgranular enclaves (cf. Didier 1973, Didier & Barbarin 1991) aligned with the foliation. They have been aligned ductilely in the magmatic foliation, while they have been disrupted, deformed and stretched in a semi-solid state in the tectonic foliation. The early stretching of the enclaves during the development of the magmatic foliation precludes their use as strain markers.

### *Stop #2*

### Naxos grid [-10810E, -17760N]
### Map 7641.1E Naxos Granodiorite

Walk back along the beach to the headland. In contrast to the surrounding flat plains of Livadia, Stellida rises like a pinnacle above the farmland and marshes. Whilst the Naxos granodiorite seems easily weathered (see the coastline south of Kastraki) lending itself to agricultural purposes, the unusually prominent headland at Stellida presents an anomaly.

The rocks at Stellida form part of an ancient cinter cone which has silicified a variety of dirrerent rock types, including volcanics. There is abundant evidence of hydrothermal activity, with obvious metasomatic (silicification) fronts, cinter cones, “worm burrows”, “finger structures”, “gypsum rose” flakes, drusy quartz fillings on pervasive crack networks, opaline quartz, and chert have developed (see Figs. 11.3 & 11.4)..

Fluid conduits/fractures trend to 240° NE-SW and conduits are generally at an angle to the layering preserved in the rock. The area is coated in bright red iron oxide and yellow sulphur staining. Recent quarrying of the area to supply aggregate in the construction of the airport has led to a dramatic decrease in the size of the headland. Unfortunately the contact between upper and lower plate rocks here is not well-exposed and the exact shape and position of the detachment are speculative.

There is an abundance of opaline chert, jasper and/or chalcedony at Stellida. This has been formed by silicification of banded marbles, presumably belonging to the same “series” as recognized elsewhere on Naxos.

In fact this site was known to an ancient people, who used it as a source of rock for tools and/or implements. The chert will break with a marked conchoidal fracture, and razor sharp cutting edges can be formed if correctly handled. The “cherts” when broken can take on a razor sharp cutting edge that is quite capable of inflicting significant damage on the unwary. The Naxos detachment may be of a different age, and a different generation to the Moutsouna detachment, as it juxtaposes quite different rocks in its upper plate against the Naxos granodiorite.

### *Stop #3* Overview of the Naxos dome

This location is also important for the overview of the eroded Naxos dome. The dome can be seen clearly in profile, and conservative estimates suggest that at least 1000-1500 m of rock have been gouged from its core (Fig. 11.5). Erosion dumped vast volumes of boulder conglomerate down the river valleys (marked by rounded boulders and pebbles that are so typical of beaches on Naxos).

The river valleys are marked by sculpted rock formations, and “potholes” made by rapidly whirring pebbles or boulders, typical of large volumes of rapid water flow.

This suggests that the Aegean was once affected by significantly greater rainfall. The large pediments and alluvial fans are still visible at different locations around Naxos, for example the one above Engares. This cannot be discerned from this location, unfortunately.

The geomorphology of Naxos may once have borne a strong resemblance to that of the D’Entrecasteaux Islands, Papua New Guinea. Hill et al. (1992) have shown that the giant gneiss domes of the Solomon Sea core complexes rose from the sea in the last million years.

Similarly, the giant gneiss dome of Naxos may once have risen majestically from an ancient Aegean Sea. The shedding of detritus from these giant gneiss domes may in part explain the aprons of sediment that now surround the Aegean core complexes.

# Chapter Twelve

## The Paros Detachment and its Mylonites

### Traverse 9 - Naoussa to the NW Cape

*Gordon Lister and Sue Keay*

## INTRODUCTION

The field trip ends on Paros. If time permits we will examine two localities at which there is relatively good outcrop of the detachment fault that separates the deformed Hercynian basement from the overlying schists and marbles.

This detachment fault has much in common with the Ios Detachment Fault (Forster 1996). It separates highly deformed Hercynian basement (Keay et al., in prep.) from schists and marbles metamorphosed at an earlier stage of the Alpine orogeny. A schematic overview map of the geology of northern Paros is shown in Fig. 12.1 (based on mapping by Jeff Lee and modified by the authors).

Paros is interesting on several counts: (a) it marks the boundary between the two structural domains of the central Aegean (see §2); (b) as on Ios (Forster 1996) there are several different generations of detachment faults. The youngest detachment juxtaposes non-metamorphic rocks against the lower-plate mylonites and upper plate carbonates of the Paros detachment.

The earliest formed detachment so far recognized on Paros (the Paros Detachment Fault) juxtaposes metamorphosed marbles and metasediments against mylonitized Hercynian "basement". The latter fault is well exposed and an estimate of its 3-D geometry is thus

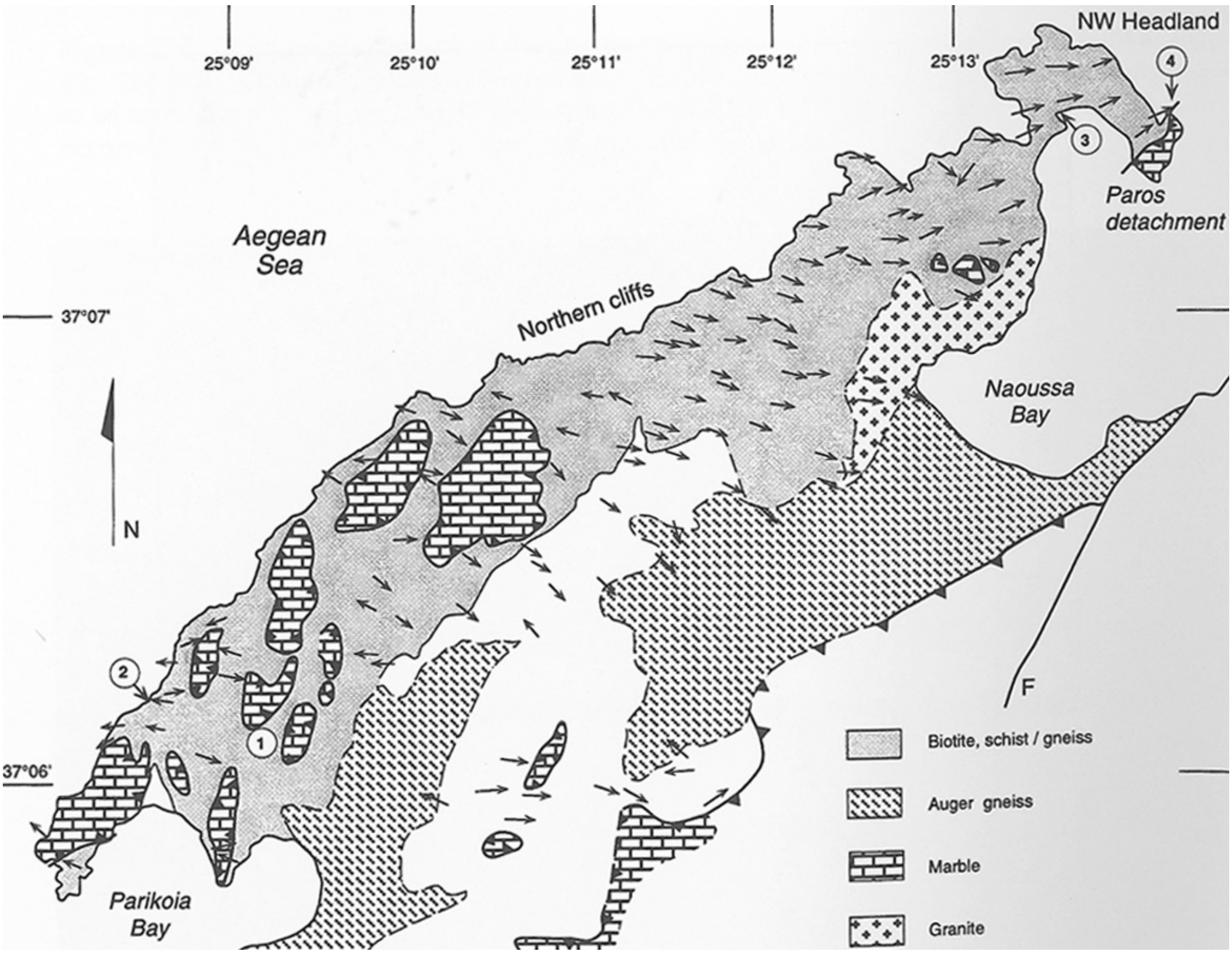


**Figure 12.1** Structural map of Paros, based on structural mapping by Jeff Lee (unpublished work). The outcrop of the Paros detachment is marked, beneath the upper plate marbles. Lineation trends in the Hercynian basement schists and gneisses are marked. These trends are characteristic of the north-western structural domain of the Cyclades.

possible. A detailed geology map of the northern part of Paros (see Fig. 12.1) shows isolated klippen above a subhorizontal detachment fault, at a slight angle to layering in the upper plate.

The two structural domains of the Aegean are marked by differently oriented lineation trends. The northwestern domain is characterized by lineation trends that vary roughly from NE-SW to E-W. We will visit several localities in this domain, on the sea cliffs NE of Parikia (the main port of Paros), and in the western headland of Naoussa bay.

Figure 12.1 also shows the main stops of the proposed traverse. Figure 12.2 shows the location of the proposed traverse on the headland NW of Naoussa.

### *Stop # 1* [37° 06.10N, 25° 09.26 E]

Drive out of Paros in the direction of Dilios. Take the turn off to Dilios, and climb a steep hill. At the top there are several vantage points from which the klippen above the Paros Detachment Fault can be observed. In the road cut, the mylonitic augengneiss and granite schist that underlies the Paros Detachment Fault can also be observed. The gneissic foliation dips 10-30° more steeply than does the gently inclined plane of the detachment fault. As observed throughout the core complexes of the Colorado River extensional corridor, the detachment fault is the youngest structure to affect this part of the tectonic development of the Aegean core complexes.

### *Stop # 2* [37° 05.88 N, 25° 08.07E]

Drive to the northern sea coast, to a small church. The relatively flat erosion surface is close to the orientation of the detachment fault, overlain by coarse marble. This is underlain by intensely foliated and intensely lineated granite schist. The fabrics have become so schistose and so anisotropic that ongoing deformation has resulted in spectacular examples of foliation boudinage (see Fig. 12.3), with dilation veins infilled with quartz. This granite schist results from the mylonitization of the Hercynian granite protolith. This is a LS tectonite with a strongly developed foliation as well as a lineation.

The central domain of the Cyclades is characterized by lineations trends that are roughly N-S oriented. Time does not permit the excursion to visit exceptional localities in which this trend is displayed (north of Pisso Livadi on the east coast of Paros). At this locality, the same (?)

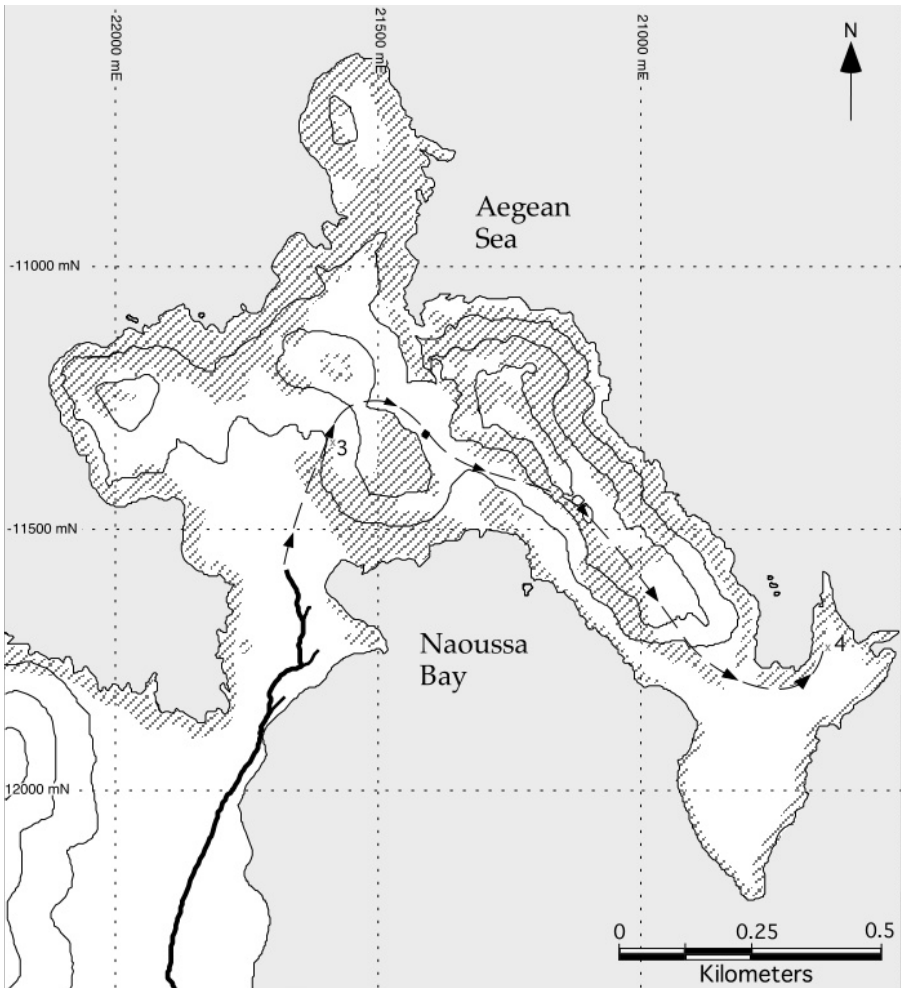


**Figure 12.2** Location map for the traverse NWof Naoussa. The traverse begins at Monastiri Bay, and ends at the approximate position of the Paros detachment.

**Figure 12.3** Close-up photograph of the granite schist beneath the Paros detachment fault at stop #2. The rock is intensely foliated and lineated. Spectacular examples of foliation boudinage are to be seen. Tension gashes have formed at high angles to the foliation, and then dilated. As this occurred they were infilled with quartz, and fold into shapes as illustrated.

Hercynian granite (Keay et al. in prep.) is mylonitized, and an intense N-S trending lineation is developed. There is evidence of the interference of two fabric forming events at this locality, and an earlier foliation may have been refolded. As a result of this interference (presumably during N-S stretching, a well-developed L-tectonite is to be found (see Fig. 12.4). This rock is highly lineated but displays evidence of a more complex history in terms of foliation development.

### *Stop # 3* Monastiri Beach

Starting from the bar overlooking the sun loungers, umbrellas and volleyball nets of Monastiri beach, in a secluded section of Plastira Bay, the traverse (see Fig. 12.2) will take us along the ridge to Cape Korakas. We will pass through a deformed igneous complex, thought to be Hercynian in age. Figure 12.5 shows a view of the deformed metaigneous rocks at the start of the traverse.

The end of the traverse will show a rapid and progressive increase in deformation towards the detachment between orthogneiss and Mesozoic marble exposed at the tip of the cape. Large amounts of ductile strain have been imposed on the rocks in a ~10-50 m thick shear zone, with the development of intensely foliated and lineated mylonites and phyllonites. The actual detachment is exposed, and is a sharply delineated fault plane (see Fig. 12.6)

Throughout most of the traverse strongly foliated gently dipping layers of grey orthogneiss are cut by aplites, which are also strongly deformed. These in turn are cut by weakly deformed pegmatites. The exact timing of emplacement of these units is unknown. The gneiss appears to have formed from a muscovite/biotite granite, with alignment of the micas and stretching of feldspar phenocrysts parallel to the foliation. The aplites are dominantly K-feldspar, quartz and muscovite and display a moderately well developed E- to NE-trending lineation, defined by elongation of muscovite. Walking NE through the complex a number of cross-cutting relationships can be observed. Moving up the ridge there appears to be some changes in the appearance of the “grey” orthogneiss, suggesting it is from a slightly different granite protolith or that the original granite was heterogeneous.

On the last peak above the tip of the cape the gneiss contains large crystals of K-feldspar which display a top to the NE sense of shear. These phenocrysts progressively decrease in size as we continue north-east and the contacts between aplite and gneiss become increasingly hard to distinguish. Also note that the proportion of quartz veins cutting the complex also increases.

There are a great variety of different structural and/or magmatic interactions to be seen along this traverse. Some of the variation is clearly the result of deformation during shear zone formation (e.g. Fig. 12.7 shows a folded granitic dyke). Other interactions are either due to the

**Figure 12.4** The strongly lineated L-tectonite at Pisso Livadi, on eastern Paros. This rock is the same Hercynian mafic granite that is deformed elsewhere in the lower plate of the Paros core complex. Here however it has been affected by two periods of foliation development, so that the total accumulation of finite strain has resulted in the development of an L-tectonite.

**Figure 12.5** The deformed meta-igneous complex at Monastiri Bay, NW of Naoussa. A large number of dykes have intruded the meta-sediments and meta-igneous rocks, and these have been deformed in a major (east-directed) shear zone beneath the Paros Detachment Fault.

**Figure 12.6** Sue Keay illustrates the sense of relative movement on the Paros Detachment Fault. The fault separates relatively undeformed marbles from intensely mylonitized granite schists and phyllonites in the lower plate. The zone of intense strain is no more than ~50 m thick. Intense mylonitization of the shear zone complex ,illustrated above, has taken place.

**Figure 12.7** On both the large scale and on the small scale, dykes in the shortening field of the deformation in the shear zone are folded intensely. Examples can be found on the 500m to the 10-100 cm scale. Photo shows a folded granitic dyke.

**Figure 12.8** In this photo we illustrate dykes that have been in the stretching field of deformation associated with the shear zone. They have been stretched out parallel to the foliation. Pinch and swell structures do not appear to be related to heterogeneous deformation. Pegmatite is closely associated with the aplite.

**Figure 12.9** This photo illustrates the enigmatic nature of the interaction between magmatism and deformation. The aplite dykes have either been intruded parallel to the foliation, or they have suffered large-scale reorientation as the result of deformation in the shear zone. The pegmatites have intruded later, often using the same fractures, or developing at the edges of the bodies. In the case illustrated, the pegmatite may have ballooned an existing fracture.

**Figure 12.10** Boudinage of an aplite dyke in the granite schists at stop #2. Tension mode fractures originally perpendicular to the foliation have dilated and been rotated into the shapes shown. Foliation adjacent to a boudin neck has bowed into the dilating zone, in an attempt to minimize the amount of new space created.

timing of magmatic emplacement, or to the interaction of magmatism with deformation. For example, Fig. 12.8 shows a granitic dyke now parallel to foliation. This is due to a combination of the initial orientation in which it was intruded, as well as to the effects of ongoing deformation in the shear zone causing large scale reorientation. The later pegmatite dyke exhibits pinch and swell structures that are related either to the effects of boudinage, or to periodic ballooning of the emplacement fracture during its intrusion. Figure 12.10 shows a variety of granitic and aplitic dykes, with timing relations suggesting that the pegmatites are associated with the aplites, but intruded later. In high strain zones (such as encountered at stop #2, the same aplitic dykes are boudinaged, and or highly attenuated.

### *Stop #4* Headland

Walking across the neck of the headland we pass the remains of what we have interpreted to be an ancient arrow-making site. Angular pieces of obsidian can be found, presumably derived from volcanic glass caught up in pumice which has floated to this end of Paros and washed up on the small beach here.

The ancient people have apparently moved the pumice boulders to the top of the ridge, where they have smashed them to extract the obsidian, and then shaped the obsidian to make tools or weapons. PLEASE DO NOT DISTURB THIS SITE. It may be of value to archaeological research.

At this point the orthogneisses are subject to intense shearing and are cut by numerous quartz veins. It is very difficult to identify any compositional changes in the protolith, as you could earlier. Closer to the marble contact the orthogneiss is strongly lineated and so strongly deformed that it gives the appearance of layers of fine sheets of paper (lineation trending 8 __> 060, mylonitic foliation dipping 15 __> 085). Tiny (<1mm) garnets have developed, overprinting the assemblages in the orthogneisses.

The detachment fault is marked by calc-silicate breccia along the fault plane, but the marble itself shows remarkably little sign of deformation, even within one metre of the fault plane.

# Bibliography


Agarwal, N.K., Jacoby, I.L. & Berckhemer, H., 1976. Teleseismic P-wave travel-time residuals and deep structure of the Aegean region. Tectonophysics 31, 33-57.

Allan, T.D. & Morelli, C., 1971. A geophysical study of the Mediterranean Sea. Bollettino di Geofisica ed Applicata 13(50), 99-141.

Altherr, R., Schliestedt, M., Okrusch, M., Seidel, E., Kreuzer, H., Harre, W., Lenz, H., Wendt, I. & Wagner, G.A., 1979. Geochronology of high-pressure rocks on Sifnos (Cyclades, Greece). Contributions to Mineralogy and Petrology 70, 245-255.

Altherr, R., Kreuzer, H., Wendt, I., Lenz, H., Wagner, G.A., Keller, J., Harre, W. & Höhndorf, A., 1982. A Late Oligocene/Early Miocene high temperature belt in the Attic-Cycladic crystalline complex (SE Pelagonian, Greece). Geologisches Jahrbuch E23, 97-164.

Altherr, R., Henjes-Kunst, F., Matthews, A., Friedrichsen, H. & Hansen, B.T., 1988. O-Sr isotopic variations in Miocene granitoids from the Aegean: evidence for an origin by combined assimilation and fractional crystallization. Contributions to Mineralogy and Petrology 100, 528-541.

Andriessen, P.A.M., 1978. Isotopic age relations within the polymetamorphic complex of the island of Naxos (Cyclades, Greece). PhD thesis, RU Utrecht, Amsterdam.

Andriessen, P.A.M., Boelrijk, N.A.I.M., Hebeda, E.H., Priem, H.N.A., Verdurmen, E.A.Th. & Verschure, R.H., 1979. Dating the events of metamorphism and granite magmatism in the Alpine orogen of Naxos (Cyclades, Greece). Contributions to Mineralogy and Petrology 69, 215-225.

Andriessen, P.A.M., Banga, G. & Hebeda, E.H., 1987. Isotopic age study of pre-Alpine rocks in the basal units on Naxos, Sikinos and Ios, Greek Cyclades. Geologie en Mijnbouw 66, 3-14.

Andriessen, P.A.M. & Jansen, J.B.H., 1990. Geochronology of the thermo-tectonic evolution of the Late Alpine Barrovian metamorphism of Naxos, Greece. Terra Abstracts 2, 4.

Andriessen, P.A.M., Hebeda, E.H., Simon, O.J. & Verschure, R.H., 1991. Tourmaline K-Ar ages compared to other radiometric dating systems in Alpine anatectic leucosomes and metamorphic rocks (Cyclades and southern Spain). Chemical Geology 91, 33-48.

Angelier, J., 1978. Tectonic evolution of the Hellenic arc since the late Miocene. Tectonophysics 4, 23-36.

Avigad, D. & Garfunkel, Z., 1991. Uplift and exhumation of high pressure metamorphic terrains: the example of the Cycladic blueschist belt (Aegean Sea). Tectonophysics 188, 357-372.

Avigad, D., 1993. Tectonic juxtaposition of blueschists and greenschists in Sifnos Island (Aegean Sea) - implications for the structure of the Cycladic blueschist belt. Journal of Structural Geology 15, 1459-1469.

Avigad, D., Matthews, A. & Garfunkel, Z., 1988. The Alpine Evolution of the Cyclades: An introduction and excursion guide to the geology of the islands of Sifnos and Tinos, Excursion to the Greek Islands, Israel Geological Society Publication.

Baillie, M.G.L. & Munro, M.A.R., 1988. Irish Tree-Rings, Santorini and Volcanic Dust Veils. Nature 332, 344-346.

Baldwin, S.J. & Lister, G.S. (in prep.). Thermochronology of the South Cyclades shear zone, Ios, Greece: implications for ductile shear zones formed during continental extension.

Banga, G., 1982. A major crustal shear-zone in the Greek Islands Ios and Sikinos. Unpublished M.Sc Thesis, University of Utrecht, The Netherlands.

Barber, R.L.N., 1987. The Cyclades in the Bronze Age, University of Iowa Press, Iowa City, 283pp.

Bardossy, G., 1982. Karst bauxites: bauxite deposits on carbonate rocks, Elsevier, Amsterdam.

Bath, M., 1983. Review: The seismology of Greece. Tectonophysics 98(3-4), 165-208.

Benioff, H., 1962. Movements of major transcurrent faults. In: Continental Drift (Ed. Runcorn, S.K.). New York, Academic Press (International Geophysics Series Vol. 3), 103-134.

Boatswain, T. & Nicolson, C., 1989. ATraveller's History of Greece, Efstathiadis Group, Athens, 306pp.

Boccaletti, M., Guazzone, G. & Manetti, P., 1974. Evoluzione paleogeografica e geodinamica del Mediterraneo; i bacini marginali (Translated title: Paleogeographic and geodynamic evolution of the Mediterranean; marginal basins). In: Atti del 67 degrees Congresso della Societa Geologica Italiana; L'Italia dell'ambito dell'evoluzione del Mediterraneo (Eds. anonymous). Societa Geologica Italiana, Rome, Italy.

Bond, A. & Sparks, R.S.J., 1976. The Minoan Eruption of Santorini, Greece. Journal of the Geological Society of London 132, 1-16.

Boronkay, K. & Doutsos, T., 1994. Transpression and transtension within different structural levels in the central Aegean region. Journal of Structural Geology 16(11), 1555-1573.

Buick, I.S., 1991a. The late Alpine evolution of an extensional shear zone, Naxos, Greece. Journal of the Geological Society of London 148, 93-103.

Buick, I.S., 1991b. Mylonite fabric development on Naxos, Greece. Journal of Structural Geology 13 (6), 643-655.

Buick, I.S. & Holland, T.J.B., 1989. The P-T-t path associated with crustal extension, Naxos, Cyclades, Greece. In: Evolution of metamorphic belts (Eds. Daly, J.S., Cliff, R.A. & Yardley, B.W.D.). Geological Society Special Publication 43, 365-369.

Buick, I.S. & Holland, T.J.B., 1991. The nature and distribution of fluids during upper amphibolite facies metamorphism, Naxos (Greece). Journal of Metamorphic Geology 9(3), 301-314.

Burn, A.R. & Burn, M., 1980. The Living Past of Greece: A time-traveller's tour of historic and prehistoric places, Penguin Books, Middlesex, England, 288pp.

Chappell, B.W. & White, A.J.R., 1974. Two contrasting granite types. Pacific Geology 8, 173-174.

Davis, G.A. & Lister, G.S., 1988. Detachment faulting in continental extension: perspectives from the southwestern U.S. Cordillera, John Rodgers symposium volume. Geological Society of America Special Papers 218, 133-159.

Dermopoulos, M.P., 1990. The Tangible Past: Archaeological Sites in the Greek Islands, Efstathiadis Group, Athens, 174pp.

Didier, J., 1973. Granites and their Enclaves: the bearing of enclaves on the origin of granites, Elsevier Scientific Publishing Co., Amsterdam, 393 pp.

Didier, J. & Barbarin, B. (Eds), 1991. Enclaves and Granite Petrology, Elsevier Science Publishing Co., Amsterdam, 625 pp.

Doumas, C. G., 1983. Thera: Pompeii of the Ancient Aegean: excavations at Akrotiri, 1967-1979, Thames and Hudson, London, 168pp.

Druitt, T.H. & Francaviglia, V., 1990. An Ancient Caldera Cliff Line at Phira and its Significance for the Topography and Geology of Pre-Minoan Santorini. In: Thera and the Aegean World III, Volume Two: Earth Sciences (Eds. Hardy D.A., Keller J., Galanopoulos V.P. & Druitt T.H.). Proceedings of the Third International Congress, Santorini, Greece, 3-9 Sept. 1989. The Thera Foundation, London, 362-369.

Druitt, T.H., 1985. Vent Evolution and Lag Breccia Formation During the Cape Riva Eruption of Santorini. Journal of Geology 93, 439-454.

Druitt, T.H., Mellors, R.A., Pyle, D.M. & Sparks, R.S.J., 1989. Explosive Volcanism in Santorini, Greece. Geology Magazine 126, 95-126.

Druitt, T.H. & Francaviglia, V., 1992. Caldera Formation on Santorini and the Physiography of the Islands in the Late Bronze Age. Bulletin of Volcanology 54, 484-493.

Dürr, S., Altherr, R., Keller, J., Okrusch, M. & Seidel, E., 1978. The median Aegean crystalline belt: stratigraphy, structure, metamorphism, magmatism. In: Alps, Apennines, Hellenides (Eds. Closs, H., Roeder, D. & Schmidt, K.). Inter-union Commission on Geodynamics Scientific Report 38. Elsevier, Amsterdam-New York, International, 620pp.

Ellingham, M., Dubin, M., Jansz, N. & Fisher, J., 1992. Greece - The Rough Guide, 5th Edition, Rough Guides Ltd, London, 720pp.

Erickson, A.J., 1970. The measurement and interpretation of heat flow in the Mediterranean and Black Sea. Unpublished PhD Thesis, Massachusetts Institute of Technology, USA.

Eriksen, U., Freidrich, W.L., Buchardt, B., Tauber, H. & Thomsen, M.S., 1990. The Stronghyle Caldera: Geological, Palaeontological and Stable Isotope Evidence from Radiocarbon Dated Stromatolites from Santorini. In: Thera and the Aegean World III, Volume Two: Earth Sciences (Eds. Hardy D.A., Keller J., Galanopoulos V.P. & Druitt T.H.). Proceedings of the Third International Congress, Santorini, Greece, 3-9 Sept. 1989. The Thera Foundation, London, 139-150.

Feenstra, A., 1985. Metamorphism of bauxites on Naxos, Greece. PhD Thesis published in Geologica Ultraiectina: Mededelingen van het Instituut voor Aardwetenschappen der Rijksuniversiteit te Utrecht, No. 39, Offsetdrukkerij Kanters B.V., Alblasserdam, 206pp.

Ferrara, G., Fytikas, M., Giuliani, O. & Marinelli, G., 1980. Age of the Formation of the Aegean Active Volcanic Arc. In: Thera and the Aegean World II (Ed. Doumas C.), 49-56.

Forbes-Boyd, E., 1970. Aegean Quest: Asearch for Venetian Greece, J.M.Dent & Sons Ltd, London, 203pp.

Forster, M.A., 1996. Deformation and metamorphism of the upper plate Ios, Cyclades, Greece. M.Sc Stage I report, Monash University, Melbourne.

Forster, M.A. & Lister, G.S., 1996a. Episodes of extension on Ios, Greece. Penrose Conference on “Exhumation Processes: Normal faulting, Ductile Processes and Erosion”, Crete.

Forster, M.A. & Lister, G.S., 1996b. Separate episodes of eclogite and blueschist metamorphism in the Ios metamorphic core complex, Cyclades, Greece. In: Evolution of Metamorphic Belts. Proceedings of the Specialist Group in Geochemistry, Mineralogy and Petrology Conference 16-17 Dec. 1996, Geological Society of Australia, Abstracts, in press.

Friedrich, W.L., Eriksen, U., Tauber, H., Heinemeier, J., Thomsen, M.S. & Buchardt, B., 1988. Existence of a Water-Filled Caldera Prior to the Minoan Eruption of Santorini, Greece. Naturwissenschaften 75, 567-569.

Fytikas, M., Giuliani, O., Innocenti, F., Marinelli, G. & Mazzuoli, R., 1976. Geochronological Data on Recent Magmatism of the Aegean Sea. Tectonophysics 31, 29-34.

Fytikas, M., Innocenti, F., Kolios, N., Manetti, P., Mazzuoli, R., Poli, G., Rita, F. & Villari, L., 1986. Volcanology and Petrology of Volcanic Products from the Island of Milos and Neighbouring Islets. Journal of Volcanology and Geothermal Research 28, 297-317.

Fytikas, M., Innocenti, F., Manetti, P., Mazzuoli, R., Peccerillo, A. & Villari, L., 1984. Tertiary to Quaternary Evolution of Volcanism in the Aegean Region. In: The Geological Evolution of the Eastern Mediterranean (Eds. Dixon J.E. & Robertson A.H.F.). Geological Society of London Special Publication 17, p687-699.

Garcia-Celma, A., 1983. c-axis- and shape-fabrics in quartz-mylonites of Cap de Creus (Spain); their properties and development. PhD Thesis, Instituut of Earth Sciences, University of Utrecht, The Netherlands.

Gass, I. G., 1972. The role of lithothermal systems in the magmatic and tectonic processes. Journal of Earth Sciences 8, 261-272.

Gautier, P. & Brun, J.P., 1994. Ductile crust exhumation and extensional detachments in the central Aegean (Cyclades and Evvia Islands). Geodinamica Acta (Paris) 7/2, 57-85.

Gautier, P., Brun, J.P. & Jolivet, L., 1993. Structure and kinematics of Upper Cenozoic extensional detachment on Naxos and Paros (Cyclades islands, Greece). Tectonics 12, 1180-1194.

Georgalas, C. C., 1962. L'eruption du volcan de Santorin en 1939 - 1941; l'eruption du dome Niki. Bulletin of Volcanology 24, 295-300.

Gulen, L., 1989. Isotopic Characterisation of Aegean Magmatism and Geodynamic Evolution of Aegean Subduction. In: Crust/Mantle Recycling at Convergence Zones (Eds. Hart S.R. & Gulen, L.). NATO Advanced Studies, Institute Series C258, 143-166.

Hammer, C.U., Clausen, H.B., Freidrich, W.L. & Tauber, H., 1987. The Minoan Eruption of Santorini in Greece Date to 1645 BC? Nature 328, 517-519.

Heiken, G. & McCoy, F.W., 1984. Caldera Development During the Minoan Eruption, Thera, Cyclades, Greece. Journal of Geophysical Research 89, 8441-8462.

Heiken, G. & McCoy, F.W., 1990. Precursor Activity to the Minoan Eruption, Thera, Greece. In: Thera and the Aegean World III, Volume Two: Earth Sciences (Eds. Hardy D.A., Keller J., Galanopoulos V.P. & Druitt T.H.). Proceedings of the Third International Congress, Santorini, Greece, 3-9 Sept. 1989. The Thera Foundation, London, 79-88.

Henjes-Kunst, F., 1980. Alpidische Einformung des praalpidischen Kristallins und seiner mesozoischen Hulle auf Ios (Kykladen, Griechenland). Unpublished Ph.D thesis, University of Braunschweig, Germany.

Henjes-Kunst, F. & Kreuzer, H., 1982. Isotopic dating of pre-alpidic rocks from the island of Ios (Cyclades, Greece). Contributions to Mineralogy and Petrology 80, 245-253.

Henjes-Kunst, F., Altherr, R., Kreuzer, H. & Hansen, B.T., 1988. Disturbed U-Th-Pb systematics of young zircons and uranothorites: the case of the Miocene Aegean granitoids (Greece). Chemical Geology (Isotope Geoscience Section) 73, 125-145.

Hill, E.J., Baldwin, S.L. & Lister, G.S., 1992. Unroofing of active metamorphic core complexes in the D'Entrecasteaux Islands, Papua New Guinea. Geology 20(10), 907-910.

Huijsmans, J.P.P., 1985. Calc-alkaline lavas from the volcanic complex of Santorini, Aegean Sea, Greece; a petrological, geochemical and stratigraphic study. Geologica Ultraiectina 41, Rijkuniversiteit, Mineralogisch-geologische Instituut, Utrecht, Netherlands, 316pp.

Innocenti, F., Manetti, P., Mazzuoli, R., Pasquare, G. & Villari, L., 1981. Neogene and Quaternary Volcanism in the Eastern Mediterranean: Time-Space Distribution and Geotectonic Implication. In: Sedimentary Basins of Mediterranean Margins (Ed. Wezel F.C.). Proceedings of the Consiglio nazionale delle ricerche International Conference, Urbino, Italy, Oct 20-22 1980. Pitagorg, Bologna, Italy, 369-385.

Jackson, M., 1994. Active tectonics of the Aegean region. Annual Review Earth and Planetary Sciences 22, 239-271.

Jacoby, W.R., Agarwal, N.K. & Berckhemer, H., 1978. Crustal and upper mantle structure of the Aegean arc from travel time residuals and gravity. In: Alps, Apennines, Hellenides (Eds. Closs, H., Roeder, D. & Schmidt, K.). Inter-union Commission on Geodynamics Scientific Report 38. Elsevier, Amsterdam-New York, International, 620pp.

Jansen, J.B.H., 1973a. Geological Map of Greece, Island of Naxos, Institute for Geology and Mineral Resources, Athens.

Jansen, J.B.H., 1973b. Metamorphism on Naxos, PhD Thesis, RU Utrecht, Amsterdam.

Jansen, J.B.H. & Schuiling, R.D., 1976. Metamorphism on Naxos: Petrology and geothermal gradients. American Journal of Science 276, 1225-1253.

Jongsma, D., 1973. Heat flow in the Aegean Sea. European Geophysical Society, Meeting, Abstracts 1, 55pp.

Jongsma, D., 1974. Heat flow in the Aegean Sea. The Geophysical Journal of the Royal Astronomical Society 37(3), 337-346.

Jongsma, D., Wissmann, G., Hinz, K. & Garde, S., 1978. Result of reflection seismic surveys in the southern Aegean Sea. In: Alps, Apennines, Hellenides (Eds. Closs, H., Roeder, D. & Schmidt, K.). Inter-union Commission on Geodynamics Scientific Report 38. Elsevier, Amsterdam-New York, International, 620pp.

Kalegeropoulos, S. & Paritsis, S., 1990. Geological and Geochemical Evolution of the Santorini Volcano: A Review. In: Thera and the Aegean World III, Volume Two: Earth Sciences (Eds. Hardy D. A., Keller J., Galanopoulos V. P. & Druitt T. H.). Proceedings of the Third International Congress, Santorini, Greece, 3-9 Sept. 1989. The Thera Foundation, London, 164-171.

Keay, S.M., Lister, G.S.L. & Compston, W. (in prep.). Evidence for extensive Hercynian magmatism from Aegean basement rocks.

Keller, J., Rehren, T.H. & Stadlbauer, E., 1990. Explosive Volcanism in the Hellenic Arc: a Summary and Review. In: Thera and the Aegean World III, Volume Two: Earth Sciences (Eds. Hardy D. A., Keller J., Galanopoulos V. P. & Druitt T. H.). Proceedings of the Third International Congress, Santorini, Greece, 3-9 Sept. 1989. The Thera Foundation, London, 13-26.

Keller, J., 1981. Quaternary Tephrachronology in the Mediterranean Region. In: Tephra Studies (Eds. Self, S. & Sparks R.S.J.). NATO Advanced Study Institutes Series C 75, 227-244.

Keller, J., 1982. Mediterranean Island Arcs. In: Andesites: orogenic andesites and related rocks (Ed. Thorpe S.), Wiley, Chichester, 724pp.

Keller, J., Gillot, P.Y., Rehren, T.H. & Stadlbauer, E., 1989. Chronostratigraphic Data for the Volcanism in the Eastern Hellenic Arc: Nisyros and Kos. Terra Abstracts 1, 354.

Kissel, C. & Laj, C., 1988. The Tertiary geodynamical evolution of the Aegean arc: a palaeomagnetic reconstruction. Tectonophysics 146, 183-201.

LaMarche, V.C. & Hirschboeck, K.K., 1984. Frost Rings in Trees as Records of Major Volcanic Eruptions. Nature 307, 121-126.

Le Pichon, X. & Angelier, J., 1979. The Hellenic arc and Trench system: A key to the neotectonic evolution of the Eastern Mediterranean area. Tectonophysics 60, 1-42.

Le Pichon, X., Lyberis, N., Angelier, J. & et Renard, V., 1982. Strain distribution over the East Mediterranean ridge: A synthesis incorporating new sea-beam data. Tectonophysics 86, 243-274.

Lee, J. & Lister, G.S., 1992. Late Miocene ductile extension and detachment faulting, Mykonos, Greece. Geology 20, 121-124.

Leydecker, G., Berckhemer, H. & Delibasis, N., 1978. A study of seismicity in the Peloponnesos region by precise hypocenter determinations. In: Alps, Apennines, Hellenides (Eds. Closs, H., Roeder, D. & Schmidt, K.). Inter-union Commission on Geodynamics Scientific Report 38. Elsevier, Amsterdam-New York, International, 620pp.

Lister, G., 1990. Metamorphic core complexes - “hot-spots” in the continental crust? Proceedings of Pacific Rim 1990 Congress.

Lister, G.S., Banga, G. & Feenstra, A., 1984. Metamorphic core complexes of Cordilleran type in the Cyclades, Aegean Sea, Greece. Geology 12, 221-225.

Lister, G.S. & Raouzaios, A., 1996. The tectonic significance of a porphyroblastic blueschist facies overprint during alpine orogenesis - Sifnos, Aegean Sea, Greece. Journal of Structural Geology 18, 1417-1435.

Makris, J., 1977. Geophysical Investigations. Crustal structure of the Central Aegean Sea and the islands of Evia and Crete, Greece. Hamburger Geoph. Einzel. 34, Hamburg, Germany, 124pp.

Makris, J., 1978. The crust and upper mantle of the Aegean region obtained from seismic soundings. Tectonophysics 46(3-4), 269-284.

Makris, J. & Vees, R., 1977. Crustal structure of the Central Aegean Sea and the islands of Evia and Crete, Greece, obtained by fractional seismic experiments. Journal of Geophysics 42, 329-341.

Marangou, L. (Ed.), 1990. Cycladic Culture: Naxos. In: The 3rd Millennium BC, Nicholas P. Goulandris Foundation - Museum of Cycladic Art, Athens, 179pp.

McKenzie, D., 1972. Active tectonics of the Mediterranean region. The Geophysical Journal of the Royal Astronomical Society 30(2), 109-185.

McKenzie, D., 1978. Active tectonics of the Alpine-Himalayan belt: the Aegean sea and surrounding regions. The Geophysical Journal of the Royal Astronomical Society 55, 217-254.

Miller, E.L.M., Calvert, A.T. & Little, T.A., 1992. Strain-collapsed metamorphic isograds in a sillimanite gneiss dome, Seward Peninsula, Alaska. Geology 20(6), 487-496.

Mitropoulos, P. & Tarney, J., 1992. Significance of Mineral Composition Variations in the Aegean Island Arc. Journal of Volcanology and Geothermal Research 51, 283-303.

Mitropoulos, P., Tarney, J., Saunders, A.D. & Marsh, N.G., 1987. Petrogenesis of Cenozoic Volcanic Rocks from the Aegean Island Arc. Journal of Volcanology and Geothermal Research 32, 177-193.

Miyashiro, A., 1973. Paired and unpaired metamorphic belts. in: Experimental petrology and global tectonics. Tectonophysics 17, 241-254.

Ninkovich, D. & Hays, J. D., 1972. Mediterranean Island Arcs and the Origin of High Potash Volcanoes. Earth and Planetary Science Letters 16, 331-345.

O'Sullivan, M., 1993. The Greek Gods - an iconoclast's guide, Efstathiadis Group, Athens, 213pp.

Pichler, H. & Kussmaul, S., 1972. The Calcalkaline Volcanic Rocks of the Santorini Group (Aegean Sea, Greece). Neues Jahrbuch fur Mineralogie, Abhandlungen 116, 268-307.

Papazachos, B.C. & Comninakis, P.E., 1978. Deep structure and tectonics of the Eastern Mediterranean. Tectonophysics 46, 285-296.

Pyle, D.M., 1990. New Estimates for the Volume of the Minoan Eruption. In: Thera and the Aegean World III, Volume Two: Earth Sciences (Eds. Hardy D. A., Keller J., Galanopoulos V. P. & Druitt T. H.). Proceedings of the Third International Congress, Santorini, Greece, 3-9 Sept. 1989. The Thera Foundation, London, 113-121.

Raouzaios, A., Lister, G.S. & Foster, D.A., 1996. Oligocene exhumation and metamorphism of eclogite-blueschists from the island of Sifnos, Cyclades, Greece. Geological Society of Australia, Abstracts 41, 358.

Raouzaios, A. & Lister, G.S., 1993. Deformation and metamorphism on the island of Sifnos, Cyclades, Greece. Structures and tectonics at different lithospheric levels, Graz, Austria, 6-8 Sept. 1993. Terra Nova abstract supplement 5(2), 28.

Rehren, T.H., 1988. Geochemie und Petrologie von Nisyros (östliche Ägäis). Unpublished PhD Thesis, Freiburg.

Reynolds, S.J. & Lister, G.S., 1987. Structural aspects of fluid-rock interactions in detachment zones. Geology 15, 362-366.

Richter, I. & Strobach, K., 1978. Benioff zones of the Aegean arc. In: Alps, Apennines, Hellenides (Eds. Closs, H., Roeder, D. & Schmidt, K.). Inter-union Commission on Geodynamics Scientific Report 38. Elsevier, Amsterdam-New York, International, 620pp.

Ridley, J., 1982. Arcuate lineation trends in a deep level, ductile thrust belt, Syros, Greece. Tectonophysics 88, 347-360.

Ritsema, A.R., 1974. Fault plane mechanisms of Balkan earthquakes. In: Proceedings of the seminar on the seismotectonic map of the Balkan region (Eds. Gorshkov, G.P., Karnik, V. & Sikosek, B.). UNESCO, Skopje, Yugoslavia, 229-238.

Roesler, G., 1978. Relics of non-metamorphic sediments on Central Aegean Islands. In: Alps, Apennines, Hellenides (Eds. Closs, H., Roeder, D. & Schmidt, K.). Inter-union Commission on Geodynamics Scientific Report 38. Elsevier, Amsterdam-New York, International, 620pp.

Ryan, W.B.F., Kastens, K.A. & Cita, M.B., 1982. Geological evidence concerning compressional tectonics in the eastern Mediterranean. Tectonophysics 86(1-3), 213-242.

Scott, R.J. & Lister, G.S., 1992. Detachment faults: Evidence for a low-angle origin. Geology 20(9), 833-836.

Schuiling, R.D. & Kreulen, R., 1979. Are thermal domes heated by CO2-rich fluids from the mantle? Earth and Planetary Science Letters 43(2), 298-302.

Seidal, E., Kreuzer, H. and Harne, W. 1982. A late Oligocene/early Miocene high pressure belt in the External Hellenides. Geologisches Jahrbuch. Reihe E: Geophysik 23, 165-206.

Spakman, W., Wortel, M.J.R. & Vlaar, N.J., 1988. The Hellenic subduction zone; a tomographic image and its geodynamic implications. Geophysical Research Letters 15(1), 60-63.

Sparks, R.S.J. & Wilson, C.J.N., 1990. The Minoan Deposits: a Review of their Characteristics and Interpretation. In: Thera and the Aegean World III, Volume Two: Earth Sciences (Eds. Hardy D. A., Keller J., Galanopoulos V. P. & Druitt T. H.). Proceedings of the Third International Congress, Santorini, Greece, 3-9 Sept. 1989. The Thera Foundation, London, 89-99.

Sparks, R.S.J., Self, S. & Walker, G.P.L., 1973. Products of Ignimbrite Eruptions. Geology 1, 115-118.

Spiegelman, M. & McKenzie, D.P., 1987. Simple 2D Models for Melt Extraction at Mid-Ocean Ridges and Island Arcs. Earth and Planetary Science Letters 83, 137-152.

Sullivan, D.G., 1988. The Discovery of the Santorini Minoan Tephra in Western Turkey. Nature 333, 552-554.

Sykes, L.R., 1966. Spatial and temporal distribution of earthquakes. In: ESSA symposium on earthquake prediction, Rockville, MD., 1966. Washington, DC, US Government Printing Office, 38-43.

Ucke, C., 1988. Walking Tours on Naxos, Christoph & Michael Hofbauer Publishing House, Munchen, 214pp.

Urai, J.L., Means, W.D. & Lister, G.S., 1986. Dynamic recrystallisation of minerals. American Geophysical Union, Geophysics Monograph 16, 161-199.

Urai, J.L., Schuiling, R.D. & Jansen, J.B.H., 1990. Alpine deformation on Naxos (Greece). In: Deformation mechanisms, rheology and tectonics (Eds. Knipe, R.J. & Rutter, E.H.). Geological Society Special Publication 54, 509-522.

Vandenberg L.C. & Lister, G.S., 1996. Structural analysis of basement tectonites from the Aegean metamorphic core complex of Ios, Cyclades, Greece. Journal of Structural Geology 18, 1437-1454.

Van der Maar, P.A., 1980. The geology and petrology of Ios, Cyclades Greece. Annales Geologiques des Pays Helleniques 30, 206-224.

Van der Maar, P.A., 1981. Geological map of Greece, Island of Ios, 1:50,000. Institute for Geology and Mineral Exploration (I.G.M.E), Athens.

Van der Maar, P.A. & Jansen, J.B.H., 1983. The geology of the polymetamorphic complex on Ios, Cyclades, Greece, and its significance for the Cycladic massif. Geologische Rundschau 72, 283-299.

Vogt, P.R. & Higgs, R.H., 1969. An aeromagnetic survey of the eastern Mediterranean sea and its interpretation. Earth and Planetary Science Letters 5(7), 439-448.

Watkins, N.D., Sparks, R.S.J., Sigurdsson, H., Huang, T.C., Federman, A., Carey, S. & Ninkovich, D., 1978. Volume and Extent of the Minoan Tephra Layer from Santorini Volcano: New Evidence from Deep Sea Sediment Cores. Nature 271, 122-126.

Wijbrans, J.R. & McDougall, I., 1986. 40Ar/39Ar dating of white micas from an Alpine high pressure metamorphic belt on Naxos (Greece): the resetting of the argon isotopic system. Contributions to Mineralogy and Petrology 93, 187-194.

Wijbrans, J.R. & McDougall, I., 1988. Metamorphic evolution of the Attic Cycladic metamorphic belt on Naxos (Cyclades, Greece) utilising 40Ar/39Ar age spectrum measurements. Journal of Metamorphic Geology 6, 571-594.

Willett, D., Hall, R., Hellander, P. & Kenihan, K., 1996. Greece - a lonely planet travel survival kit, 2nd edition, Lonely Planet Publications, Hawthorn, Australia, 744pp.

Wilson, C.J.N. & Houghton, B.F., 1990. Eruptive Mechanisms in the Minoan Eruption: Evidence From Pumice Vesicularity. In: Thera and the Aegean World III, Volume Two: Earth Sciences (Eds. Hardy D. A., Keller J., Galanopoulos V. P. & Druitt T. H.). Proceedings of the Third International Congress, Santorini, Greece, 3-9 Sept. 1989. The Thera Foundation, London, 122-128.

Woodside, J. & Bowin, C., 1970. Gravity anomalies and inferred crustal structure in the eastern Mediterranean Sea. Geological Society of America Bulletin 81(4), 1107-1122.